

Algebraic complete axiomatisation of ZX-calculus with a normal form via elementary matrix operations

Quanlong Wang
Cambridge Quantum Computing Ltd.

Abstract

In this paper we give a complete axiomatisation of qubit ZX-calculus via elementary transformations which are basic operations in linear algebra. This formalism has two main advantages. First, all the operations of the phases are algebraic ones without trigonometry functions involved, thus paved the way for generalising complete axiomatisation of qubit ZX-calculus to qudit ZX-calculus and ZX-calculus over commutative semirings. Second, we characterise elementary transformations in terms of ZX diagrams, so a lot of linear algebra stuff can be done purely diagrammatically.

1 Introduction

ZX-calculus was introduced by Coecke and Duncan [4] as a graphical language for quantum computing. It is quite intuitive but still mathematically restrict as formalised in the framework of compact closed categories. The diagrams of ZX-calculus are mainly generated by so-called Z-spiders and X-spiders (based on Z and X quantum observables with a spider-like shape). Any operation performed on a ZX diagram is just a replacement of a part of the diagram with another diagram according to a diagrammatic equality. Such an operation is called a rewriting which is local in the sense that other parts of the operated diagram won't be affected by the rewriting. The property of being local can be seen as an advantage of ZX-calculus, since one has no need to remember any previous steps when rewriting a diagram.

Since its invention, ZX-calculus has been focused on unitaries which are the core of quantum computing [14]. Actually, the first proof of universality of ZX-calculus (which means each matrix of size $2^m \times 2^n$ can be represented by a ZX diagram) was based on representation of unitaries in terms of Z and X phases [4]. Moreover, ZX-calculus has exhibited its power in the application field of quantum circuit optimisation [2, 9, 5]. On the other hand, ZX-calculus has been first proved to be complete for overall qubit quantum computing in [12] and incorporated in [6], which means quantum computation done by matrices can purely be done in ZX-calculus. Afterwards, there came a few different complete axiomatisations of ZX-calculus [7, 8, 15]. However,

all of these universal axiomatisations are non-algebraic in the sense that there are always some rules with trigonometry functions involved, which makes the application of non-algebraic rules quite difficult. This inconvenience was rescued in [18] by introducing an algebraic complete axiomatisation of ZX-calculus. Nevertheless, except for [8] whose completeness was established internally via a normal form of ZX diagrams, the other complete axiomatisations obtained their completeness externally, either deployed the completeness of ZW-calculus [6], or utilised pre-existing completeness of ZX-calculus. Could there be a universally complete axiomatisation of ZX-calculus which is both algebraic and internally established?

In this paper, we give a definite answer to that question by providing an algebraic complete axiomatisation of ZX-calculus with a normal form via elementary matrix operations. The idea of using elementary matrices comes from a simple observation: all of the elementary matrices of size 2×2 already existed in the previous complete axiomatisations of ZX-calculus [6] and [18]. So it is natural to generalise these expressions for arbitrary elementary matrix of size $2^n \times 2^n$. To focus on the completeness proof, the representation of arbitrary elementary row switching operations in ZX-calculus as presented in [19] is not given in this paper, which will be included in the further work [16]. Based on the representation of elementary matrices in ZX, we obtain a normal form for any vectors, then any matrix can be represented by a diagram due to the map-state duality. This normal form leads to a proof of completeness, though full of nontrivial techniques. In addition, we gain an advantage that no scalable techniques are needed, while seriously considered in [3].

2 Algebraic ZX-calculus

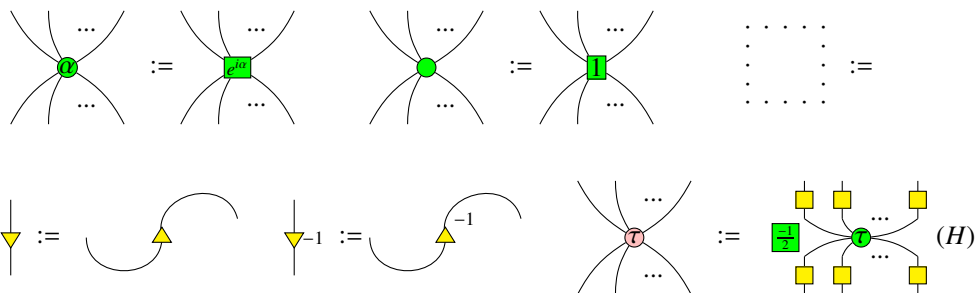
In this section, we give generators and rules for algebraic ZX-calculus which is shown to be complete via a normal form. We assume that we are working in a compact closed category \mathcal{C} .

$R_{Z,a}^{(n,m)} : n \rightarrow m$		$I : 1 \rightarrow 1$	
$H : 1 \rightarrow 1$		$\sigma : 2 \rightarrow 2$	
$C_a : 0 \rightarrow 2$		$C_u : 2 \rightarrow 0$	
$T : 1 \rightarrow 1$		$T^{-1} : 1 \rightarrow 1$	

Table 1: Generators of algebraic ZX-calculus, where $m, n \in \mathbb{N}$, $a \in \mathbb{C}$.

Remark 2.1 In Table 1, C_a and C_u compose the compact structure of \mathfrak{C} , while σ comprises the symmetric structure of \mathfrak{C} .

For simplicity, we make the following conventions:



where $\alpha \in \mathbb{R}$, $\tau \in \{0, \pi\}$.

Remark 2.2 The generator $R_{Z,a}^{(n,m)}$ can be equivalently expressed in terms of other generators and the following three diagrams:

$$\begin{array}{c} \bullet \\ \diagup \quad \diagdown \end{array} \quad \bullet \quad \begin{array}{c} \square \\ \diagup \quad \diagdown \end{array} \quad (1)$$

Remark 2.3 Comparing to the original generators of ZX-calculus as in [4], the generators $R_{Z,a}^{(n,m)}$, T and T^{-1} are new ones, but they have been firstly introduced in [13], and essentially shown to be representable in terms of original generators in [12] and [6]. The H node has a slight difference with the normal Hadamard node in a global scalar, which leads to the X spider defined in (H) distinguished from the normal X spider by a global scalar, in addition that only X -phase angles of 0 and π are defined now.

There is a standard interpretation $\llbracket \cdot \rrbracket$ for the ZX diagrams:

$$\left[\left[\begin{array}{c} \overbrace{\quad\quad\quad}^n \\ \diagdown \quad \diagup \\ \quad \square \quad \\ \diagup \quad \diagdown \\ \underbrace{\quad\quad\quad}_m \end{array} \right] \right] = |0\rangle^{\otimes m} \langle 0|^{\otimes n} + a |1\rangle^{\otimes m} \langle 1|^{\otimes n}, \quad \left[\left[\begin{array}{c} \overbrace{\quad\quad\quad}^n \\ \diagdown \quad \diagup \\ \quad \circ \quad \\ \diagup \quad \diagdown \\ \underbrace{\quad\quad\quad}_m \end{array} \right] \right] = \sum_{\substack{0 \leq i_1, \dots, i_m, j_1, \dots, j_n \leq 1 \\ i_1 + \dots + i_m \equiv j_1 + \dots + j_n \pmod{2}}} |i_1, \dots, i_m\rangle \langle j_1, \dots, j_n|,$$

$$\left[\left[\begin{array}{c} \square \\ | \end{array} \right] \right] = \begin{pmatrix} 1 & 1 \\ 1 & -1 \end{pmatrix}, \quad \left[\left[\begin{array}{c} \triangle \\ | \end{array} \right] \right] = \begin{pmatrix} 1 & 1 \\ 0 & 1 \end{pmatrix}, \quad \left[\left[\begin{array}{c} \triangle^{-1} \\ | \end{array} \right] \right] = \begin{pmatrix} 1 & -1 \\ 0 & 1 \end{pmatrix}, \quad \left[\left[\begin{array}{c} \otimes \\ | \end{array} \right] \right] = \begin{pmatrix} 0 & 1 \\ 1 & 0 \end{pmatrix}, \quad \left[\left[\begin{array}{c} | \\ | \\ | \end{array} \right] \right] = \begin{pmatrix} 1 & 0 \\ 0 & 1 \end{pmatrix},$$

$$\left[\left[\begin{array}{c} \diagdown \quad \diagup \\ \diagup \quad \diagdown \end{array} \right] \right] = \begin{pmatrix} 1 & 0 & 0 & 0 \\ 0 & 0 & 1 & 0 \\ 0 & 1 & 0 & 0 \\ 0 & 0 & 0 & 1 \end{pmatrix}, \quad \left[\left[\begin{array}{c} \frown \\ | \end{array} \right] \right] = \begin{pmatrix} 1 \\ 0 \\ 0 \\ 1 \end{pmatrix}, \quad \left[\left[\begin{array}{c} \smile \\ | \end{array} \right] \right] = (1 \ 0 \ 0 \ 1), \quad \left[\left[\begin{array}{c} \dots \\ \vdots \\ \dots \end{array} \right] \right] = 1,$$

$$\llbracket D_1 \otimes D_2 \rrbracket = \llbracket D_1 \rrbracket \otimes \llbracket D_2 \rrbracket, \quad \llbracket D_1 \circ D_2 \rrbracket = \llbracket D_1 \rrbracket \circ \llbracket D_2 \rrbracket,$$

where

$$a \in \mathbb{C}, \quad |0\rangle = \begin{pmatrix} 1 \\ 0 \end{pmatrix}, \quad \langle 0| = (1 \ 0), \quad |1\rangle = \begin{pmatrix} 0 \\ 1 \end{pmatrix}, \quad \langle 1| = (0 \ 1).$$

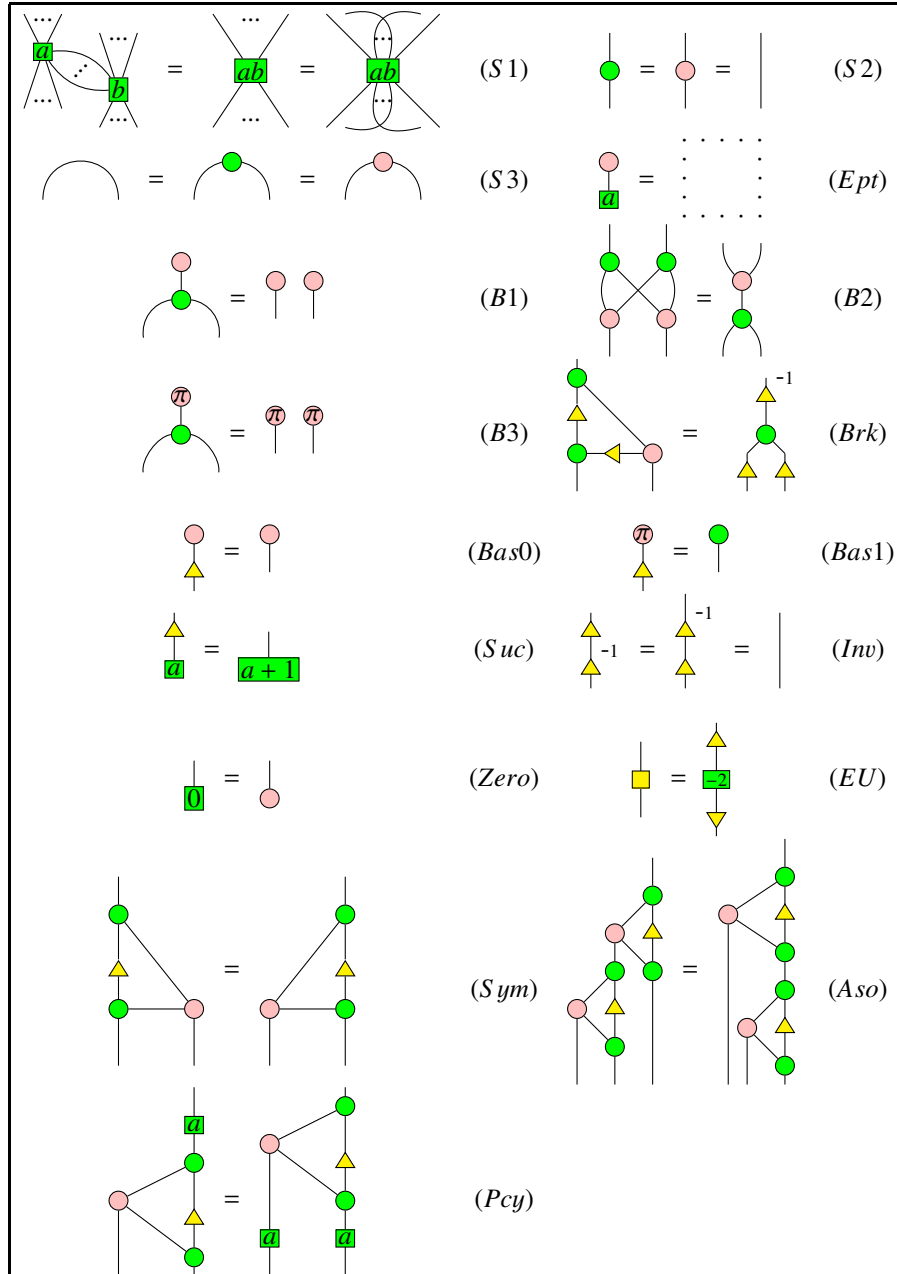



Figure 1: Algebraic rules, $a, b \in \mathbb{C}$. The upside-down flipped versions of the rules are assumed to hold as well.

Remark 2.4 As pointed out in [18], the last three rules (Sym), (Aso), and (Pcy) are

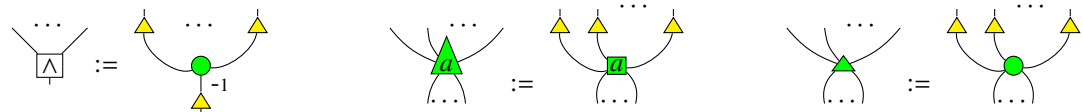
all about the properties of the W state (in a map form via map-state duality) : (Sym) means the W state is symmetric, (Aso) means the W state is associative, and (Pcy) means any phase can be copied by the W state.

It can be verified that the rules in Figure 1 still hold under the standard interpretation $\llbracket \cdot \rrbracket$, which means the algebraic ZX-calculus is sound.

3 Derivable equalities mainly from previous results

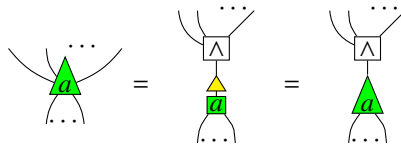
In this section, we derive equalities from algebraic rules in Figure 1. Some equalities have been essentially derived (up to scalars) in previous papers, but we prove them again due to generators and rules changed in the current formalism.

For simplicity, we give two denotations as follows:



(2)

Clearly, they have the following relation

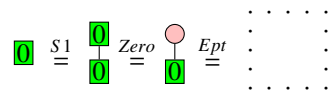


(3)

Lemma 3.1 [18] $\frac{\pi}{a} = \frac{1}{a-1}$ (Sca)

Proof:  □

Corollary 3.2 [18] $0 = \dots$ (Zos)

Proof:  □

Lemma 3.3 [18] $a \ b = \frac{1}{(a+1)(b+1)-1}$ (Sml)

Proof: $\begin{array}{|c|} \hline a \\ \hline \\ \hline b \\ \hline \end{array} \stackrel{Sca}{=} \begin{array}{|c|} \hline \pi \\ \hline \\ \hline a+1 \\ \hline \end{array} \begin{array}{|c|} \hline \pi \\ \hline \\ \hline b+1 \\ \hline \end{array} \stackrel{B3}{=} \begin{array}{|c|} \hline \pi \\ \hline \bullet \\ \hline a+1 \quad b+1 \\ \hline \end{array} \stackrel{S1}{=} \begin{array}{|c|} \hline \pi \\ \hline \\ \hline (a+1)(b+1) \\ \hline \end{array} \stackrel{Sca}{=} \begin{array}{|c|} \hline (a+1)(b+1)-1 \\ \hline \end{array} \quad \square$

Corollary 3.4 $\bullet \begin{array}{|c|} \hline \frac{-1}{2} \\ \hline \end{array} = \begin{array}{|c|} \hline \vdots \\ \hline \end{array} \quad (Siv)$

Proof: $\bullet \begin{array}{|c|} \hline \frac{-1}{2} \\ \hline \end{array} = \begin{array}{|c|} \hline 1 \\ \hline \\ \hline \frac{-1}{2} \\ \hline \end{array} \stackrel{Sml}{=} \begin{array}{|c|} \hline 0 \\ \hline \end{array} \stackrel{Zos}{=} \begin{array}{|c|} \hline \vdots \\ \hline \end{array} \quad \square$

Lemma 3.5 $\begin{array}{|c|} \hline \square \\ \hline \\ \hline \square \\ \hline \end{array} = \bullet \quad (H2)$

Proof: $\begin{array}{|c|} \hline \square \\ \hline \\ \hline \square \\ \hline \end{array} \stackrel{S2}{=} \begin{array}{|c|} \hline \bullet \\ \hline \\ \hline \bullet \\ \hline \end{array} \stackrel{Siv}{=} \begin{array}{|c|} \hline \frac{-1}{2} \\ \hline \\ \hline \bullet \\ \hline \end{array} \stackrel{H}{=} \begin{array}{|c|} \hline \bullet \\ \hline \\ \hline \bullet \\ \hline \end{array} \stackrel{S2}{=} \begin{array}{|c|} \hline \bullet \\ \hline \end{array} \quad \square$

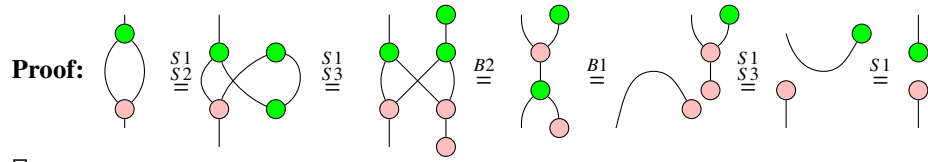
Lemma 3.6 Suppose $\tau \in \{0, \pi\}$. Then $\begin{array}{|c|} \hline \vdots \\ \hline \bullet \\ \hline \vdots \\ \hline \end{array} \stackrel{n}{=} \begin{array}{|c|} \hline \tau \\ \hline \square \\ \hline \tau \\ \hline \end{array} \stackrel{m}{=} \begin{array}{|c|} \hline \tau \\ \hline \square \\ \hline \tau \\ \hline \end{array} \quad (H)$

Proof: The proof directly follows from the definition of pink nodes (H), (H2), (Siv) and (Sca). We also call this derived equality (H), since together with the definition of pink nodes (H) they compose the colour-change rule. \square

Lemma 3.7 Suppose $\tau, \sigma \in \{0, \pi\}$. Then $\begin{array}{|c|} \hline \tau \\ \hline \vdots \\ \hline \sigma \\ \hline \vdots \\ \hline \end{array} = \begin{array}{|c|} \hline \tau+\sigma \\ \hline \vdots \\ \hline \tau+\sigma \\ \hline \vdots \\ \hline \end{array} = \begin{array}{|c|} \hline \tau+\sigma \\ \hline \vdots \\ \hline \tau+\sigma \\ \hline \vdots \\ \hline \end{array} \quad (S1)$

Proof: The proof directly follows from (S1), (H), (H2) and (Siv). We also call this derived equality (S1), since together with the green version of (S1) they compose the spider fusion rule. \square

Lemma 3.8 [1] $\begin{array}{|c|} \hline \bullet \\ \hline \circlearrowleft \\ \hline \bullet \\ \hline \end{array} = \begin{array}{|c|} \hline \bullet \\ \hline \\ \hline \bullet \\ \hline \end{array} \quad (Hopf)$



□

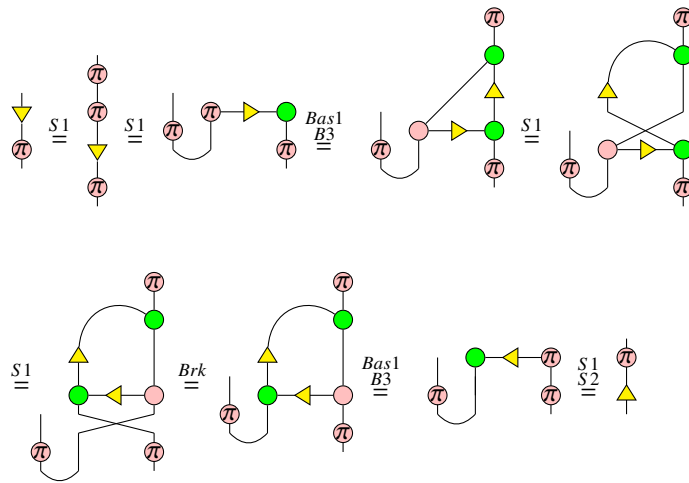
Lemma 3.9 [18] $\begin{array}{c} \bullet \\ \uparrow \\ \triangleleft^{-1} \end{array} = \begin{array}{c} \pi \\ \uparrow \end{array} (Bas1')$



□

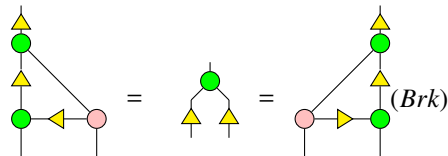
Lemma 3.10 [18] $\begin{array}{c} \nabla \\ \uparrow \\ \pi \end{array} = \begin{array}{c} \pi \\ \uparrow \\ \triangleleft \end{array}$

Proof:

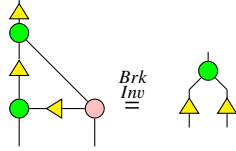


□

Lemma 3.11

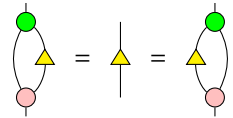


Proof:

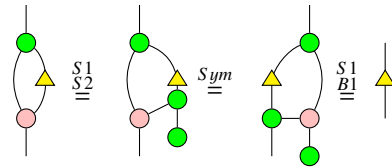


The second equality can be obtained via the symmetry of green and pink spiders. We call this derived equality (Brk) as well, since it is a variant of the (Brk). \square

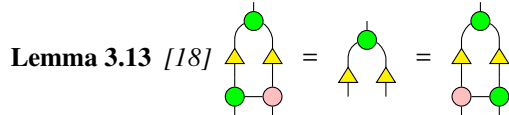
Lemma 3.12 [18]



Proof:

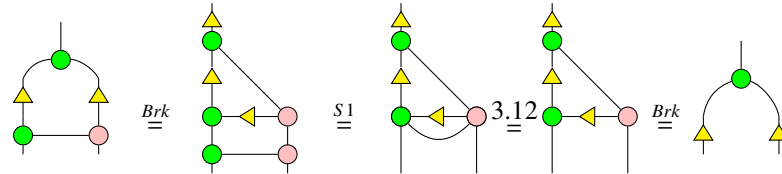


The second equality can be obtained via the symmetry of green and pink spiders. \square

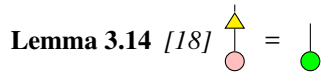


Lemma 3.13 [18]

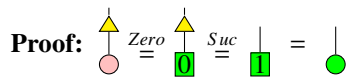
Proof:



The second equality can be obtained via the symmetry of green and pink spiders. \square



Lemma 3.14 [18]



Proof:

\square

Lemma 3.15

Proof:

□

Corollary 3.16

Lemma 3.17 [18]

(4)

Proof:

The other part can be obtained by the symmetry of green spider. □

Lemma 3.18 [18]

(5)

Proof:

The second equality can be obtained by the symmetry of green spider. □

Lemma 3.19 [1] $\pi = \text{[diagram]}$

Proof: $\text{[diagram]} \stackrel{Eu}{=} \text{[diagram]} \stackrel{S1}{=} \text{[diagram]} \stackrel{3.15}{=} \text{[diagram]} \stackrel{Suc}{=} \text{[diagram]} \stackrel{S1}{=} \pi$ □

Lemma 3.20 [1] Suppose $m \geq 0$. Then $\text{[diagram]} = \text{[diagram]}$ (Pic)

Proof:

$\text{[diagram]} \stackrel{3.19}{=} \text{[diagram]} \stackrel{B1}{=} \text{[diagram]} \stackrel{H}{=} \text{[diagram]} \stackrel{Ept}{=} \text{[diagram]}$

$\text{[diagram]} \stackrel{S1}{=} \text{[diagram]} \stackrel{B2}{=} \text{[diagram]} \stackrel{B3}{=} \text{[diagram]} \stackrel{S1}{=} \text{[diagram]}$

The general case follows directly from the above two special cases. □

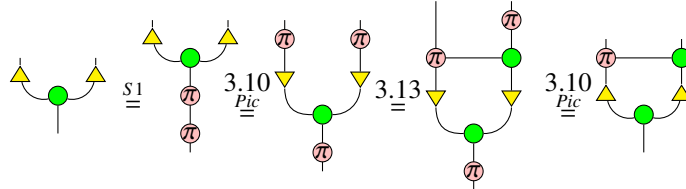
Corollary 3.21 $\text{[diagram]} = \text{[diagram]}$ (Pic)

Proof: It follows directly from Lemma 3.20 and the colour-change rule (H). We call this equality (Pic) as well. □

Corollary 3.22

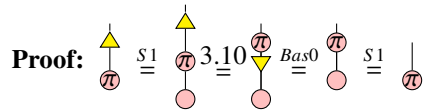
$\text{[diagram]} = \text{[diagram]} = \text{[diagram]}$ (Brk1') (6)

Proof:



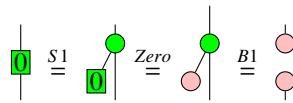
The second equality can be proved by symmetry of green spider. □

Lemma 3.23 =



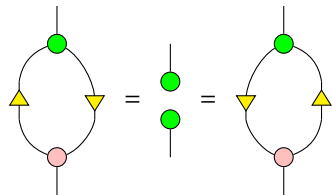
Lemma 3.24 [18] = (Zero')

Proof:

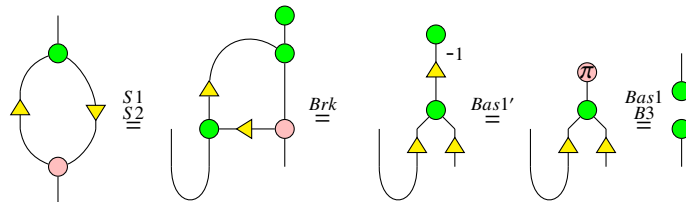


□

Lemma 3.25 [18]

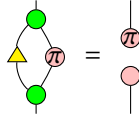


Proof:

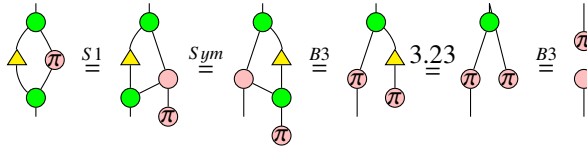


□

Lemma 3.26

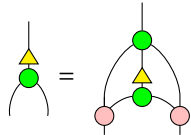


Proof:

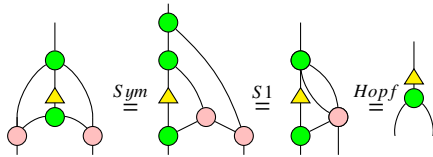


□

Lemma 3.27

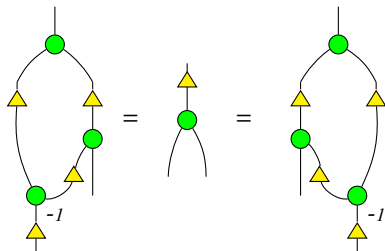


Proof:

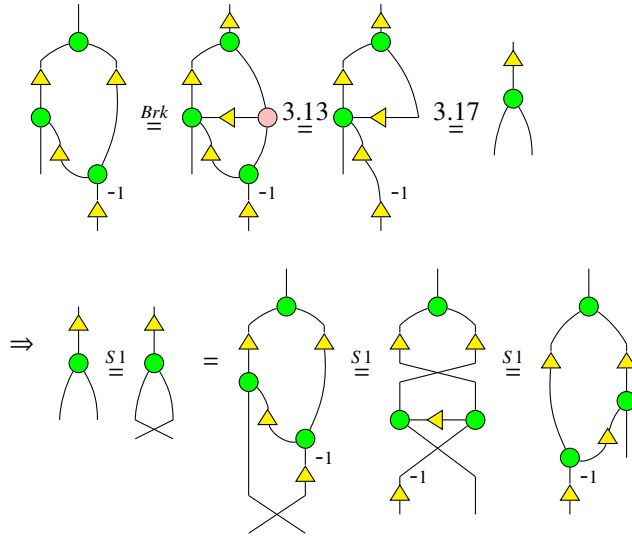


□

Lemma 3.28 [18]

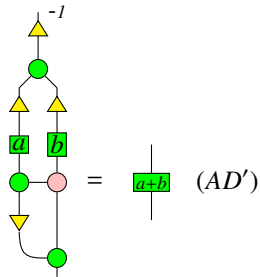


Proof:

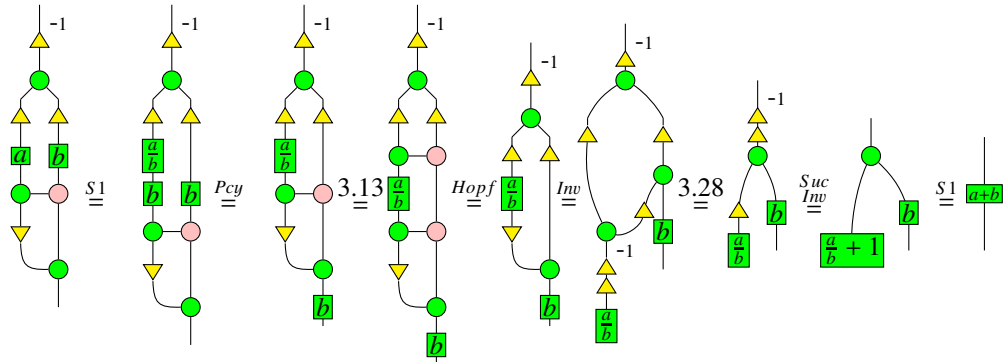


□

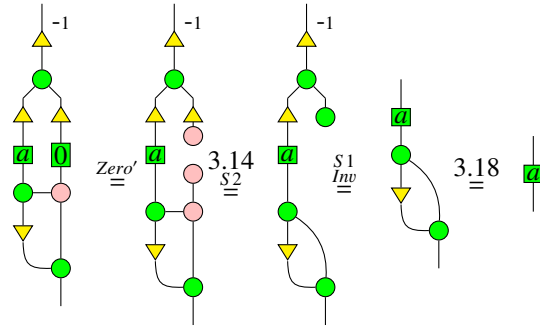
Lemma 3.29 [18]



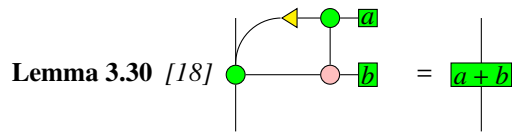
Proof: If $b \neq 0$, then



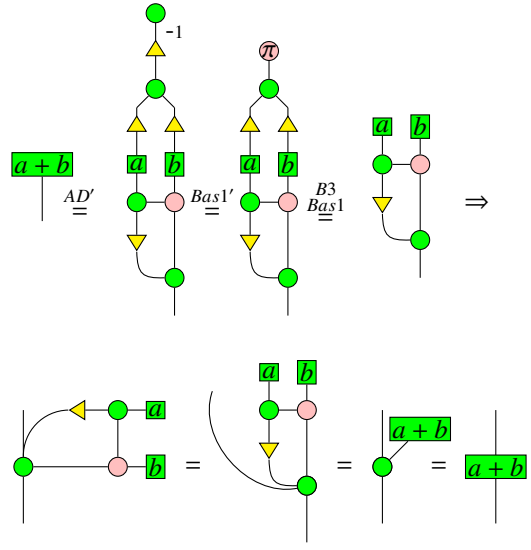
If $b = 0$, then



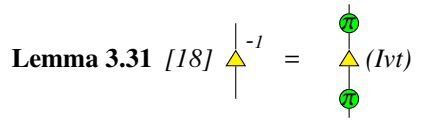
□



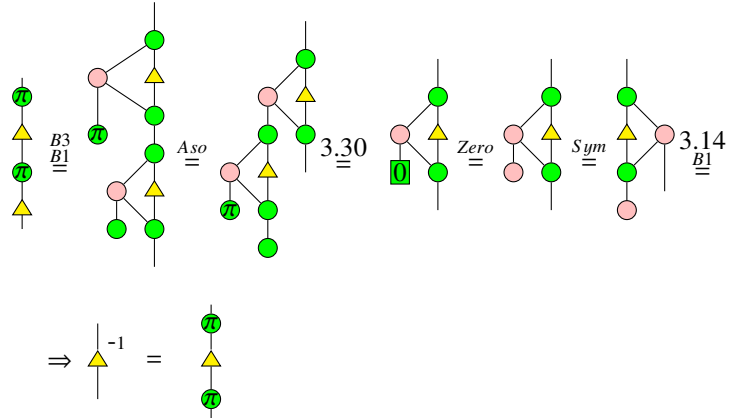
Proof:



□



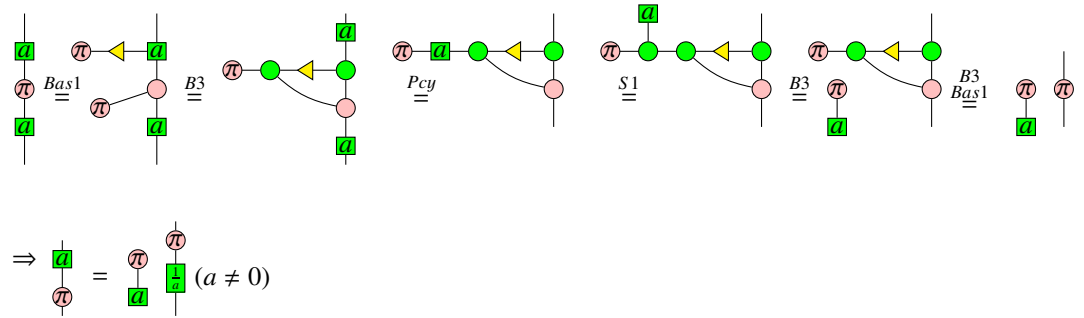
Proof:



□

Lemma 3.32 [18] $\begin{array}{c} \pi \\ \pi \end{array} = \begin{array}{c} \pi \\ \pi \\ \pi \end{array}$

Proof:

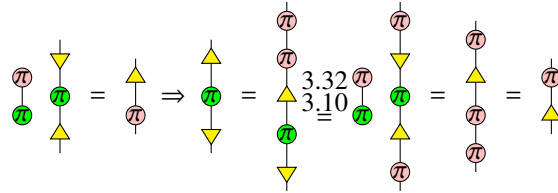
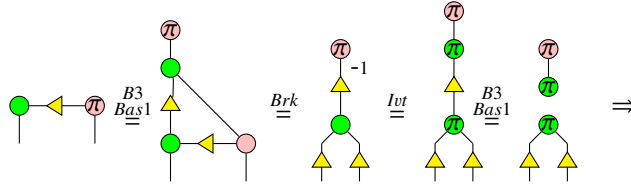


The proof completes when setting $a = e^{i\alpha}$.

□

Lemma 3.33 [18] $\begin{array}{c} \triangle \\ \pi \\ \triangle \end{array} = \begin{array}{c} \pi \\ \triangle \end{array}$

Proof:

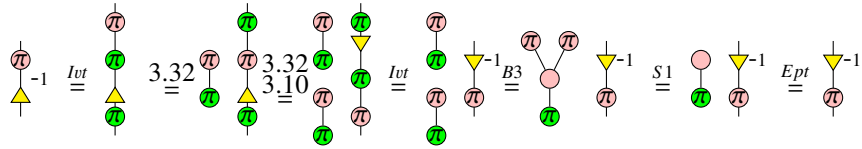


□

Corollary 3.34 [18]

$$\begin{array}{c} \pi \\ \triangleleft^{-1} \\ \triangle \\ \pi \end{array} = \begin{array}{c} \triangle \\ \pi \end{array} \quad (7)$$

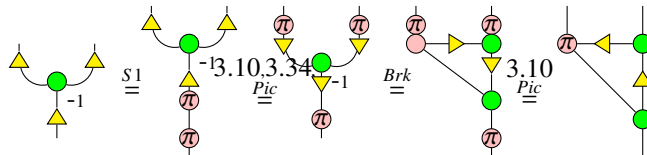
Proof:



□

Lemma 3.35 [18]

Proof:



The second equality can be obtained via symmetry.

□

Lemma 3.36 [18]

$$= \quad (8)$$

Proof:

$$\stackrel{3.10}{=} \stackrel{Pic}{=} \stackrel{3.12}{=} \quad \square$$

Lemma 3.37 [18]

$$=$$

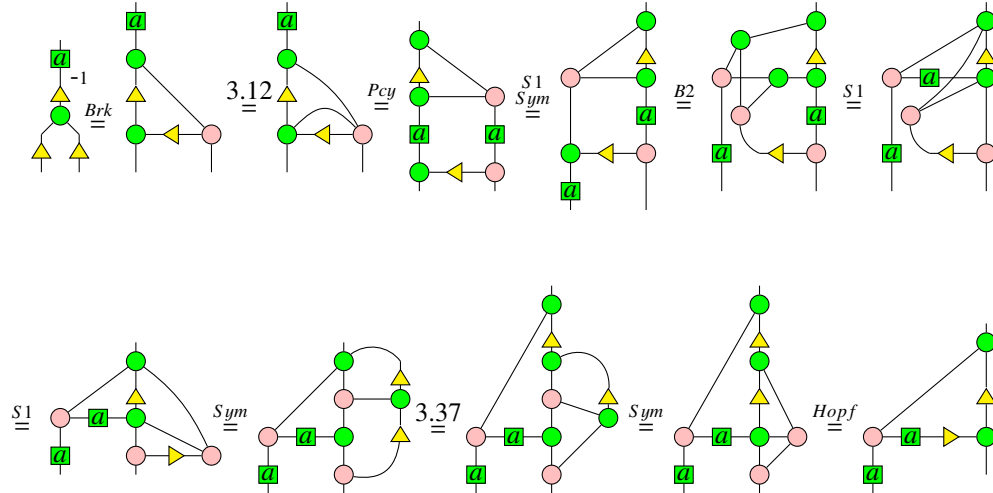
Proof:

$$\stackrel{B1}{\stackrel{Sym}{\equiv}} \stackrel{Aso}{\equiv} \stackrel{B1}{\equiv} \stackrel{Sym}{\equiv} \quad \square$$

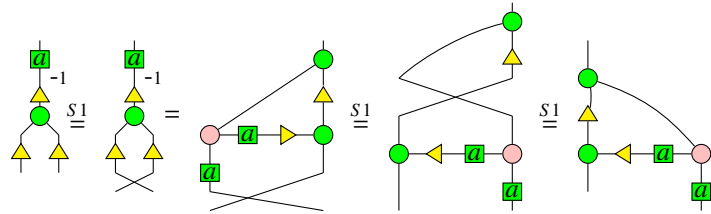
Lemma 3.38 [18]

$$\stackrel{(Brkp)}{=} \quad \square$$

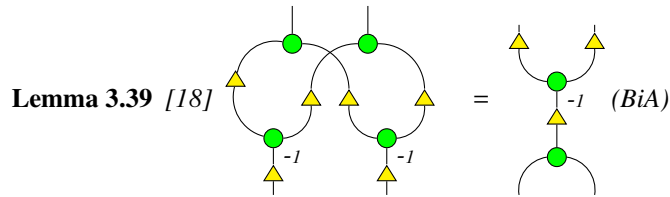
Proof:



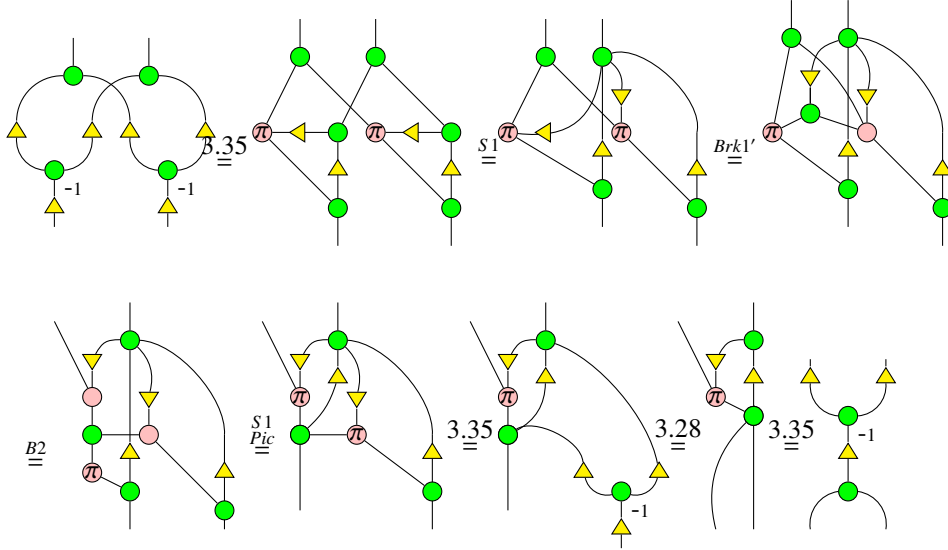
Therefore,



□

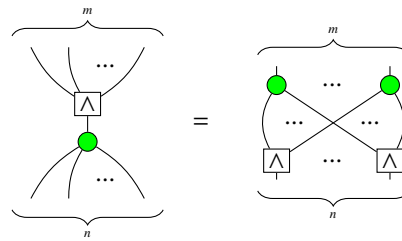


Proof:

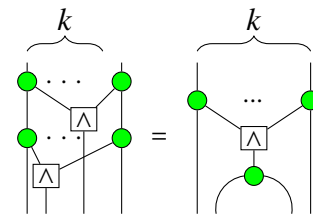


□

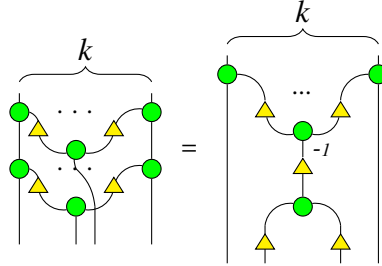
Corollary 3.40 [18]



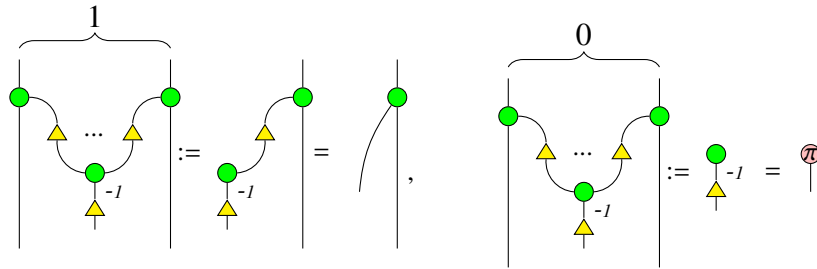
Corollary 3.41 ([11]) *For any $k \geq 0$, we have*



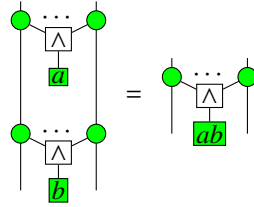
or equivalently,



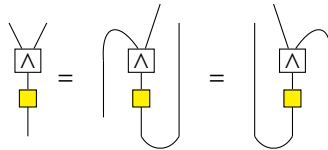
where



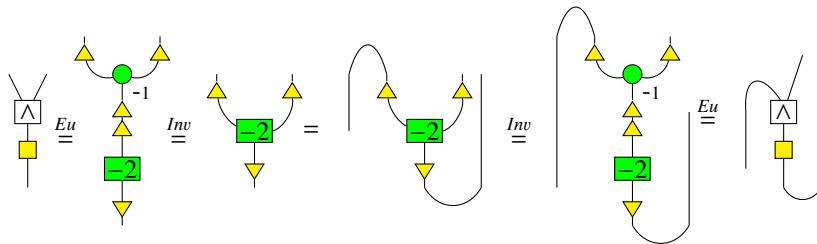
Corollary 3.42



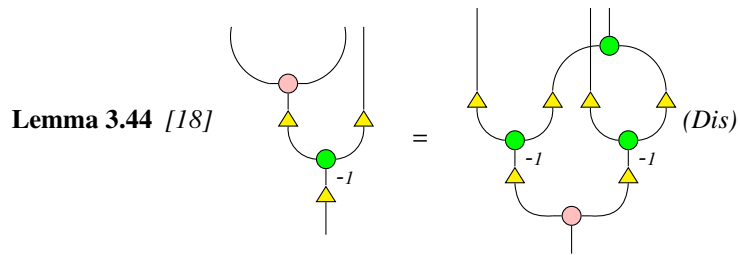
Lemma 3.43 [18]



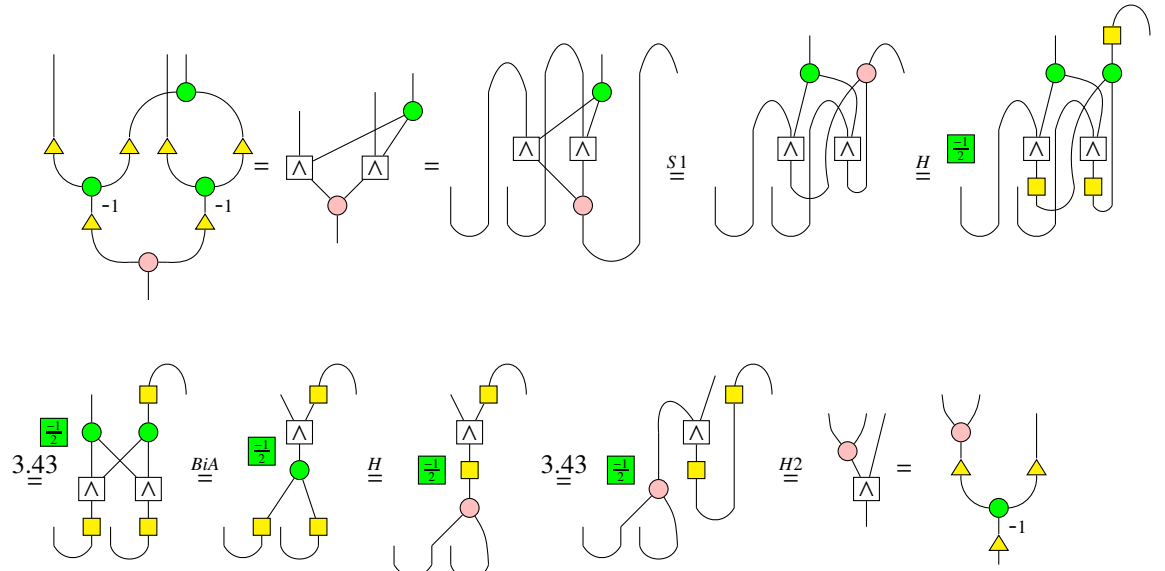
Proof:



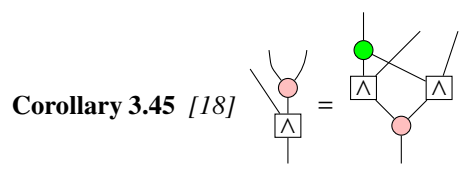
The second equality can be obtained by symmetry. □



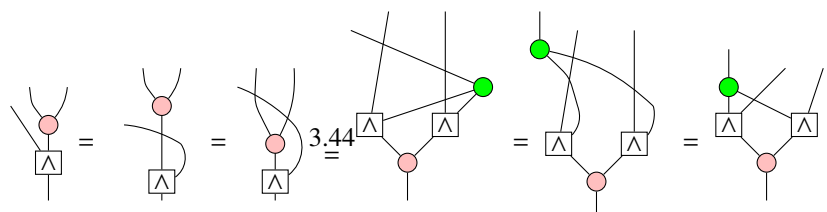
Proof:



□



Proof:

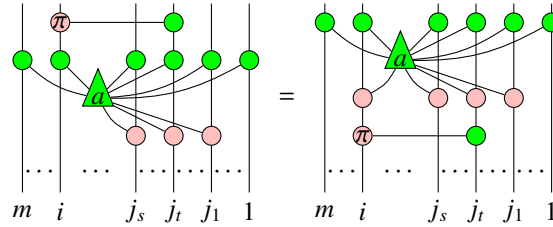


□

4 Newly derivable equalities

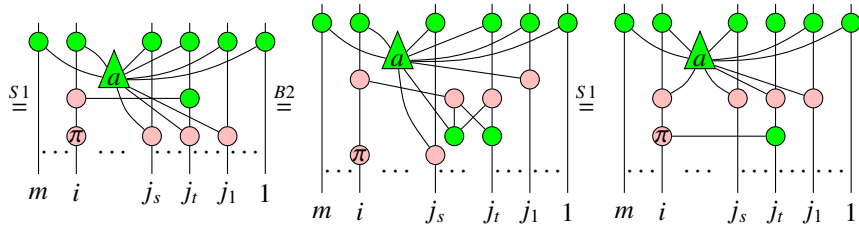
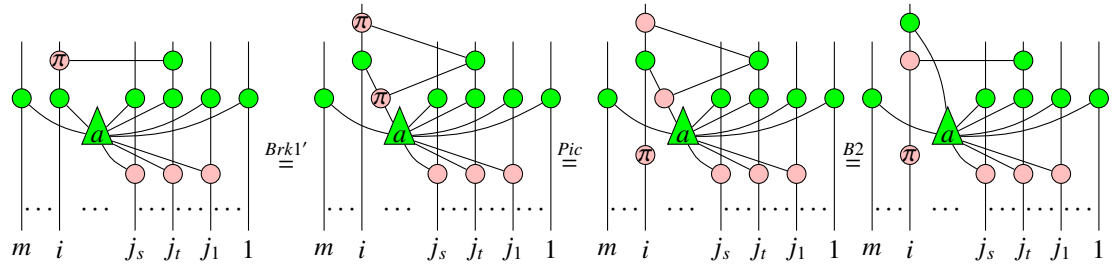
In this section, we derive all the equalities needed for the proof of completeness while relatively new to previous results.

Proposition 4.1 *Let $i, j_1, \dots, j_t, \dots, j_s \in \{1, \dots, m\}, i \notin \{j_1, \dots, j_t, \dots, j_s\}$. Then we have*



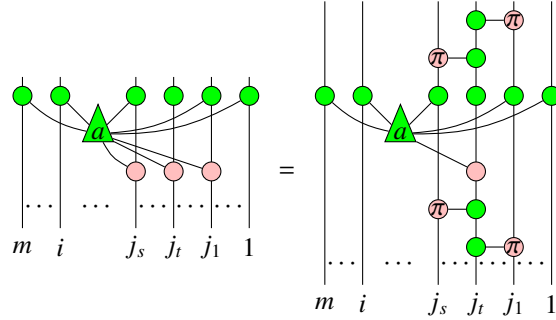
where the node a is connected to $j_1, \dots, j_t, \dots, j_s$ via pink nodes.

Proof:

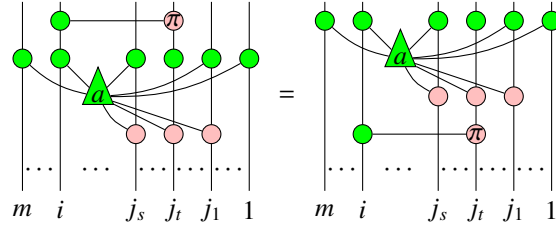


□

Corollary 4.2

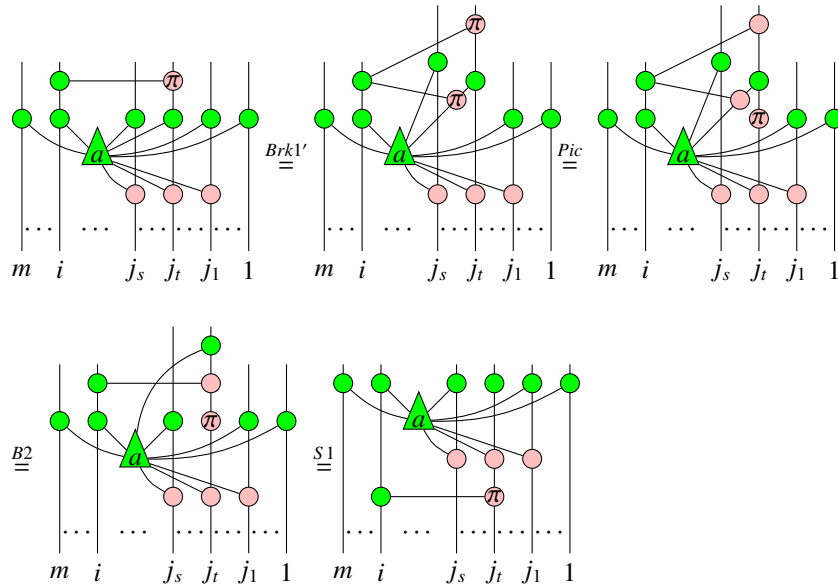


Proposition 4.3 Let $i, j_1, \dots, j_t, \dots, j_s \in \{1, \dots, m\}, i \notin \{j_1, \dots, j_t, \dots, j_s\}$. Then we have



where the node a is connected to $j_1, \dots, j_t, \dots, j_s$ via pink nodes.

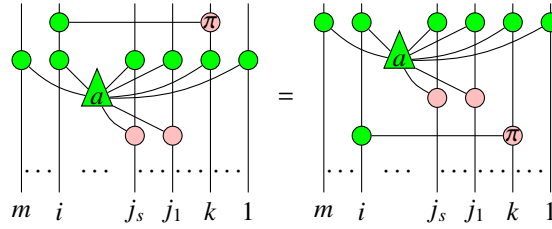
Proof:



□

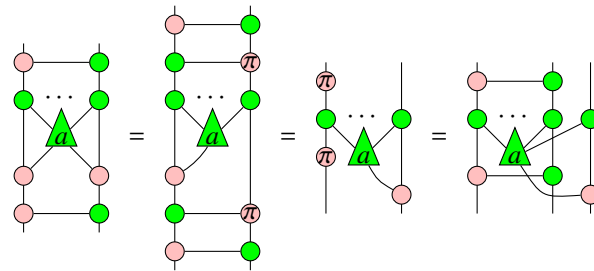
Similarly, we have

Proposition 4.4 Let $i, k, j_1, \dots, j_s \in \{1, \dots, m\}, i, k \notin \{j_1, \dots, j_s\}$. Then we have



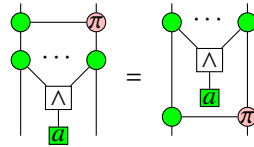
where the node a is connected to j_1, \dots, j_s via pink nodes.

Corollary 4.5

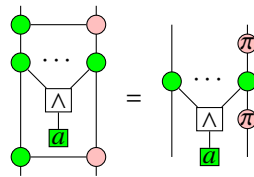


In the same way, we have

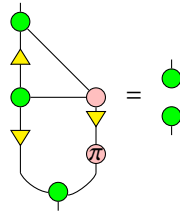
Proposition 4.6



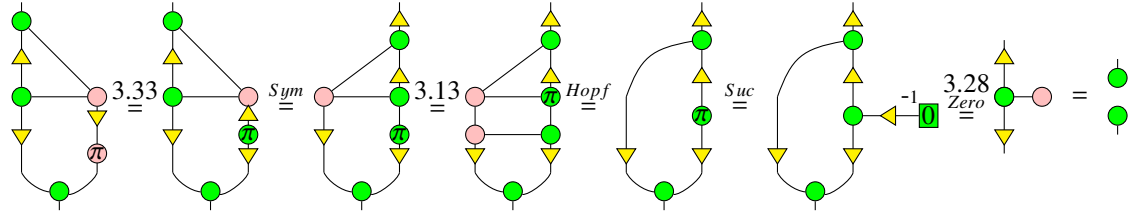
Corollary 4.7



Lemma 4.8

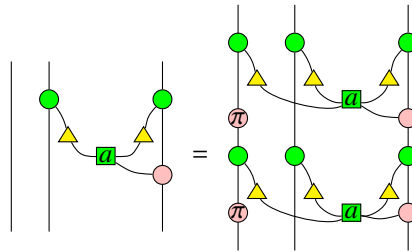


Proof:

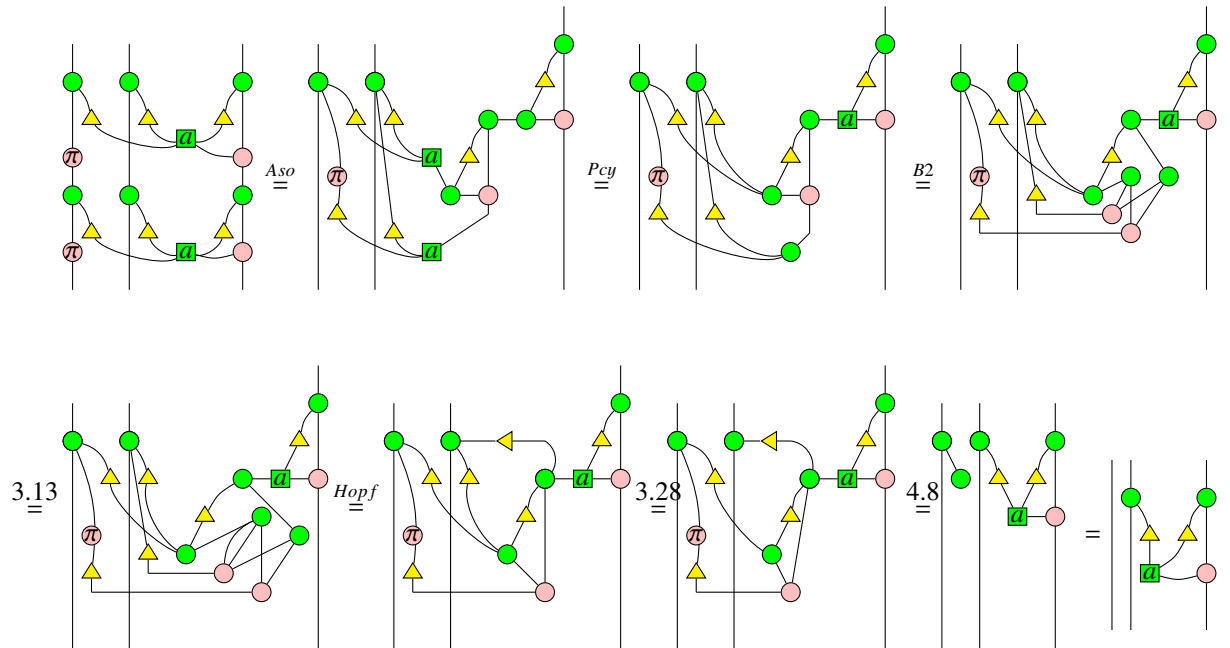


□

Lemma 4.9

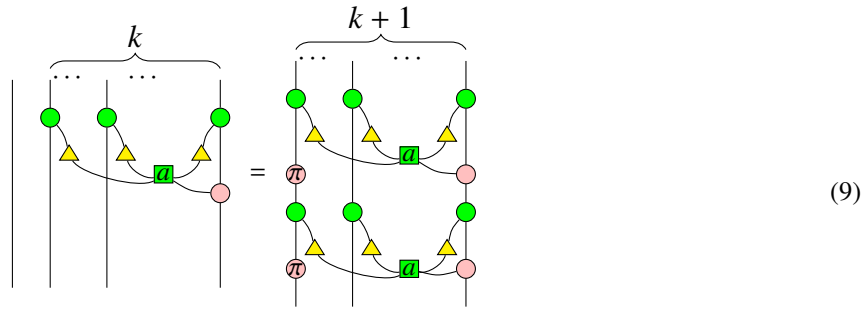


Proof:

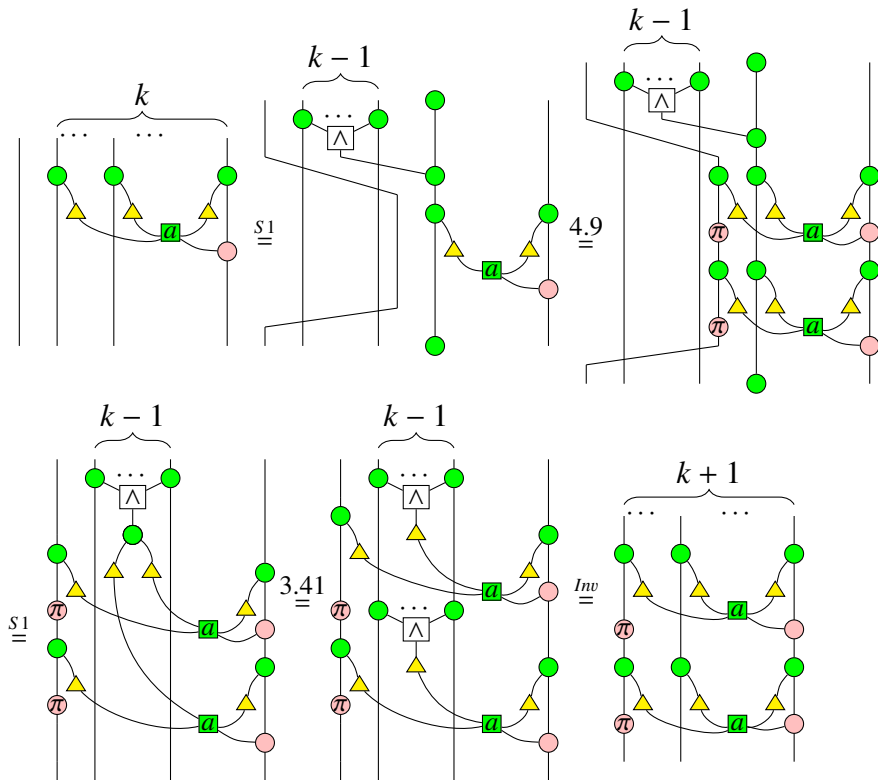


□

Proposition 4.10 For any $k \geq 1$, we have

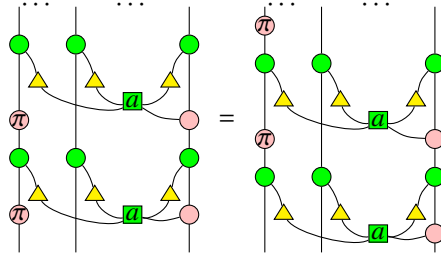


Proof:



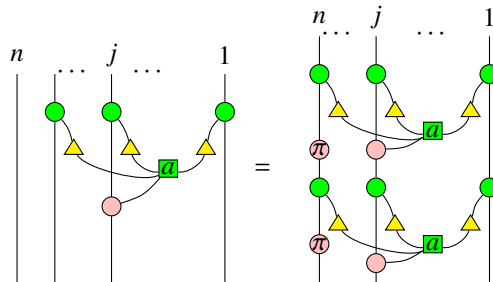
□

Corollary 4.11



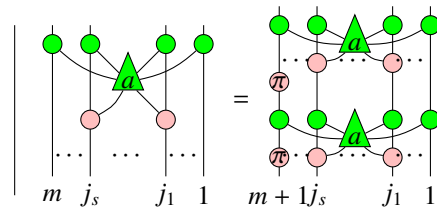
This can be immediately obtained by plugging pink π phase gates from the top and the bottom of the left-most line of diagrams on both sides of (9).

Corollary 4.12



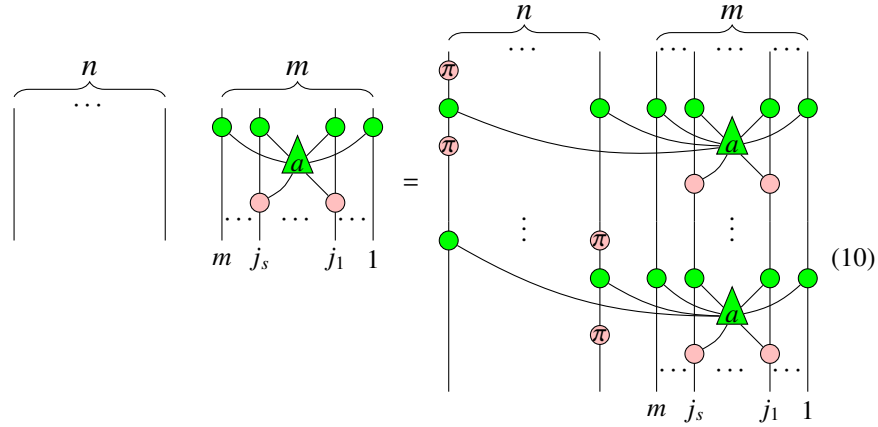
This can be obtained by swapping the 1-th and the j -th lines of diagrams on both side of (9).

Corollary 4.13



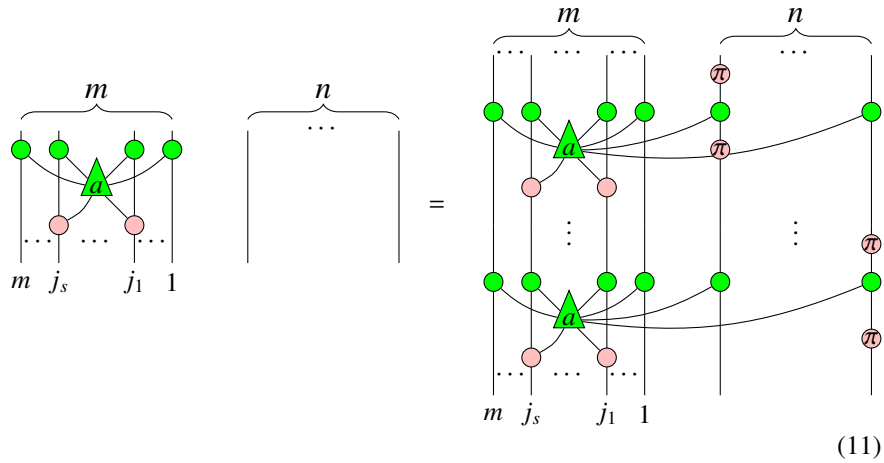
This follows directly from Proposition 4.10 and Corollary 4.2.

Corollary 4.14



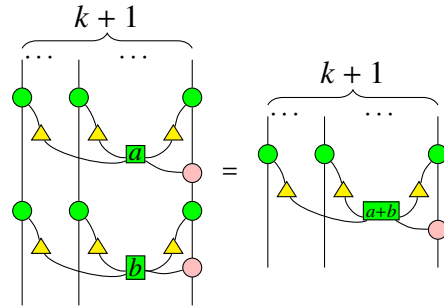
where on the RHD of (10), there are 2^n green triangles labeled by a on the right-most m wires, each green triangle is connected to the left-most n wires via green dots which are surrounded by k pairs of red π s with $0 \leq k \leq n$, and different green triangles have different distribution of pairs of red π s, that's why there are $\binom{n}{0} + \binom{n}{1} + \dots + \binom{n}{n} = 2^n$ green triangles labeled by a .

Corollary 4.15

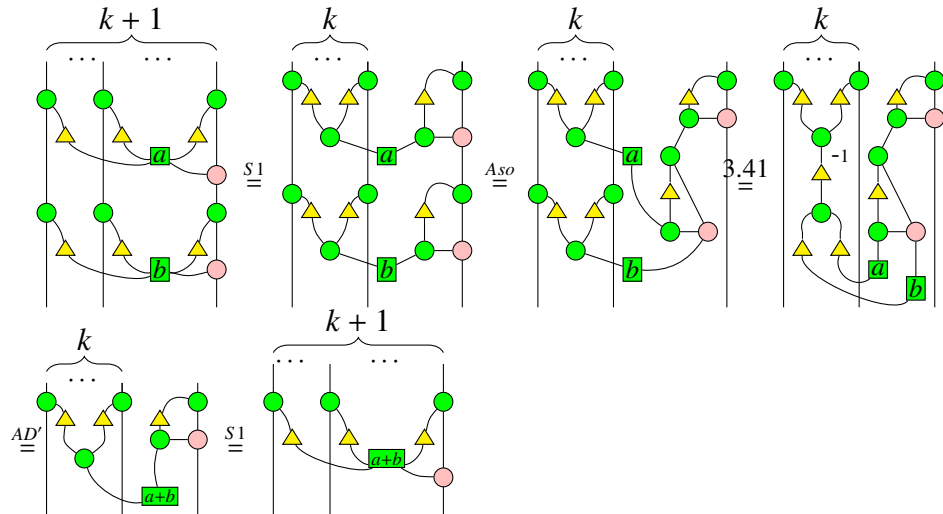


where on the RHD of (10), there are 2^n green triangles labeled by a on the left-most m wires, each green triangle is connected to the right-most n wires via green dots which are surrounded by k pairs of red π s with $0 \leq k \leq n$, and different green triangles have different distribution of pairs of red π s, that's why there are $\binom{n}{0} + \binom{n}{1} + \dots + \binom{n}{n} = 2^n$ green triangles labeled by a .

Proposition 4.16 For any $k \geq 1$, we have

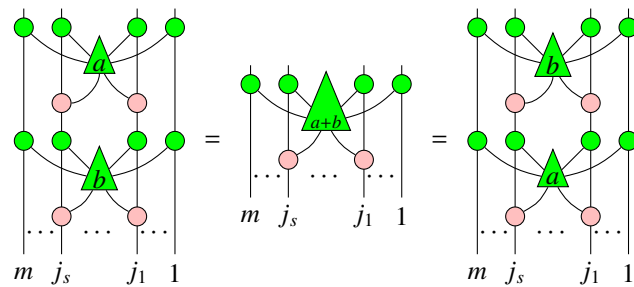


Proof:

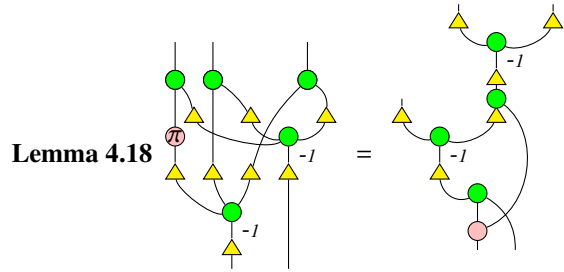


□

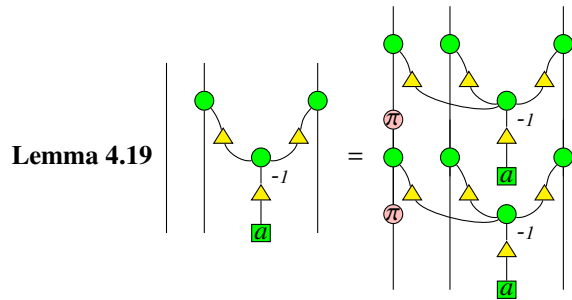
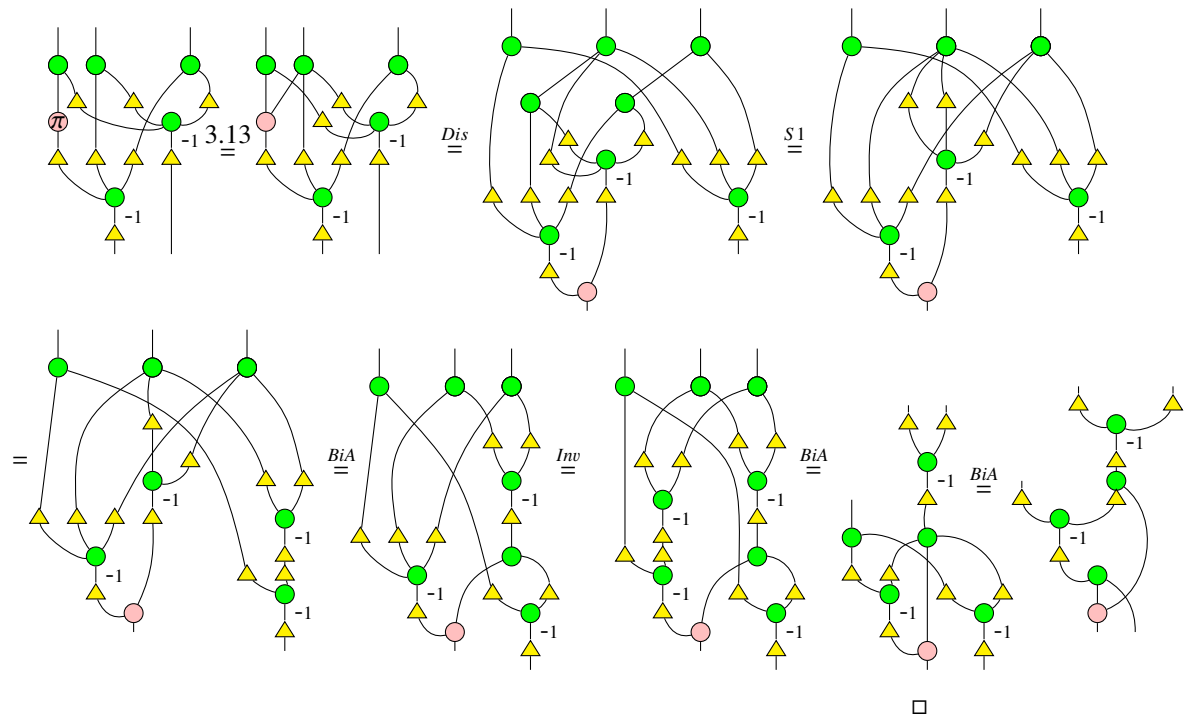
Corollary 4.17



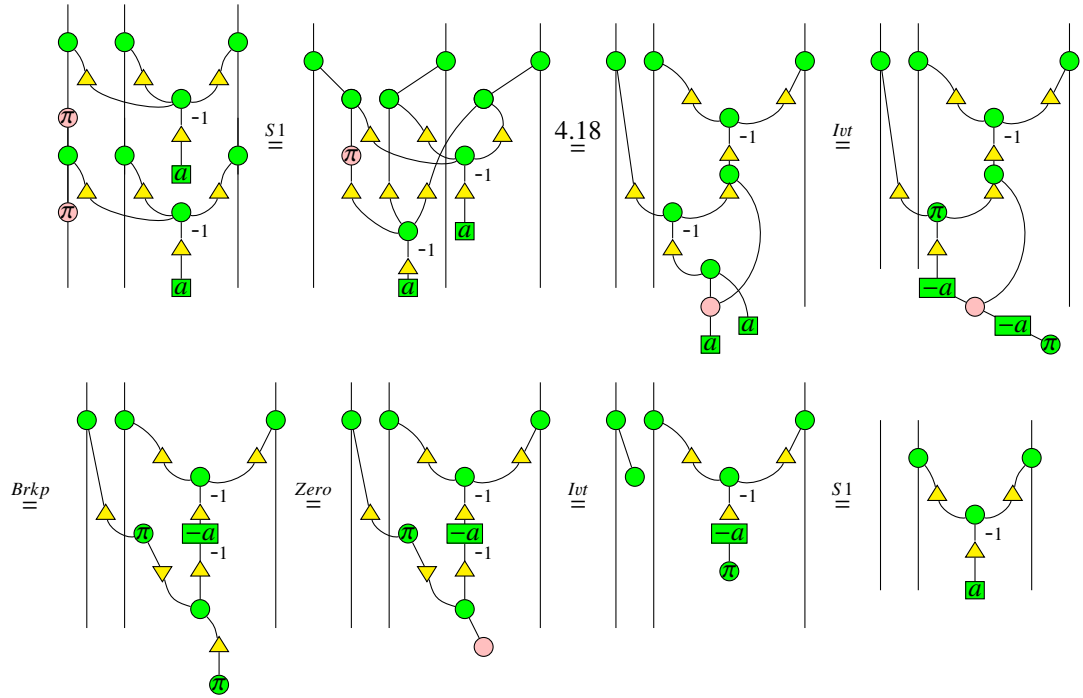
This can be directly obtained from Proposition 4.16 and Corollary 4.2.



Proof:

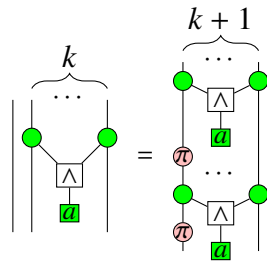


Proof:

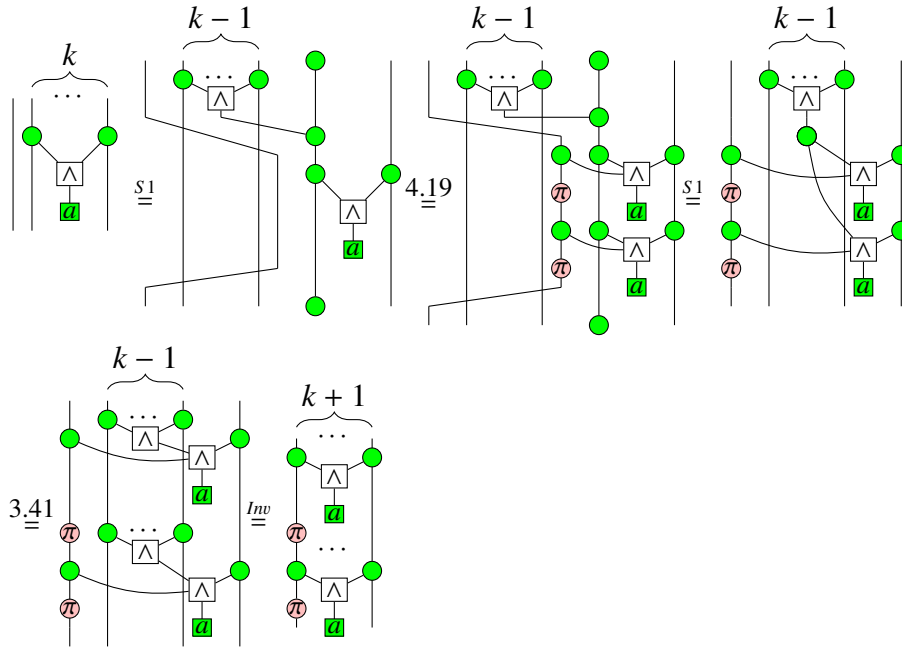


□

Proposition 4.20 For any $k \geq 1$, we have

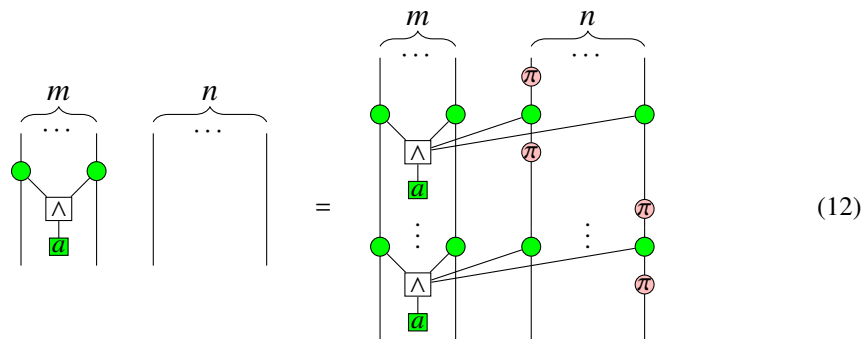


Proof:



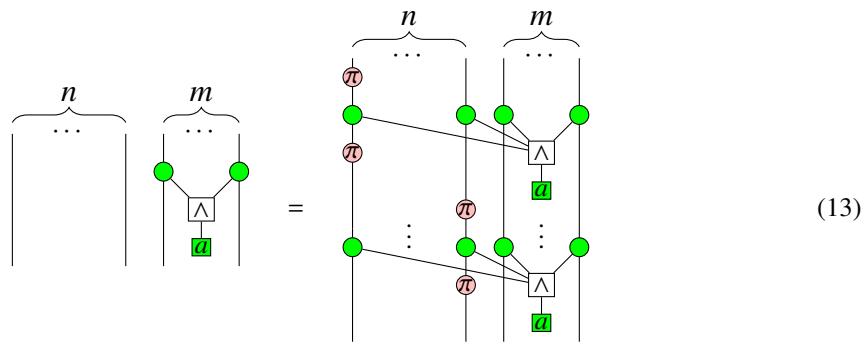
□

Corollary 4.21

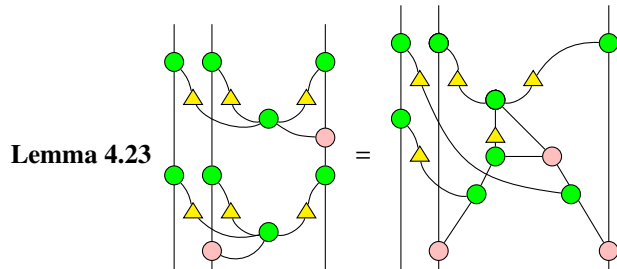


where on the RHD of (12), there are 2^n AND gates on the left-most m wires, each AND gate is accompanied by k pairs of red π s on the left-most n wires with $0 \leq k \leq n$, and different AND gates have different distribution of pairs of red π s, that's why there are $\binom{n}{0} + \binom{n}{1} + \dots + \binom{n}{n} = 2^n$ AND gates.

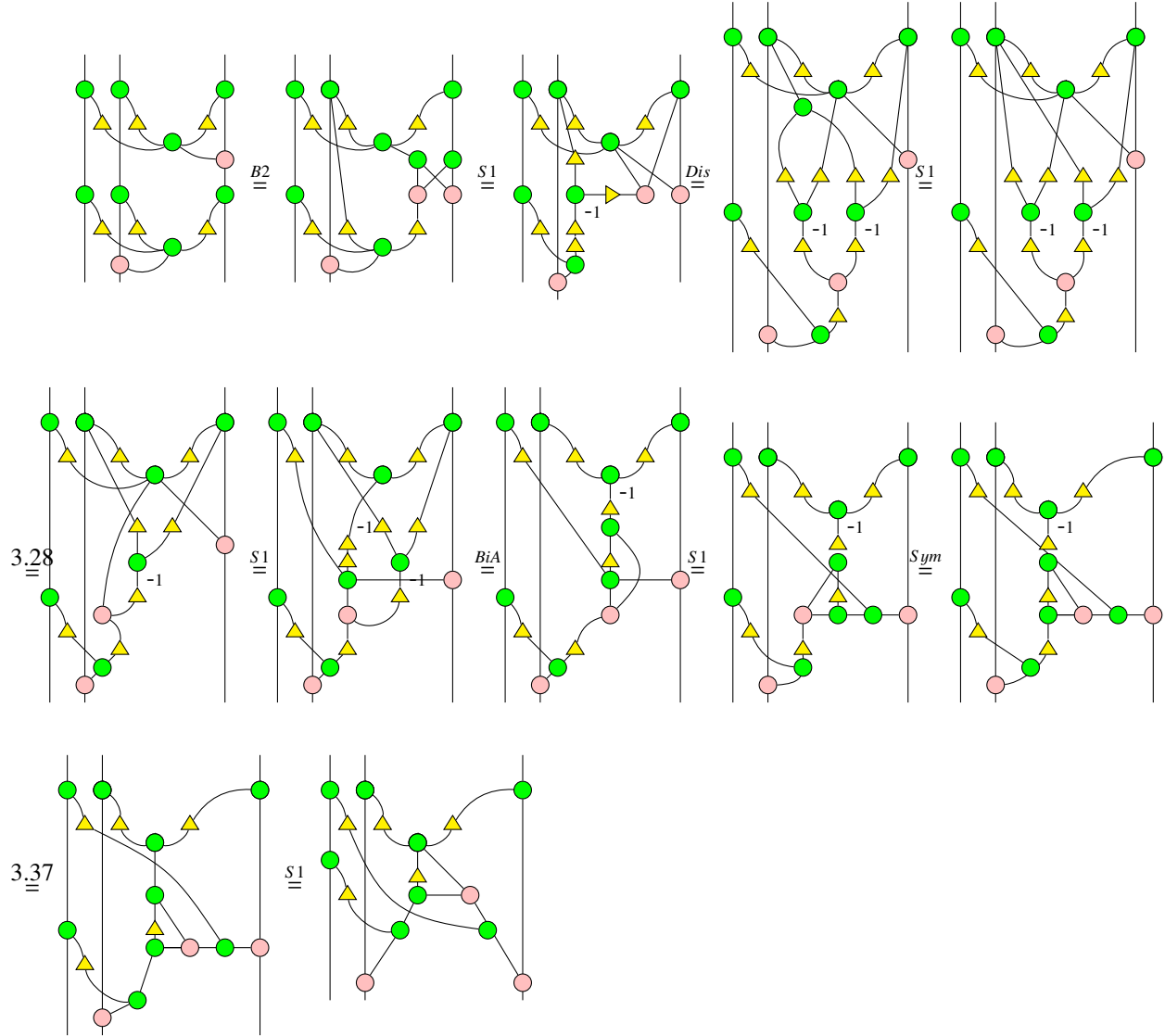
Corollary 4.22



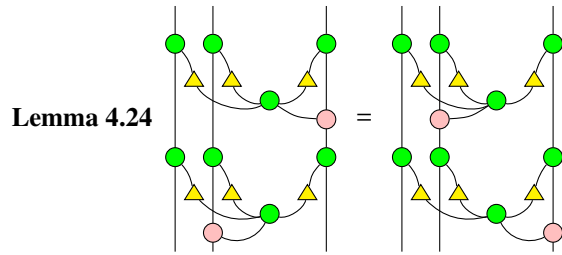
where on the RHD of (13), there are 2^n AND gates on the right-most m wires, each AND gate is accompanied by k pairs of red π s on the left-most n wires with $0 \leq k \leq n$, and different AND gates have different distribution of pairs of red π s, that's why there are $\binom{n}{0} + \binom{n}{1} + \dots + \binom{n}{n} = 2^n$ AND gates.



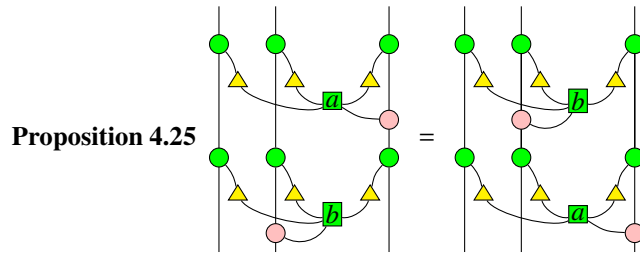
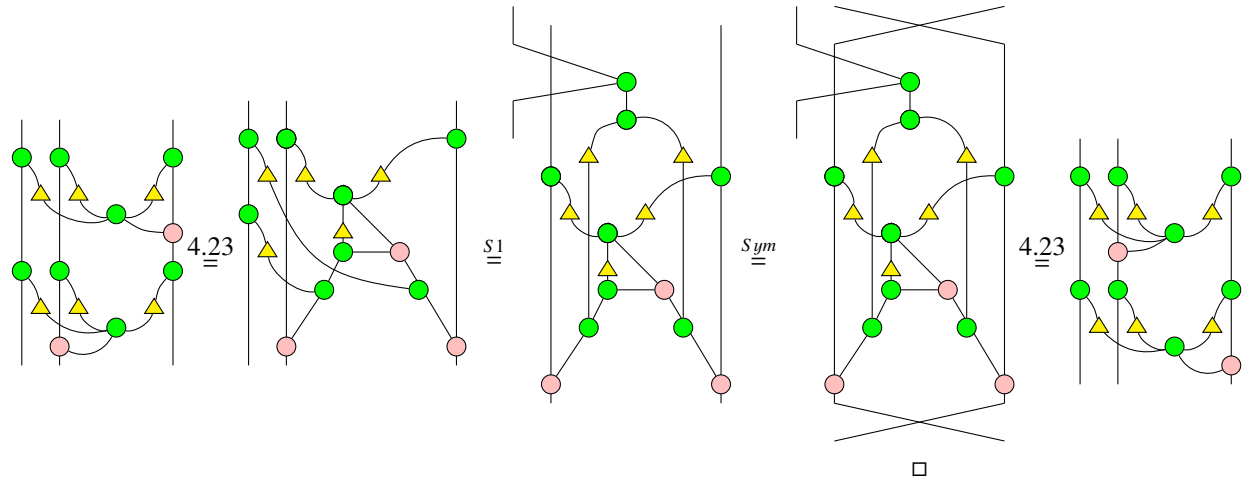
Proof:



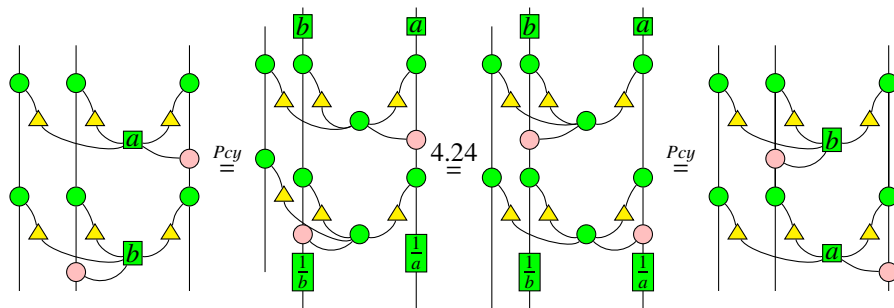
□



Proof:

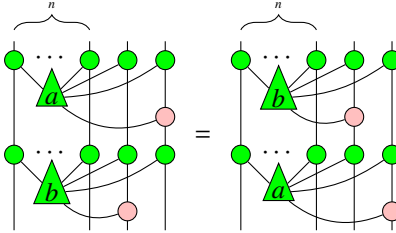


Proof: If $a = 0$ or $b = 0$, then the equality holds trivially. Now we assume $ab \neq 0$. Then

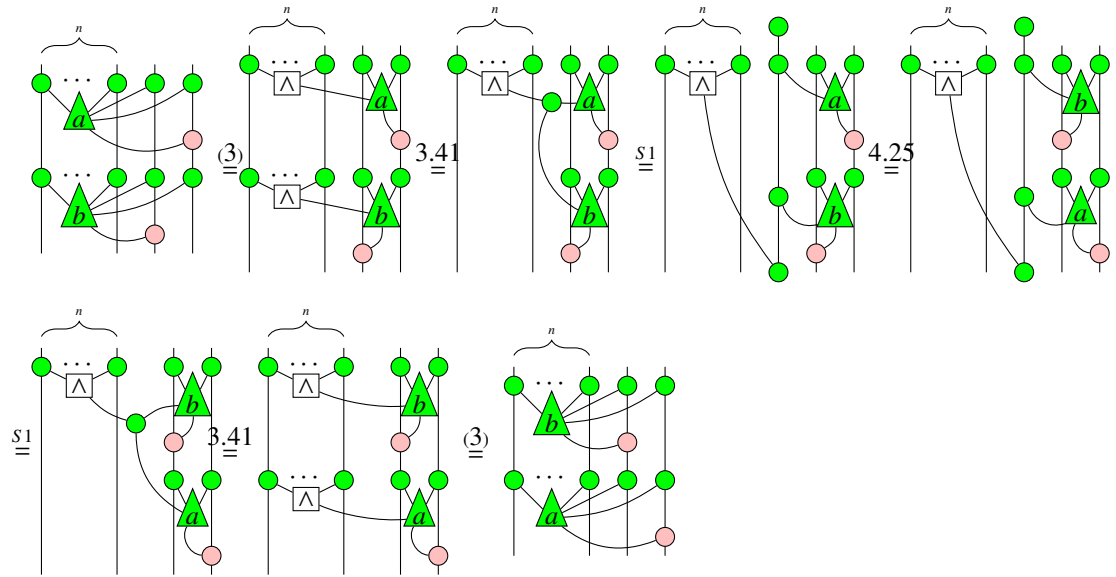


□

Proposition 4.26 *Let $n \geq 0$. Then we have*

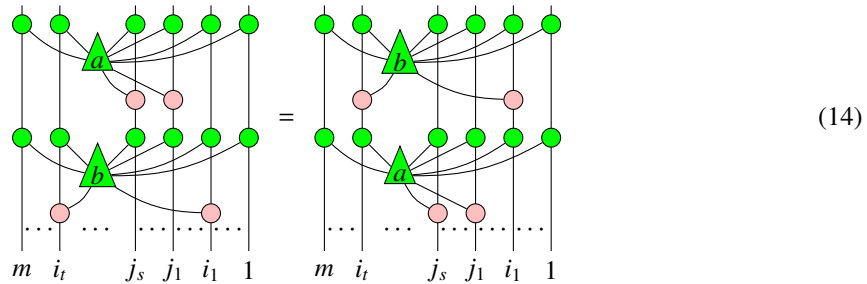


Proof:

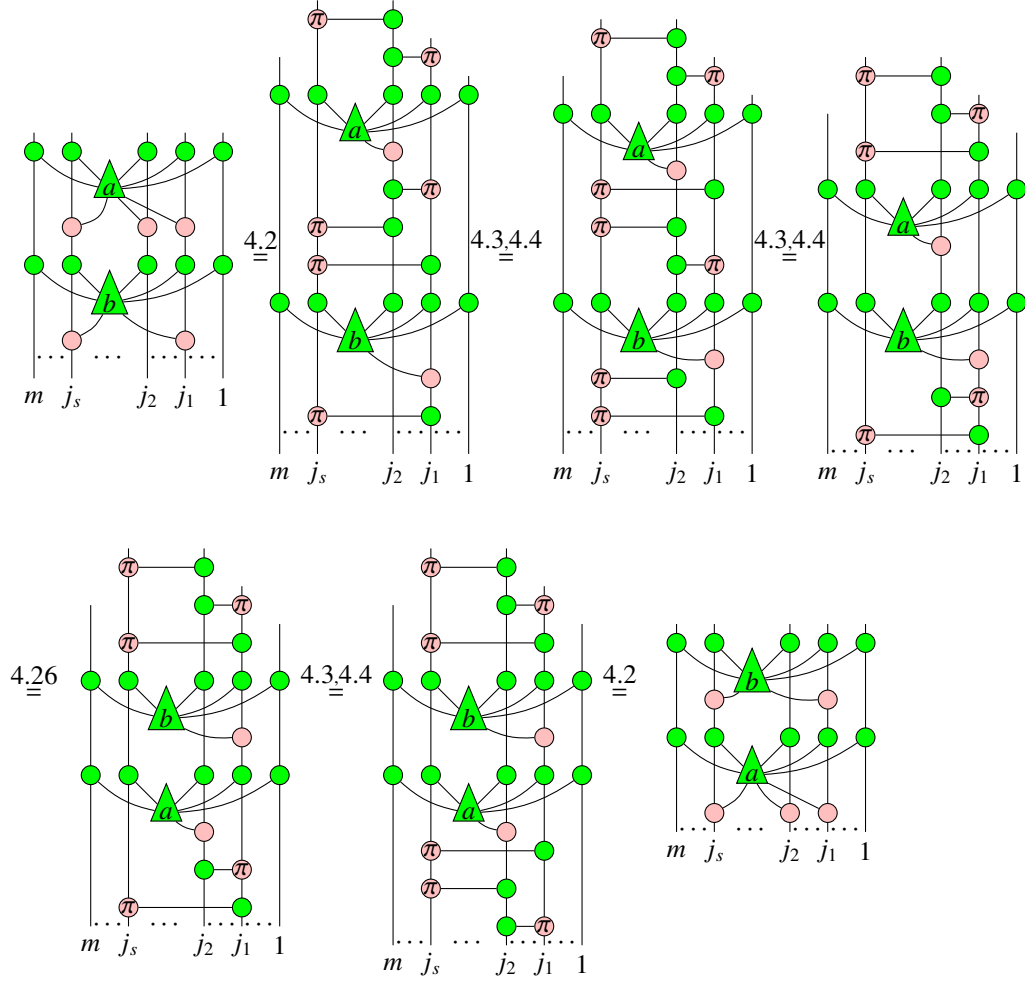


□

Proposition 4.27 *Assume that node a is connected to j_1, \dots, j_s via pink nodes and node b is connected to i_1, \dots, i_t via pink nodes, where $i_1, \dots, i_t, j_1, \dots, j_s \in \{1, \dots, m\}$, and $\{i_1, \dots, i_t\} \neq \emptyset, \{j_1, \dots, j_s\} \neq \emptyset$. Then we have*

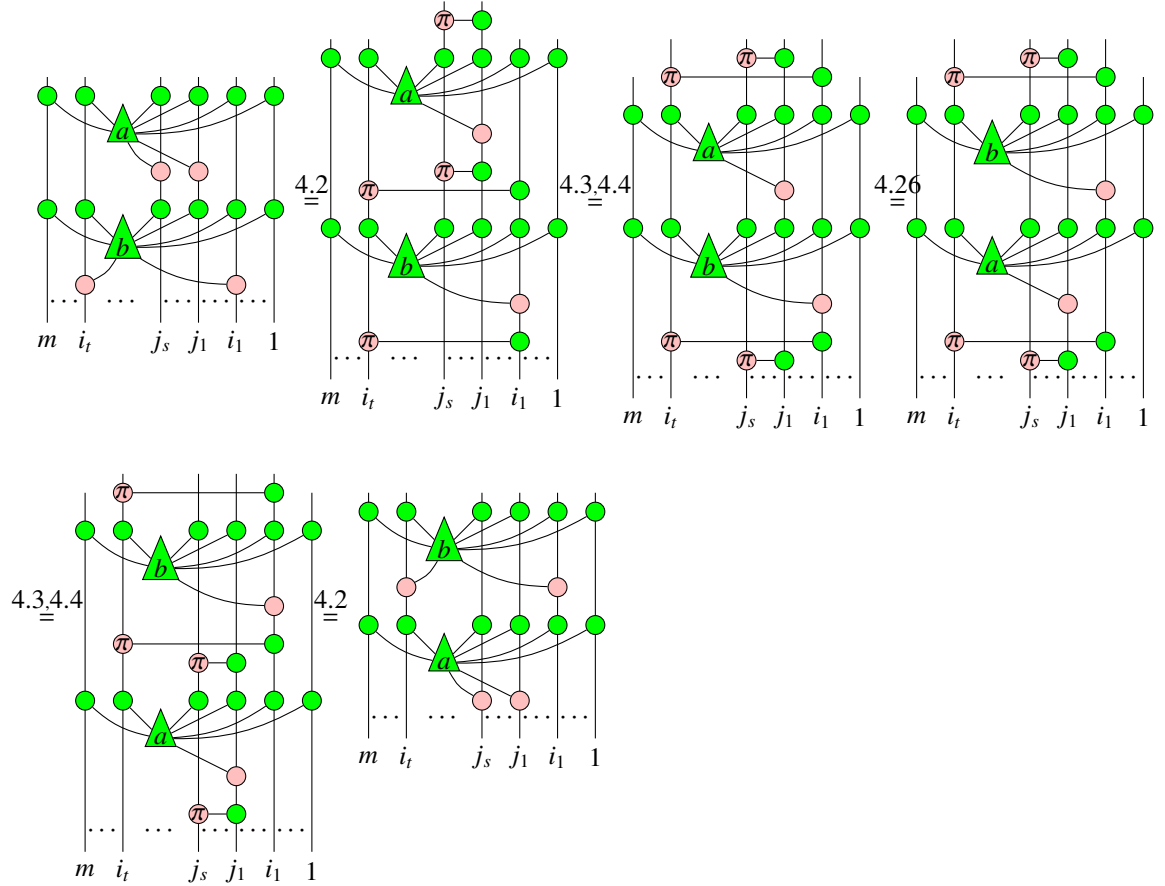


Proof: If $\{i_1, \dots, i_t\} = \{j_1, \dots, j_s\}$, then (14) follows directly from Corollary 4.17. Below we assume that $\{i_1, \dots, i_t\} \neq \{j_1, \dots, j_s\}$. If $\{i_1, \dots, i_t\} \subseteq \{j_1, \dots, j_s\}$, then we assume w.l.o.g. that $i_1 = j_1, i_t = j_s, j_2 \notin \{i_1, \dots, i_t\}$, then we have



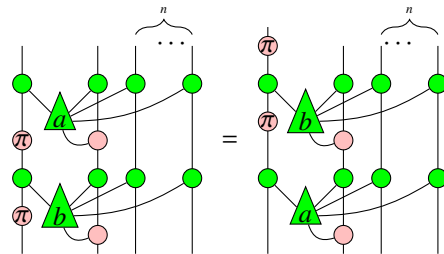
If symmetrically $\{j_1, \dots, j_s\} \subseteq \{i_1, \dots, i_t\}$, then it can be proved similarly as the last case. If $\{i_1, \dots, i_t\} \not\subseteq \{j_1, \dots, j_s\}$ and $\{j_1, \dots, j_s\} \not\subseteq \{i_1, \dots, i_t\}$, then we assume w.l.o.g.

that $j_1 \notin \{i_1, \dots, i_t\}, i_1 \notin \{j_1, \dots, j_s\}$. Then we have

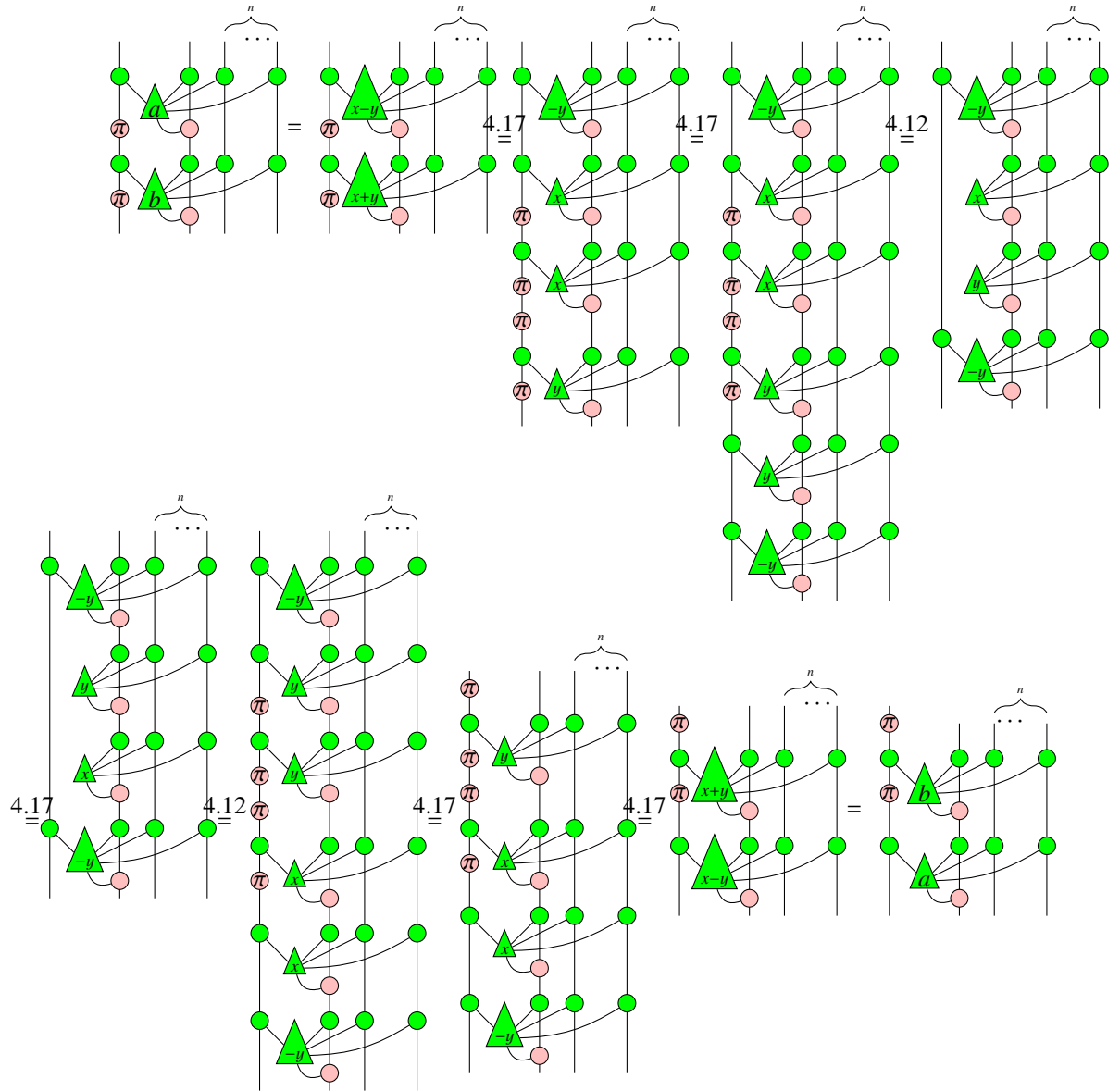


□

Proposition 4.28 Assume that $n \geq 0$. Then

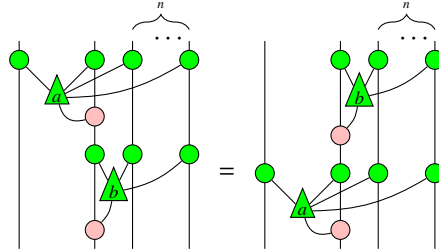


Proof: Let $x = \frac{a+b}{2}$, $y = \frac{b-a}{2}$. Then $a = x - y$, $b = x + y$.



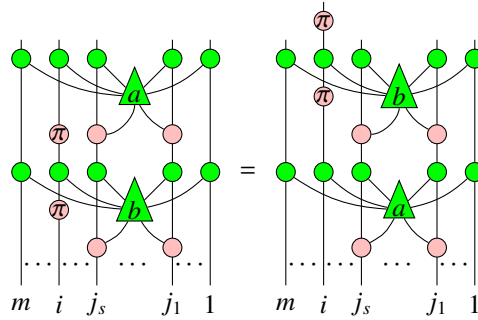
□

Corollary 4.29 Assume that $n \geq 0$. Then



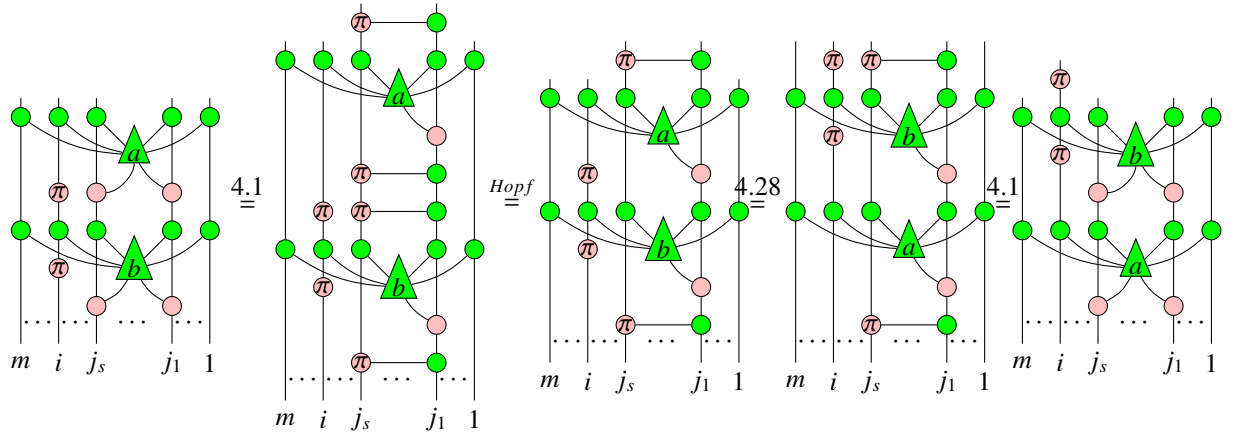
This follows directly from Proposition 4.28 and Corollary 4.12.

Corollary 4.30

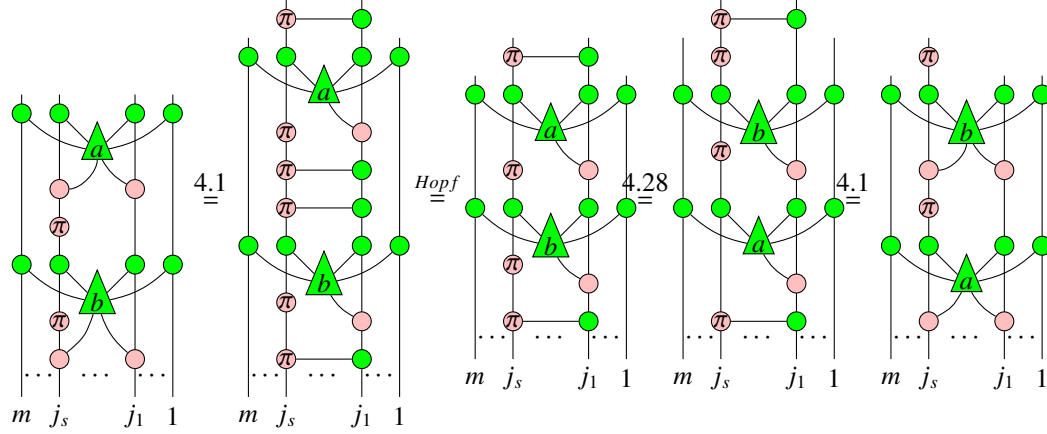


where the node a and b are connected to j_1, \dots, j_s via pink nodes, and two red π nodes are located on the i -th line, $i \notin \{j_1, \dots, j_s\}$ or $i \in \{j_1, \dots, j_s\}, |\{j_1, \dots, j_s\}| \geq 2$.

Proof: If $i \notin \{j_1, \dots, j_s\}$, then we have

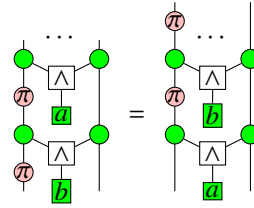


If $i \in \{j_1, \dots, j_s\}, |\{j_1, \dots, j_s\}| \geq 2$, we assume w.l.g that $i = j_s \neq j_1$. Then we have

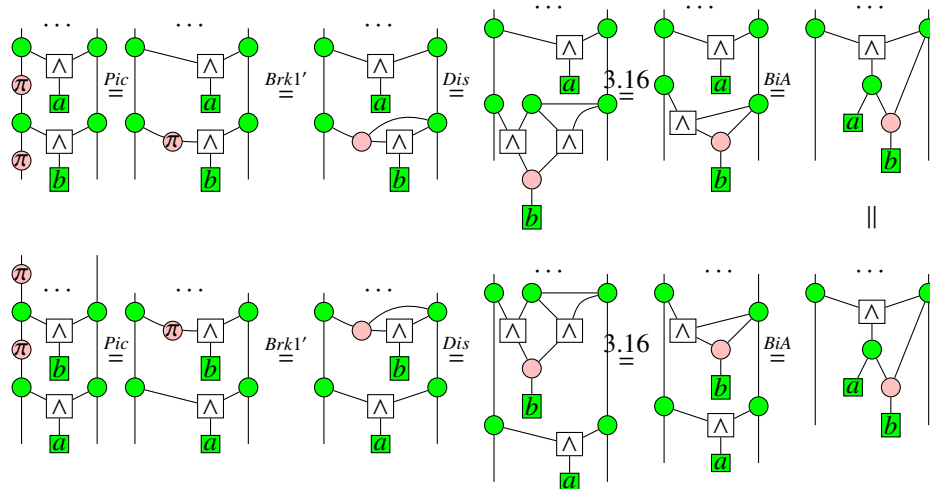


□

Proposition 4.31

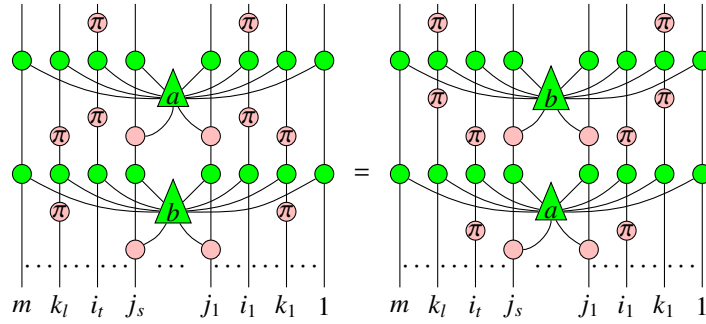


Proof:



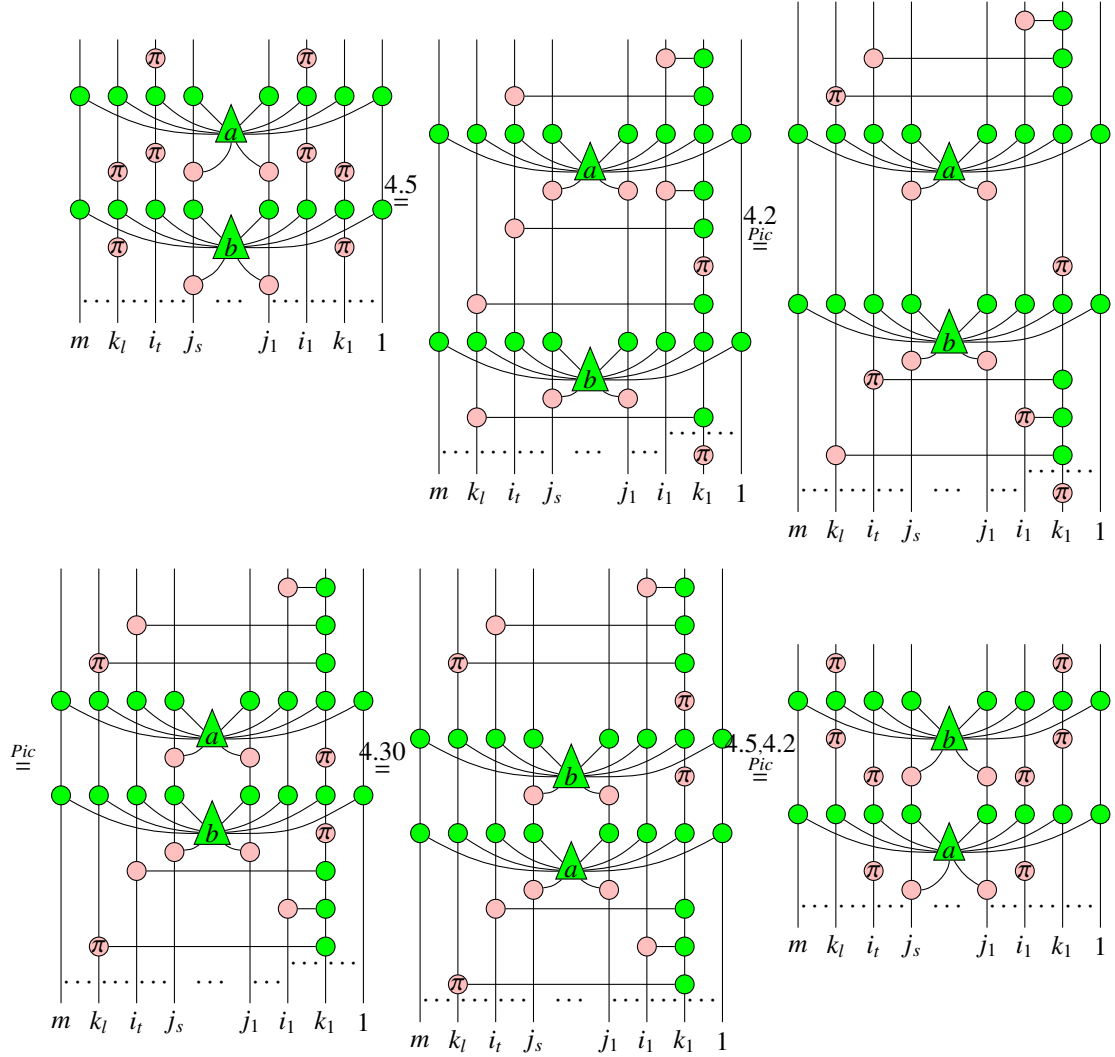
□

Proposition 4.32 Suppose the nodes a and b are connected to j_1, \dots, j_s via pink nodes, pairs of red π nodes separated by green nodes connected to a are located on i_1, \dots, i_t , and pairs of red π nodes separated by green nodes connected to b are located on k_1, \dots, k_l , $\{i_1, \dots, i_t\} \cap \{j_1, \dots, j_s\} = \emptyset$, $\{k_1, \dots, k_l\} \cap \{j_1, \dots, j_s\} = \emptyset$. Then we have



Proof: If $\{i_1, \dots, i_t\} \cup \{k_1, \dots, k_l\} = \emptyset$, then it is just the case of Corollary 4.17. Other-

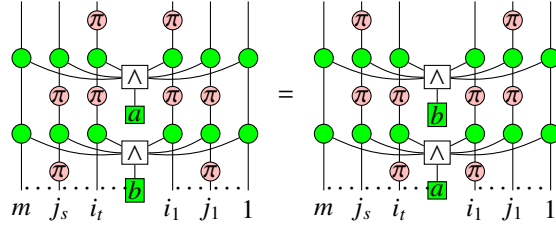
wise, we assume w.l.g that $|{k_1, \dots, k_l}| \geq 1$. Then we have



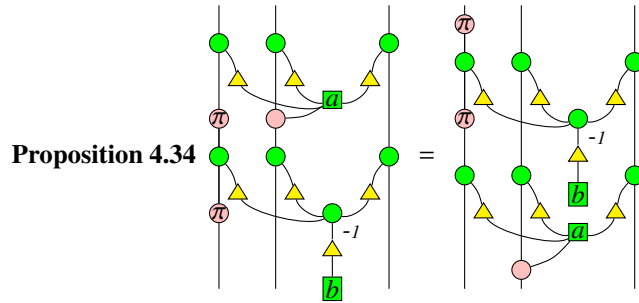
□

Proposition 4.33 Suppose the pairs of red π nodes separated by green nodes connected to a are located on i_1, \dots, i_t , and pairs of red π nodes separated by green nodes

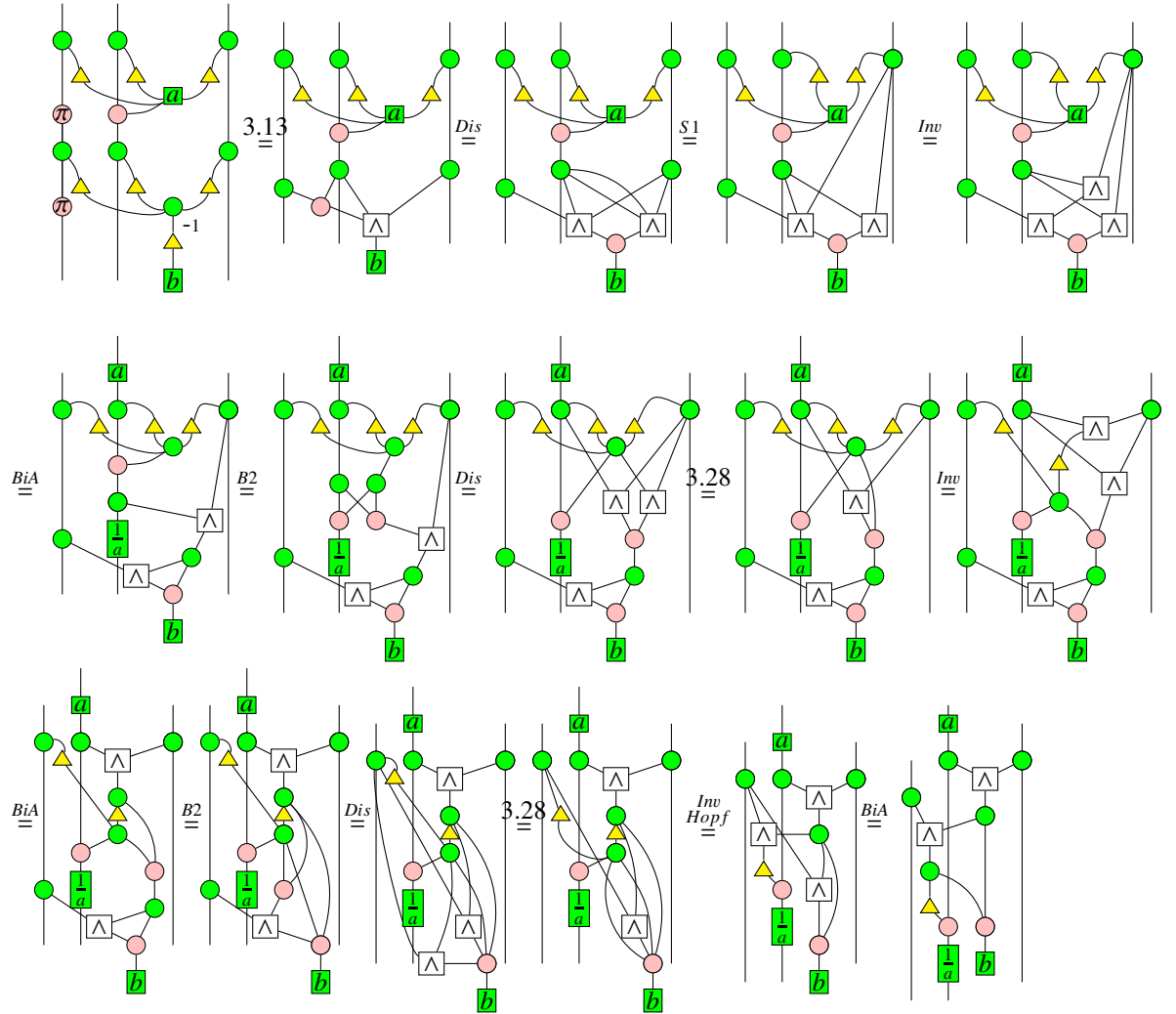
connected to b are located on j_1, \dots, j_s . Then we have

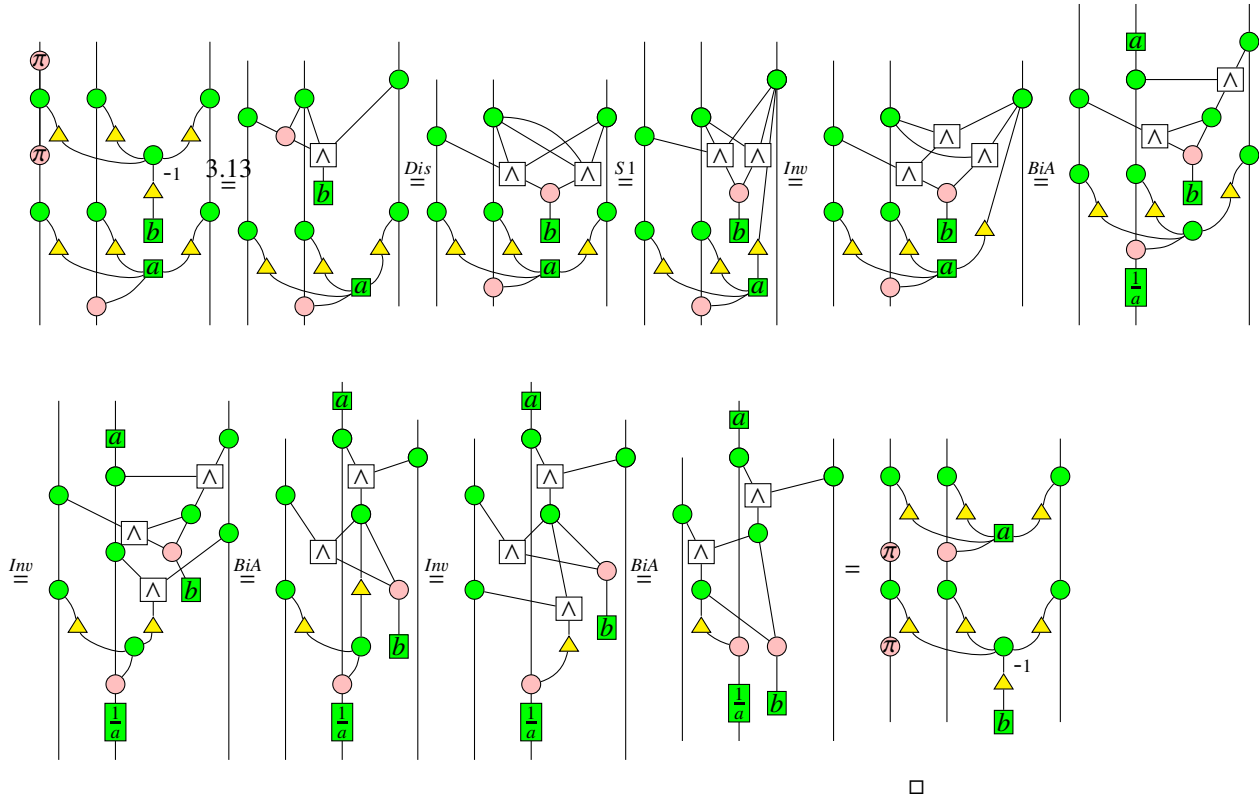


Proof: If $\{i_1, \dots, i_t\} \cup \{j_1, \dots, j_s\} = \emptyset$, then it is just the case of Corollary 4.17. Otherwise, it follows from Proposition 4.31 using the same techniques as in the proof of Proposition 4.32. \square



Proof: If $a = 0$, then the equality holds trivially. Now we assume $a \neq 0$. Then



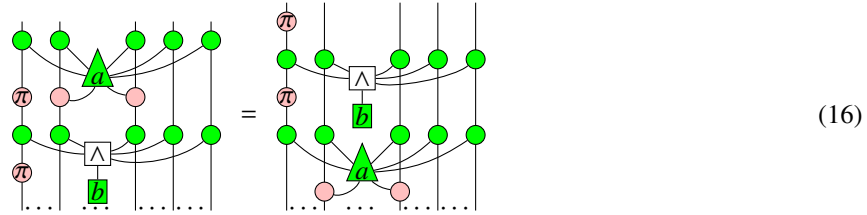


Proposition 4.35 Suppose the node a is connected to j_1, \dots, j_s via pink nodes, and a pair of red π nodes separated by green nodes connected to b are located on k , where $k \notin \{j_1, \dots, j_s\}, |\{j_1, \dots, j_s\}| \geq 1$, or $k \in \{j_1, \dots, j_s\}, |\{j_1, \dots, j_s\}| \geq 2$. Then we have

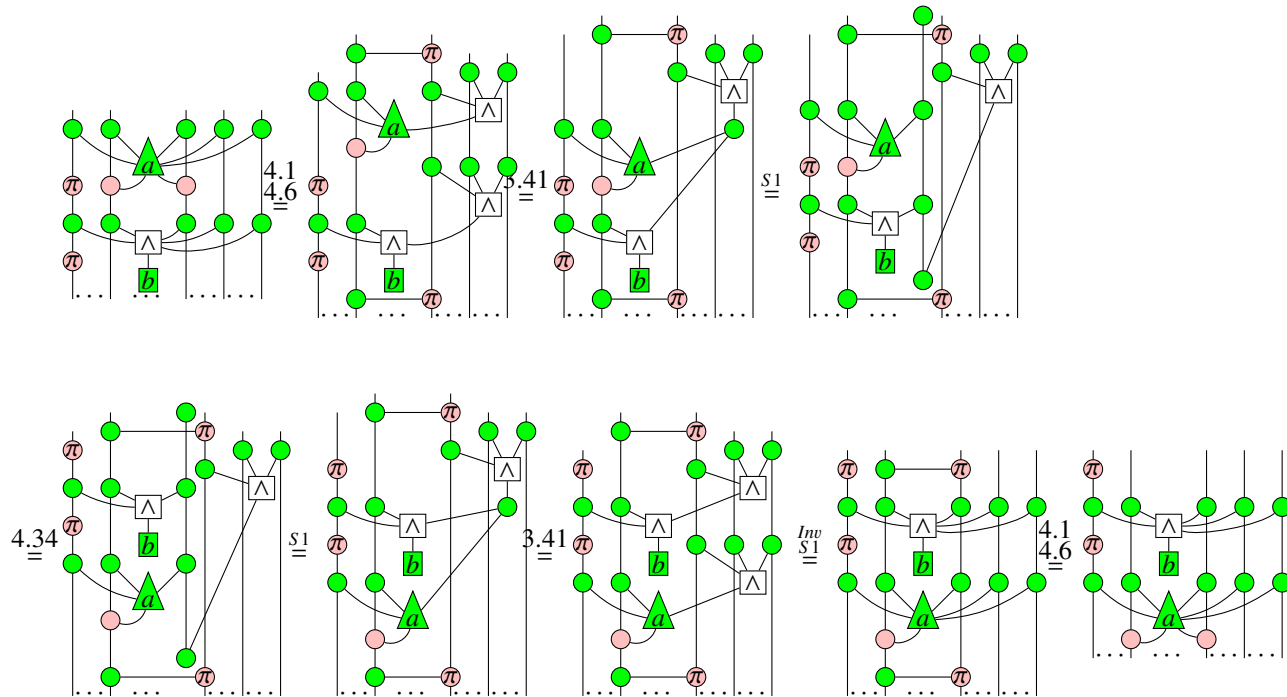
(15)

Proof: If $k \notin \{j_1, \dots, j_s\}, |\{j_1, \dots, j_s\}| \geq 1$, then by rearranging the order of lines by

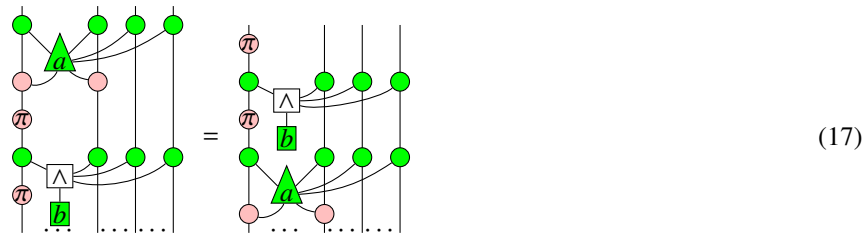
swapping, (15) is equivalent to



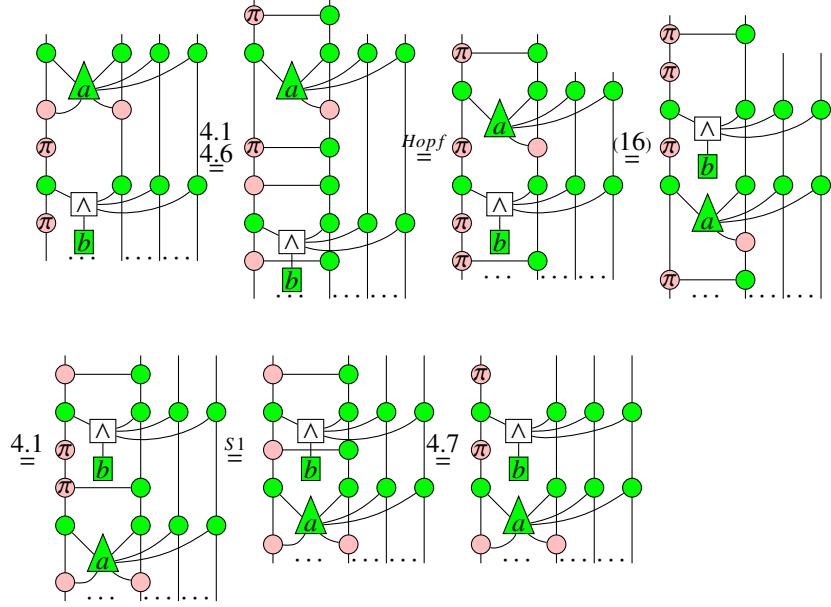
We have



If $k \in \{j_1, \dots, j_s\}$, $|\{j_1, \dots, j_s\}| \geq 2$, we assume w.l.g that $k = j_s$, then (15) is equivalent to

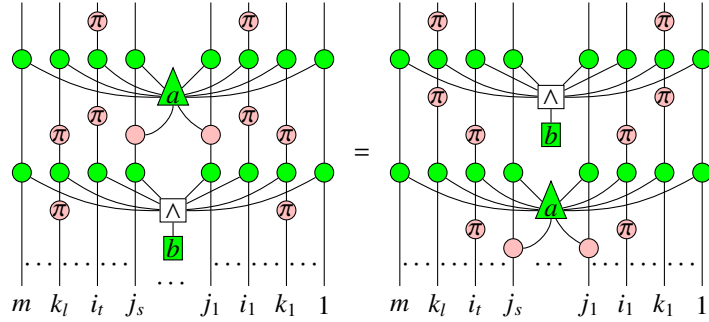


We have

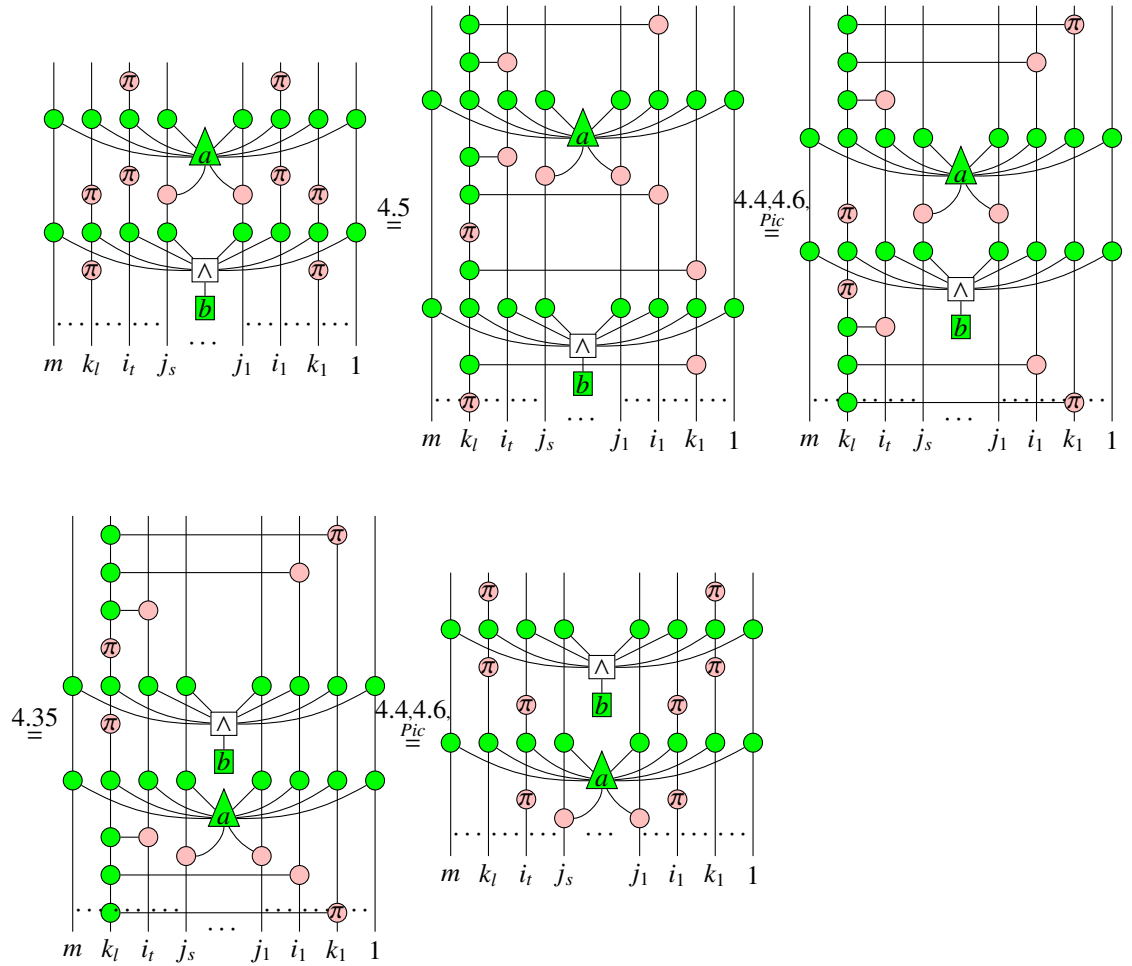


□

Proposition 4.36 *Suppose the node a is connected to j_1, \dots, j_s via pink nodes, pairs of red π nodes separated by green nodes connected to a are located on i_1, \dots, i_t , and pairs of red π nodes separated by green nodes connected to b are located on k_1, \dots, k_l , $\{i_1, \dots, i_t\} \neq \{k_1, \dots, k_l\}$. Either $\{k_1, \dots, k_l\} \neq \emptyset, \{k_1, \dots, k_l\} \cap \{j_1, \dots, j_s\} = \emptyset, |\{j_1, \dots, j_s\}| \geq 1$; or $\{k_1, \dots, k_l\} \neq \emptyset, |\{k_1, \dots, k_l\} \cap \{j_1, \dots, j_s\}| = 1, |\{j_1, \dots, j_s\}| \geq 2$; or symmetrically, $\{i_1, \dots, i_t\} \neq \emptyset, \{i_1, \dots, i_t\} \cap \{j_1, \dots, j_s\} = \emptyset, |\{j_1, \dots, j_s\}| \geq 1$; or $\{i_1, \dots, i_t\} \neq \emptyset, |\{i_1, \dots, i_t\} \cap \{j_1, \dots, j_s\}| = 1, |\{j_1, \dots, j_s\}| \geq 2$. Then we have*

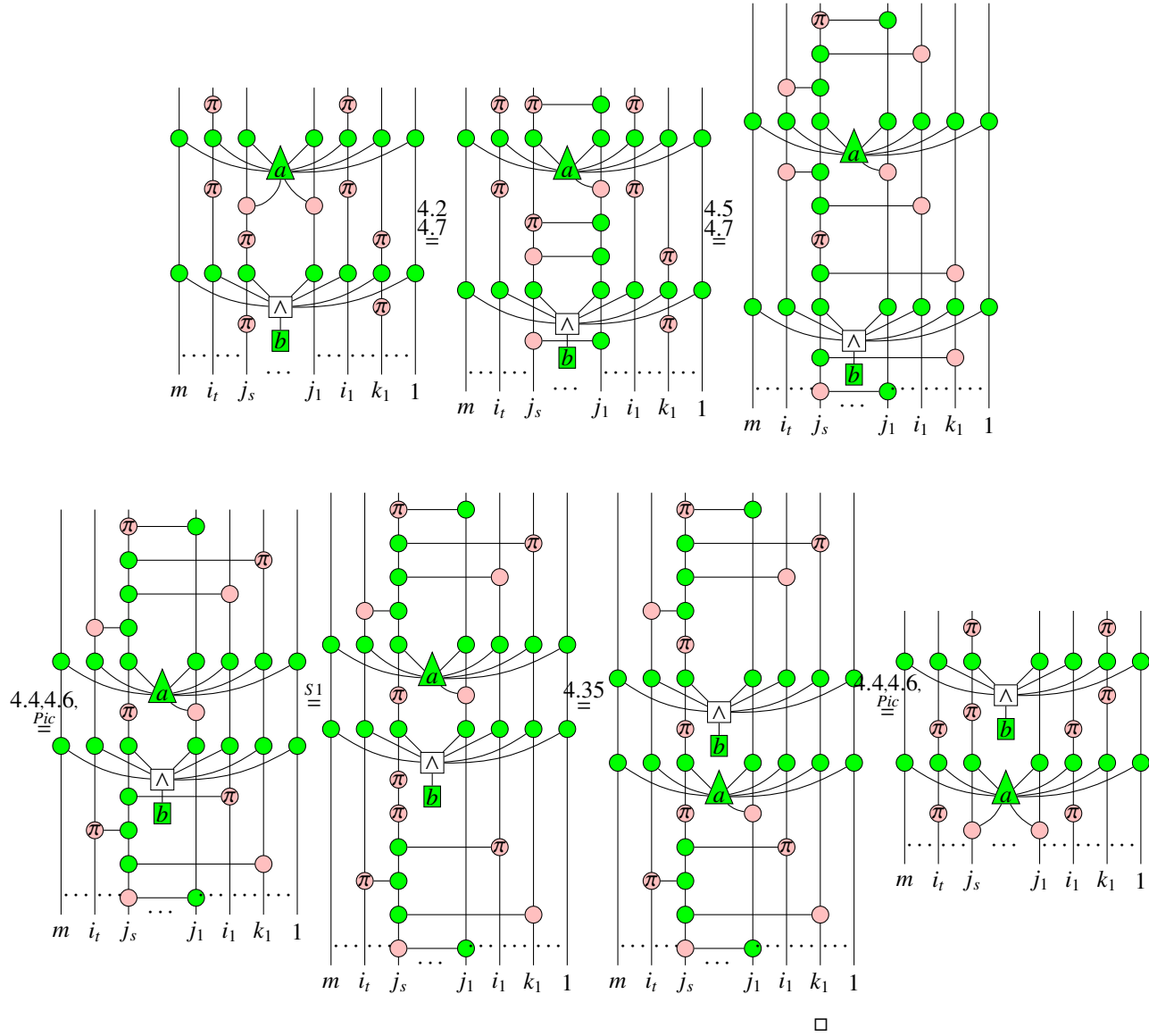


Proof: We assume w.l.g that $k_l \notin \{i_1, \dots, i_t\}$. If $k_l \notin \{j_1, \dots, j_s\}$. Then we have

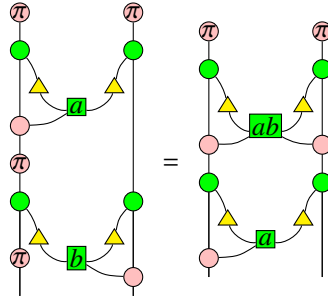


(18)

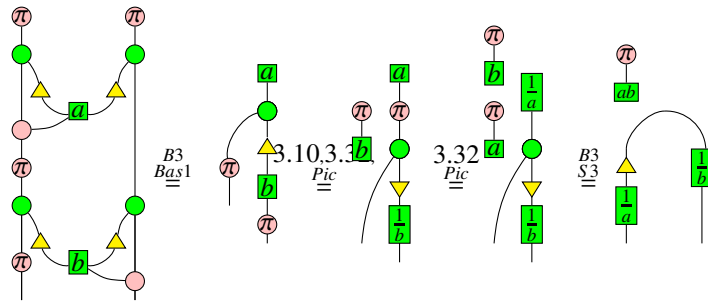
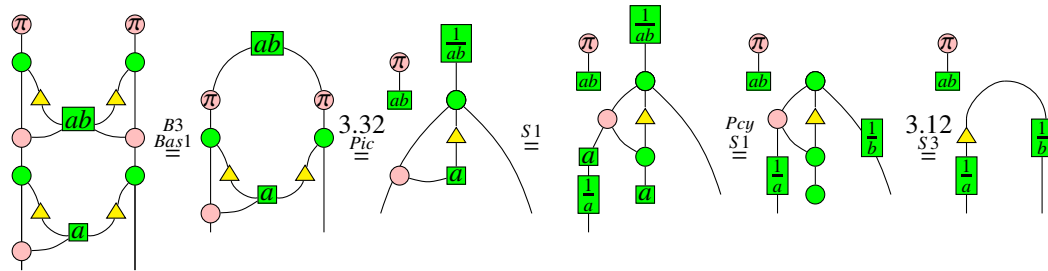
If $|\{j_1, \dots, j_s\}| \geq 2$, $k_l \in \{j_1, \dots, j_s\}$, we assume w.l.g that $k_l = j_s \neq j_1$. Then we have



Proposition 4.37

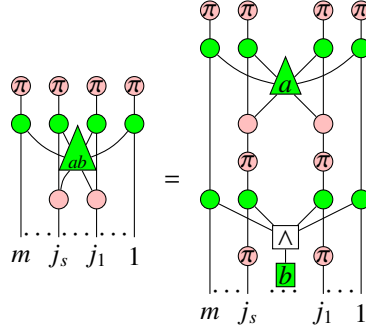


Proof: If $ab = 0$, it can be easily verified. Below we assume that $ab \neq 0$. Then we have



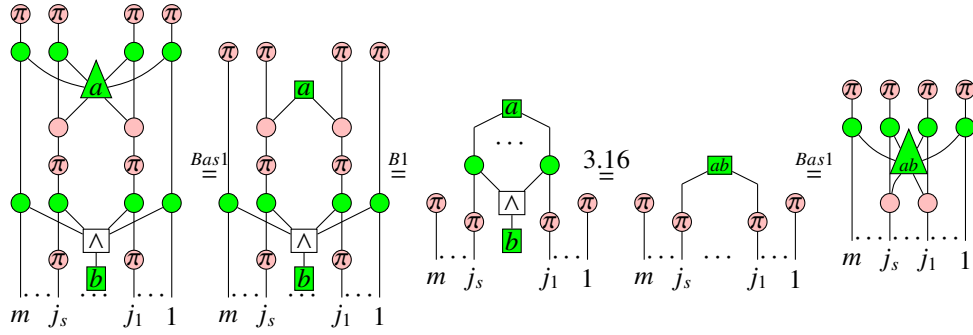
□

Proposition 4.38



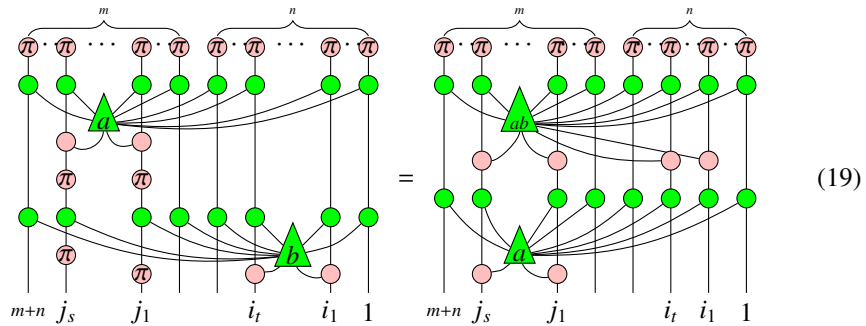
where the node ab is connected to j_1, \dots, j_s via pink nodes.

Proof:

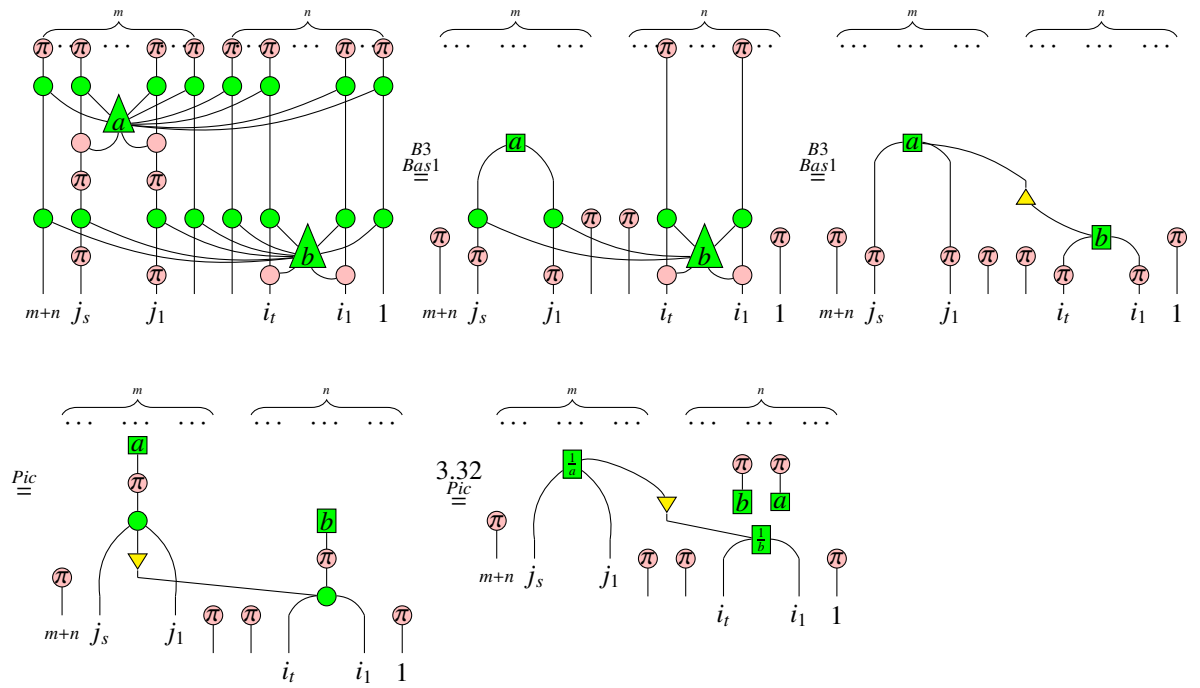


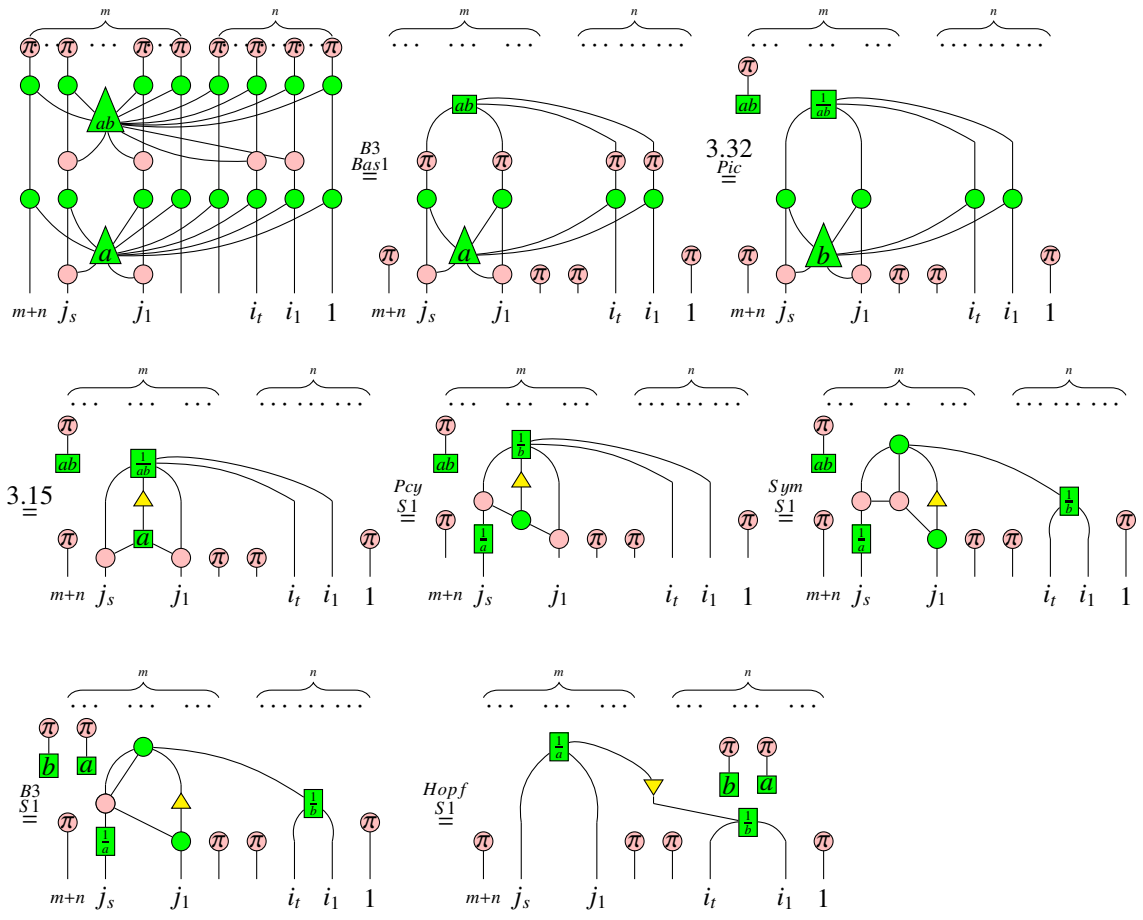
□

Proposition 4.39 Suppose the node a is connected to j_1, \dots, j_s via pink nodes, the node b is connected to i_1, \dots, i_t via pink nodes, pairs of red π nodes separated by green nodes connected to b are located on j_1, \dots, j_s . Furthermore, $\emptyset \neq \{i_1, \dots, i_t\} \subseteq \{1, \dots, n\}, \emptyset \neq \{j_1, \dots, j_s\} \subseteq \{n+1, \dots, n+m\}$.

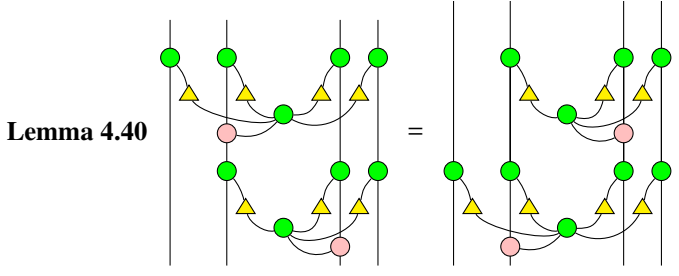


Proof: If $ab = 0$, then it is easy to prove. We assume that $ab \neq 0$. Then

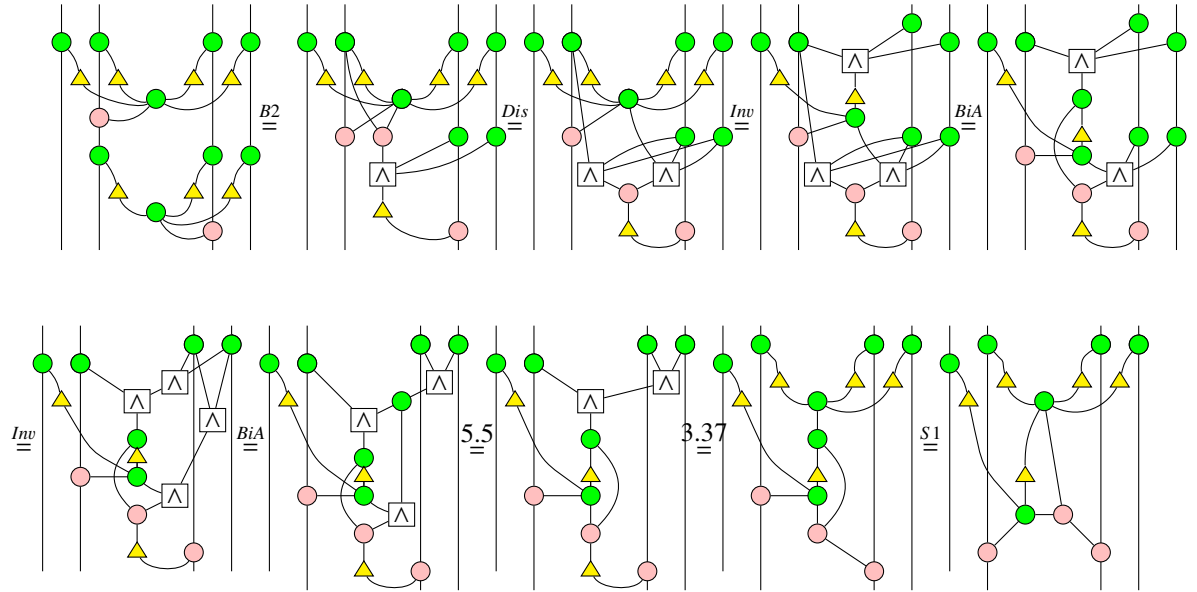


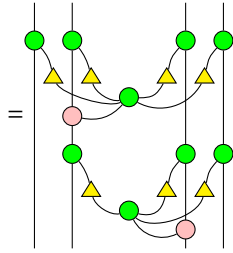
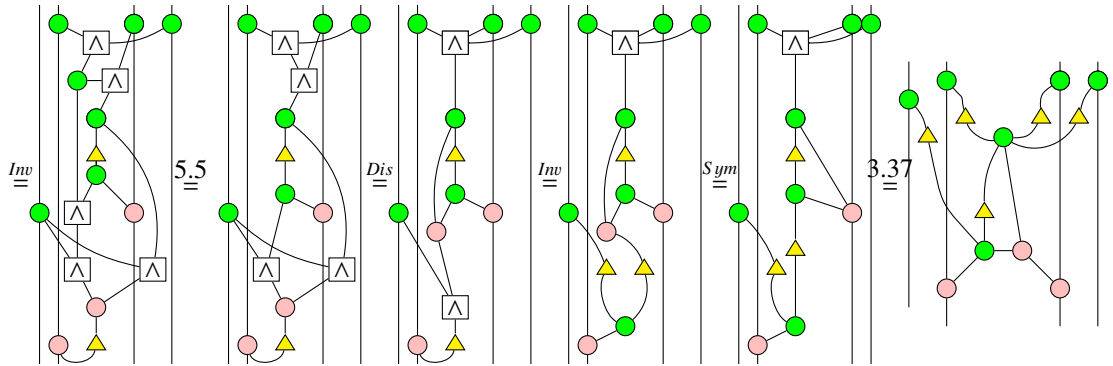
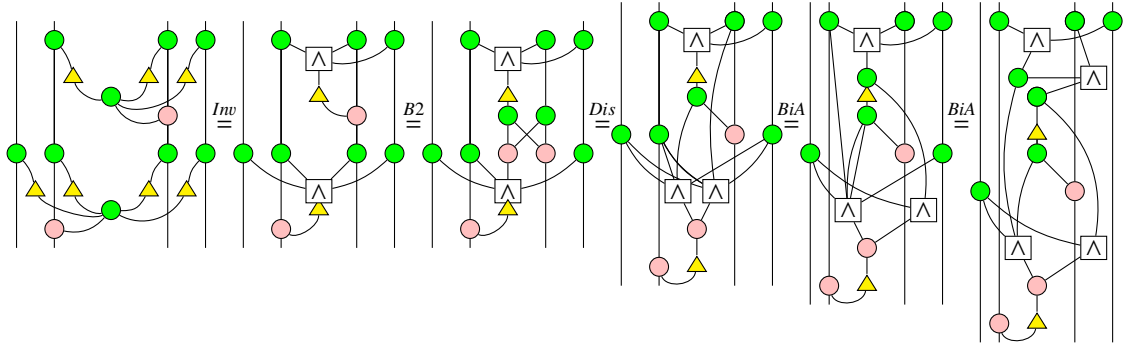


□

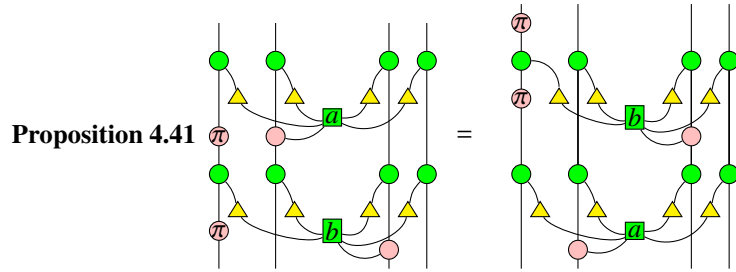


Proof:

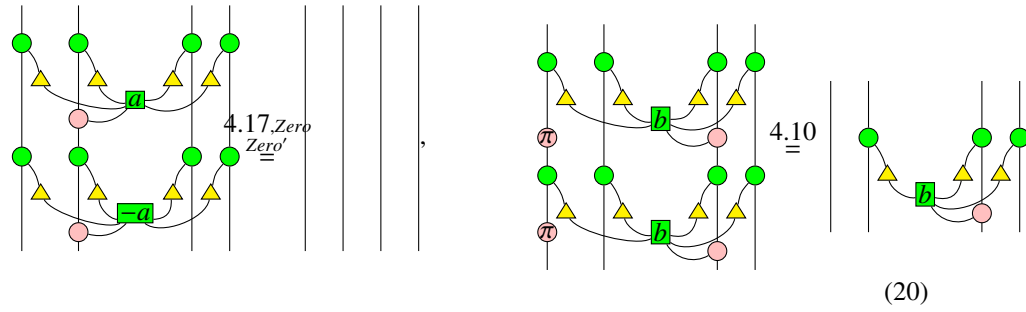




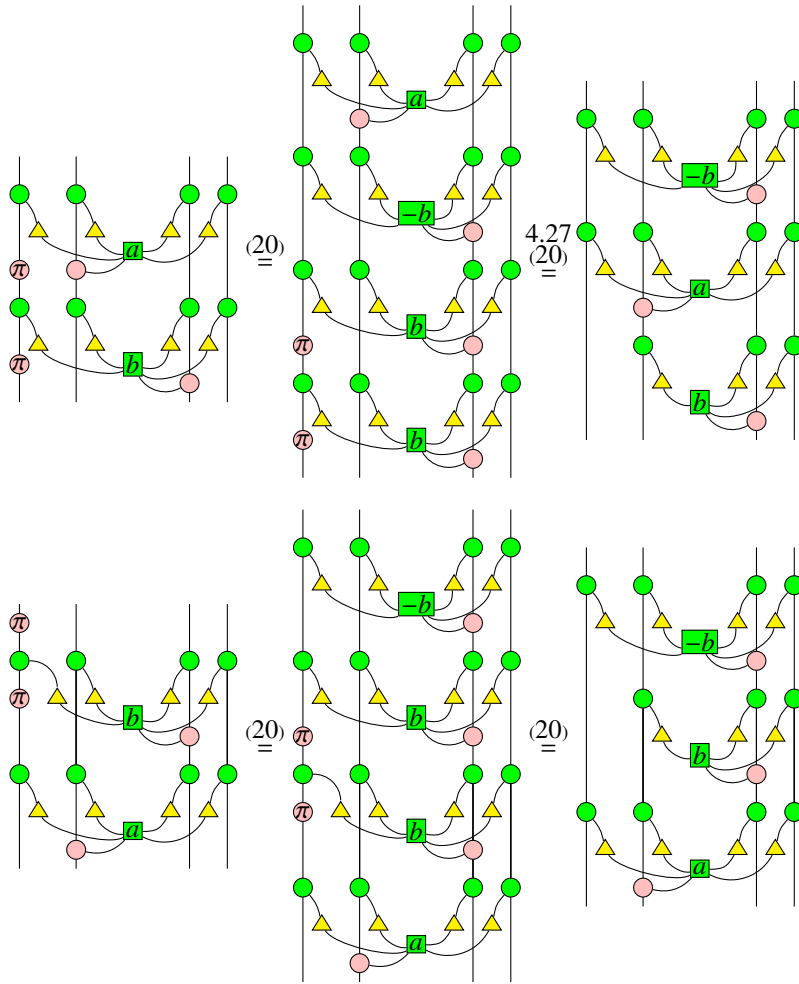
□



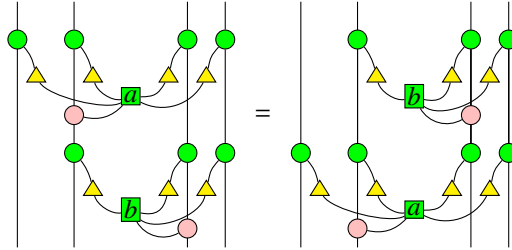
Proof: If $a = 0$ or $b = 0$, then the equality holds trivially. Now we assume $ab \neq 0$. First we note that the following equalities hold:



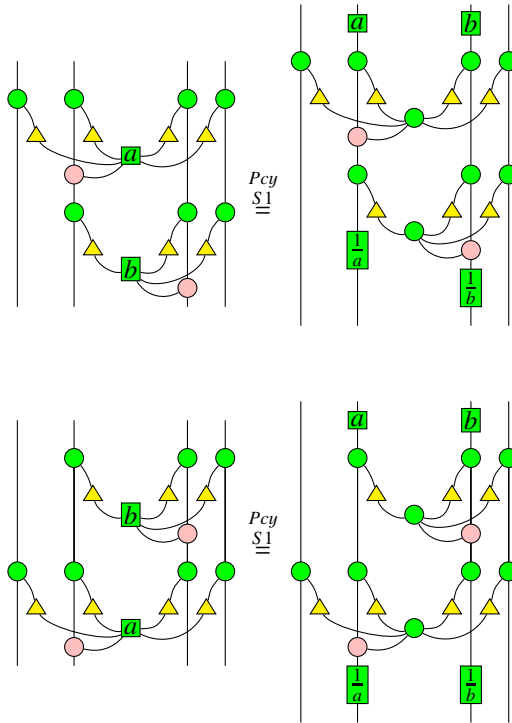
Since



Then it is equivalent to prove

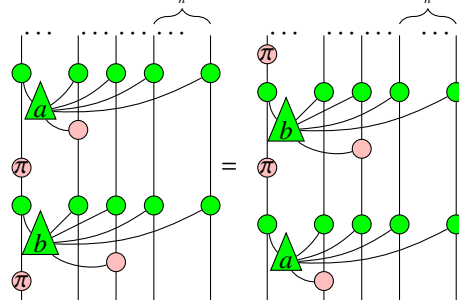


Furthermore,

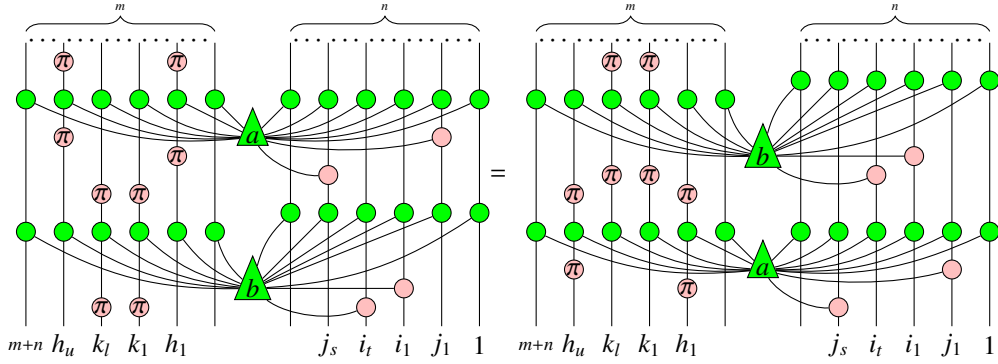


Therefore it is equivalent to prove Lemma 4.40 which has been done. \square

Corollary 4.42

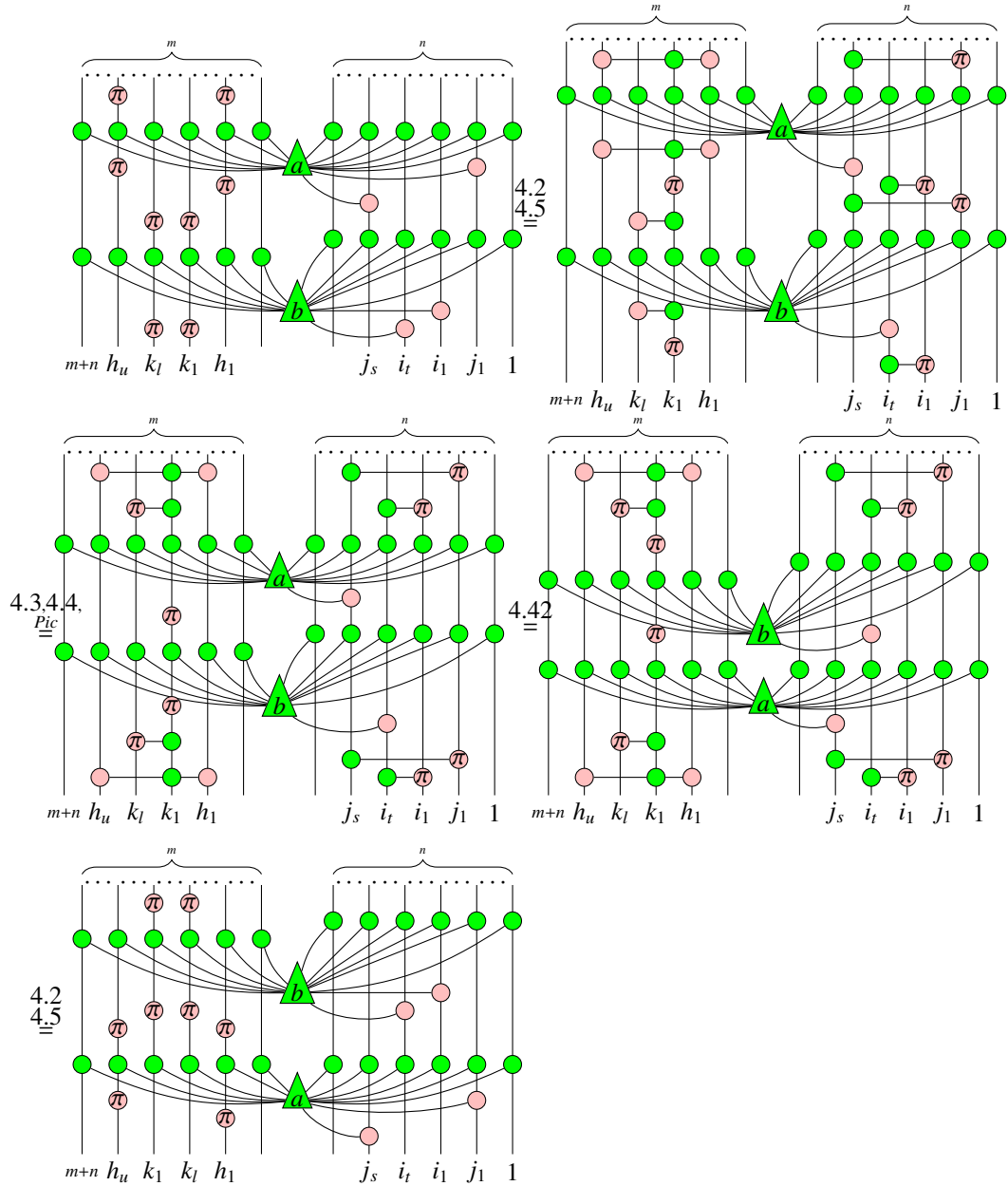


Proposition 4.43 Suppose the node a is connected to j_1, \dots, j_s via pink nodes, the node b is connected to i_1, \dots, i_t via pink nodes, pairs of red π nodes separated by green nodes connected to a are located on h_1, \dots, h_u , pairs of red π nodes separated by green nodes connected to b are located on k_1, \dots, k_l . Furthermore, $\emptyset \neq \{i_1, \dots, i_t\} \subseteq \{1, \dots, n\}$, $\emptyset \neq \{j_1, \dots, j_s\} \subseteq \{1, \dots, n\}$, $\{h_1, \dots, h_u\} \subseteq \{n+1, \dots, n+m\}$, $\{k_1, \dots, k_l\} \subseteq \{n+1, \dots, n+m\}$. Then



Proof: If $\{i_1, \dots, i_t\} = \{j_1, \dots, j_s\}$, then it is just the case of Proposition 4.32. If $\{h_1, \dots, h_u\} = \{k_1, \dots, k_l\}$, then it is just the case of Proposition 4.27. Therefore, we

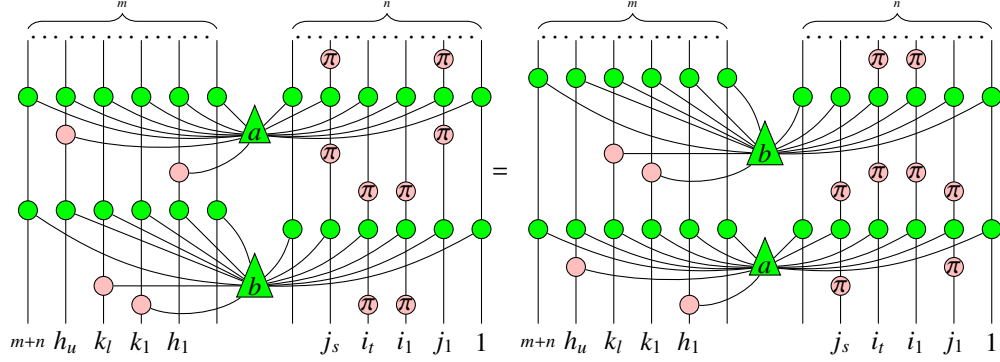
assume w.l.g that $k_1 \notin \{h_1, \dots, h_u\}, i_t \notin \{j_1, \dots, j_s\}$. Then we have



□

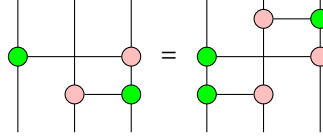
Corollary 4.44 Suppose the node a is connected to h_1, \dots, h_u via pink nodes, the node b is connected to k_1, \dots, k_l via pink nodes, pairs of red π nodes separated by

green nodes connected to a are located on j_1, \dots, j_s , pairs of red π nodes separated by green nodes connected to b are located on i_1, \dots, i_t . Furthermore, $\{i_1, \dots, i_t\} \subseteq \{1, \dots, n\}, \{j_1, \dots, j_s\} \subseteq \{1, \dots, n\}, \emptyset \neq \{h_1, \dots, h_u\} \subseteq \{n+1, \dots, n+m\}, \emptyset \neq \{k_1, \dots, k_l\} \subseteq \{n+1, \dots, n+m\}$. Then



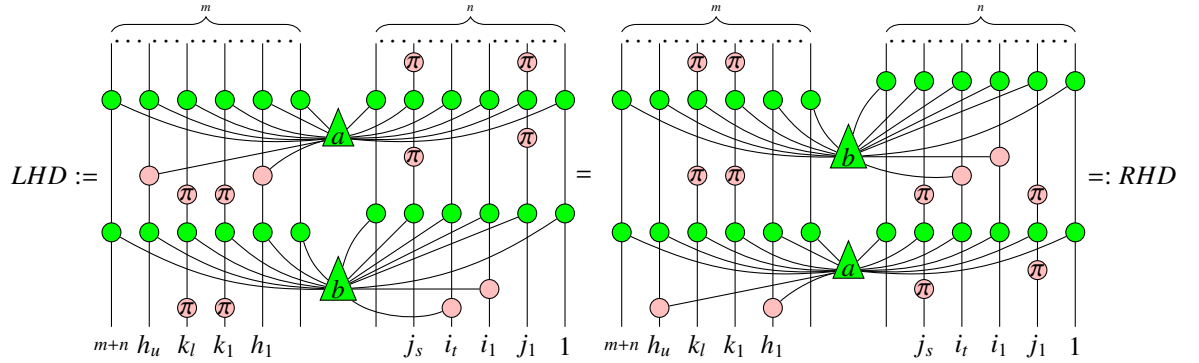
This can be obtained from Proposition 4.43 by swapping the left m wires to the right.

Lemma 4.45

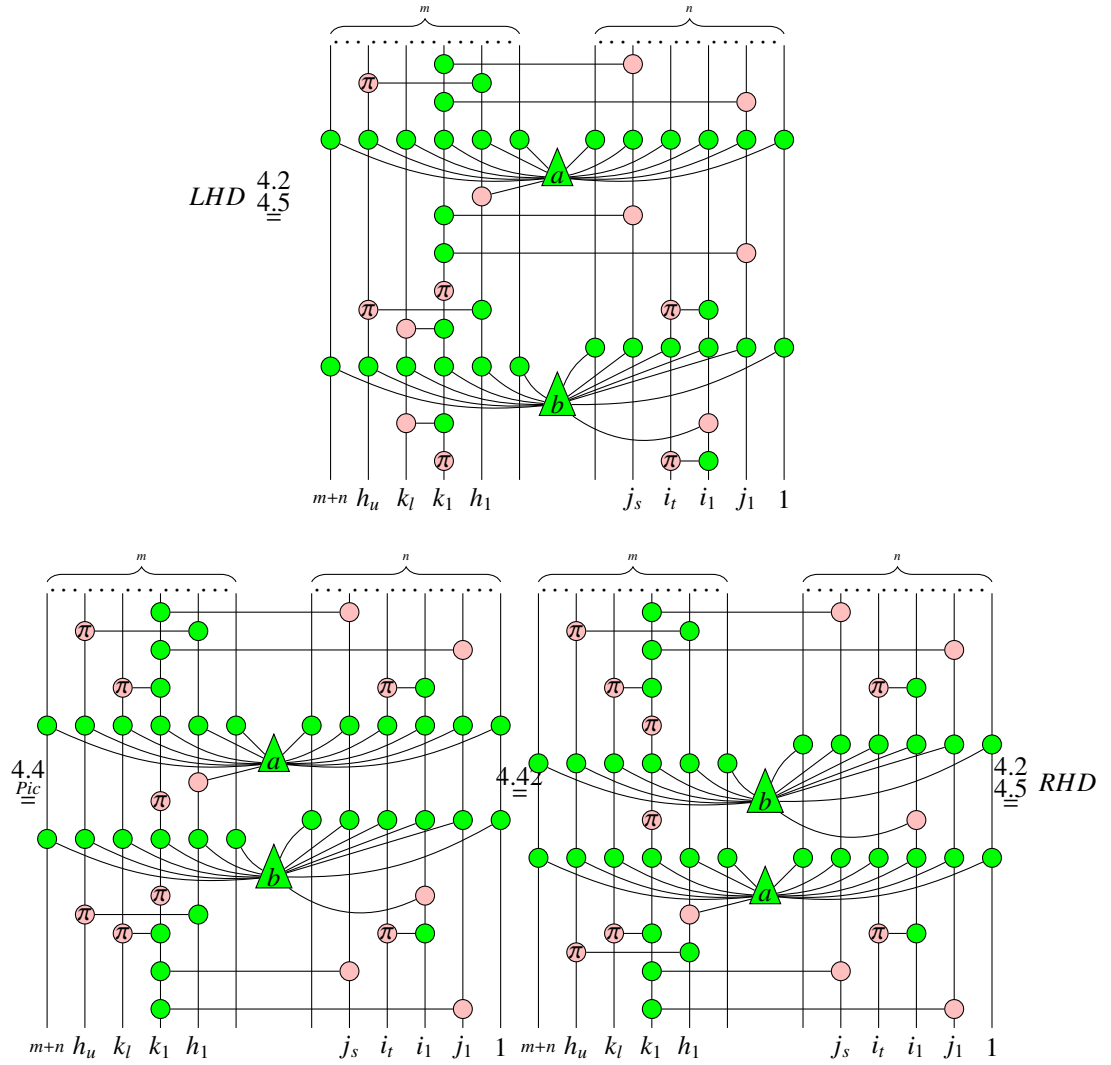


This can be easily obtained mainly by using the (B2) rule.

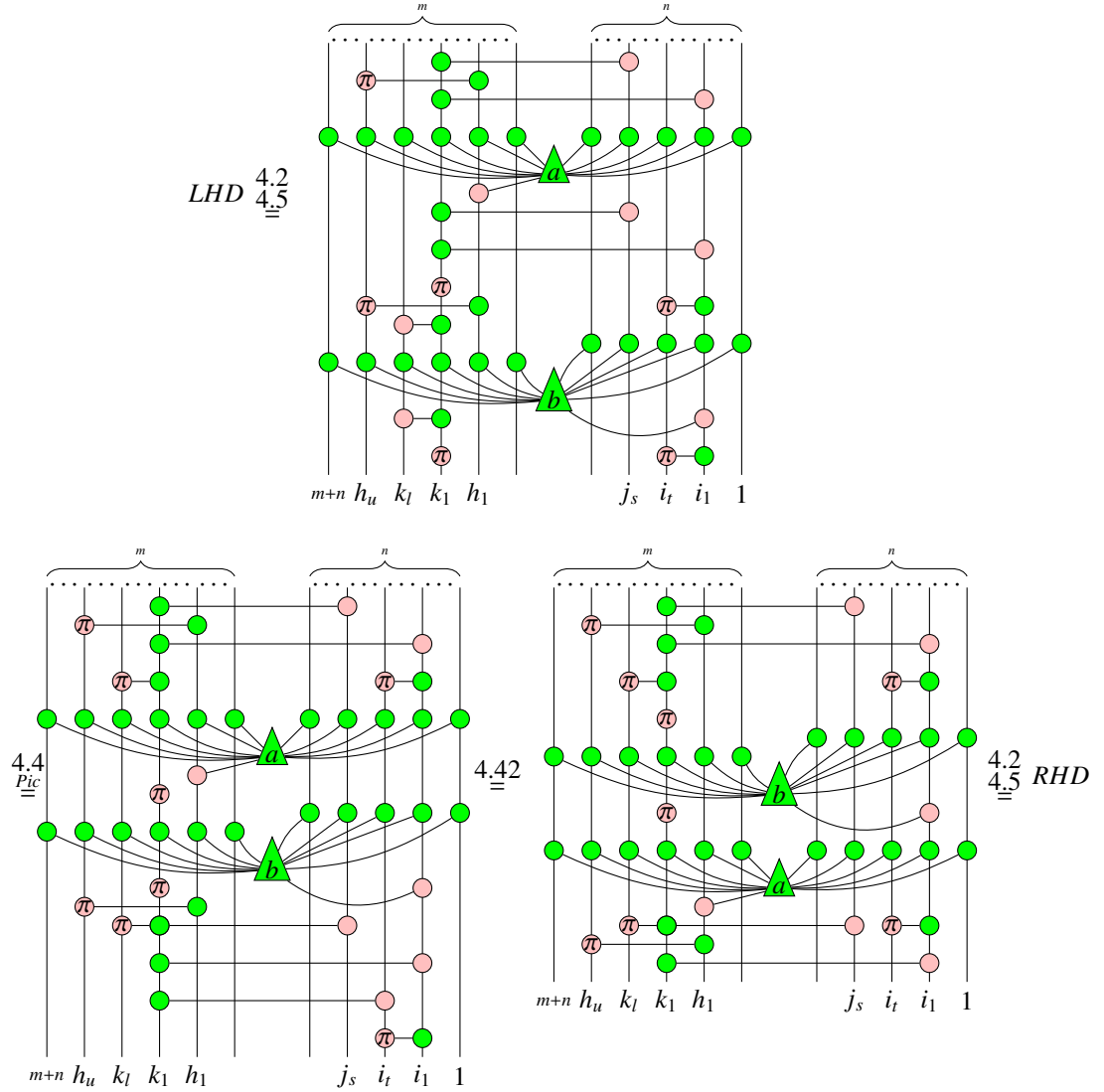
Proposition 4.46 Suppose the node a is connected to h_1, \dots, h_u via pink nodes, the node b is connected to i_1, \dots, i_t via pink nodes, pairs of red π nodes separated by green nodes connected to a are located on j_1, \dots, j_s , pairs of red π nodes separated by green nodes connected to b are located on k_1, \dots, k_l . Furthermore, $\emptyset \neq \{i_1, \dots, i_t\} \subseteq \{1, \dots, n\}, \{j_1, \dots, j_s\} \subseteq \{1, \dots, n\}, \emptyset \neq \{h_1, \dots, h_u\} \subseteq \{n+1, \dots, n+m\}, \emptyset \neq \{k_1, \dots, k_l\} \subseteq \{n+1, \dots, n+m\}, \{h_1, \dots, h_u\} \neq \{k_1, \dots, k_l\}$. Then



Proof: We assume w.l.g that $k_1 \notin \{h_1, \dots, h_u\}$. If $\{i_1, \dots, i_t\} \cap \{j_1, \dots, j_s\} = \emptyset$, then



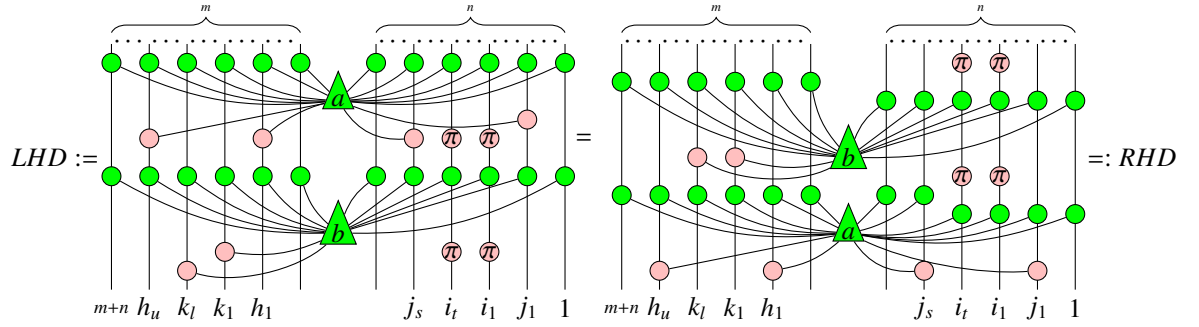
If $\{i_1, \dots, i_t\} \cap \{j_1, \dots, j_s\} \neq \emptyset$, we assume w.l.g that $j_1 = i_1$, then



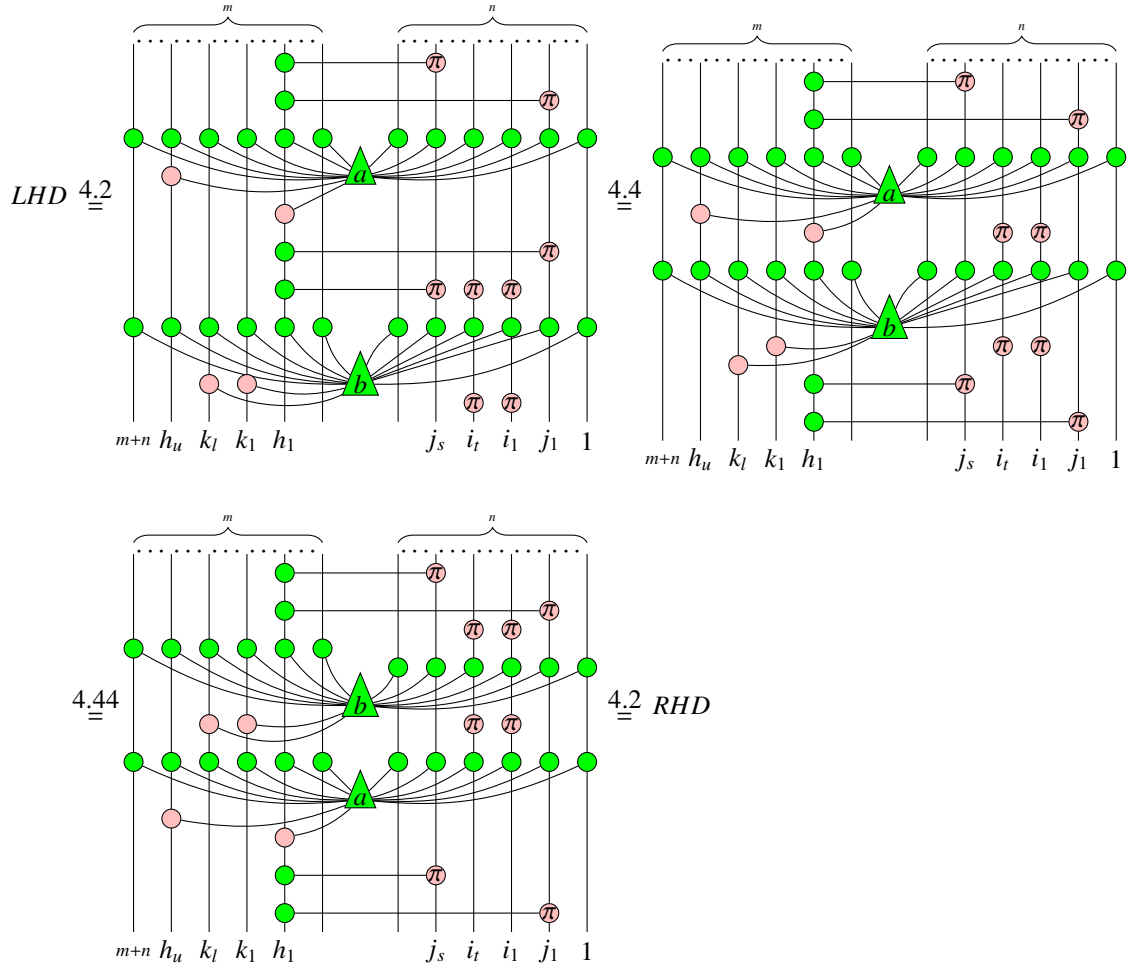
□

Proposition 4.47 Suppose the node a is connected to h_1, \dots, h_u on the left m wires via pink nodes, and is connected to j_1, \dots, j_s on the right n wires via pink nodes; the node b is connected to k_1, \dots, k_l via pink nodes, pairs of red π nodes separated by green nodes connected to b are located on i_1, \dots, i_t . Furthermore, $\{i_1, \dots, i_t\} \subseteq \{1, \dots, n\}, \emptyset \neq \{j_1, \dots, j_s\} \subseteq \{1, \dots, n\}, \emptyset \neq \{h_1, \dots, h_u\} \subseteq \{n+1, \dots, n+m\}, \emptyset \neq$

$\{k_1, \dots, k_l\} \subseteq \{n+1, \dots, n+m\}, \{h_1, \dots, h_u\} \neq \{k_1, \dots, k_l\}$. Then

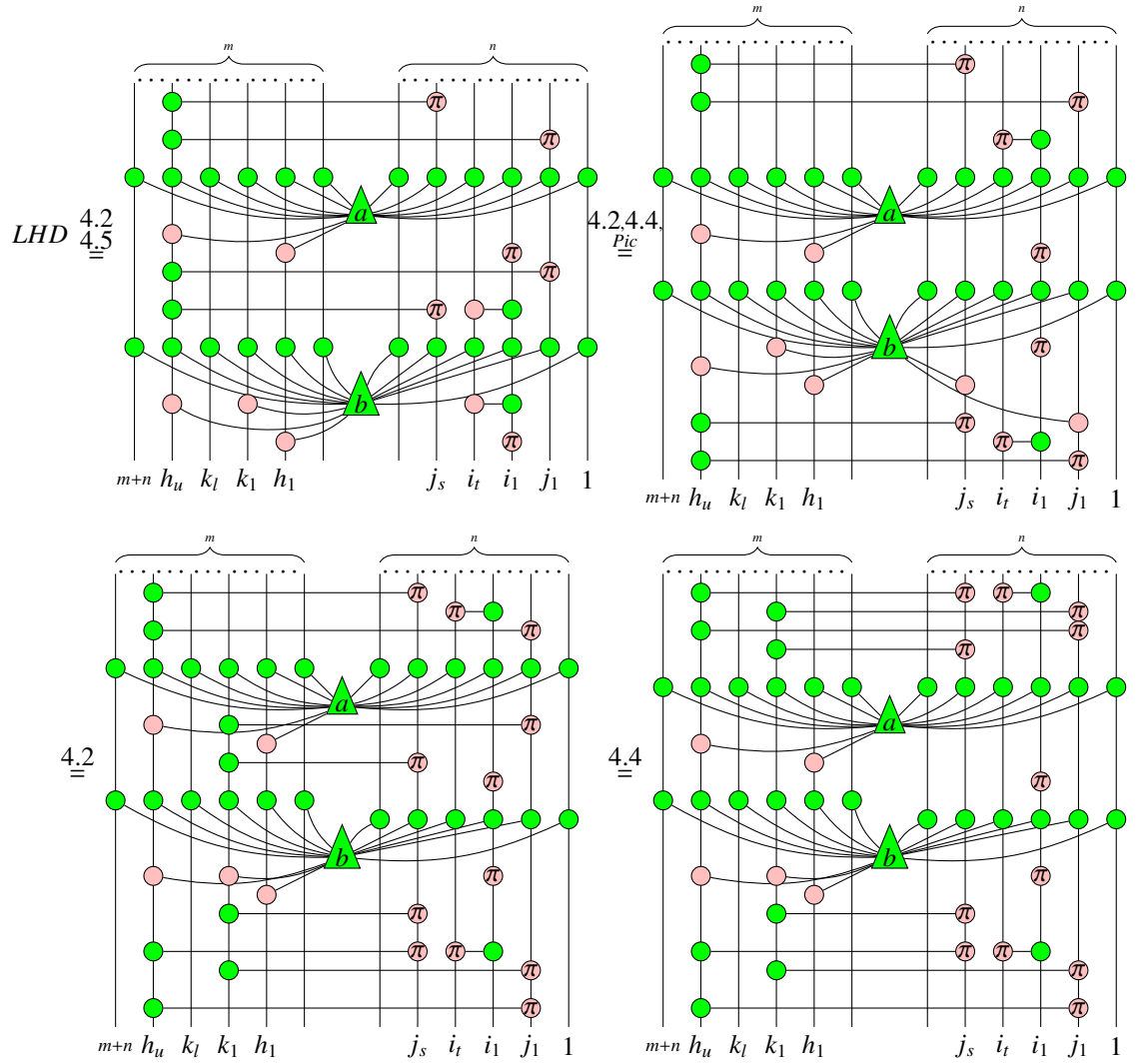


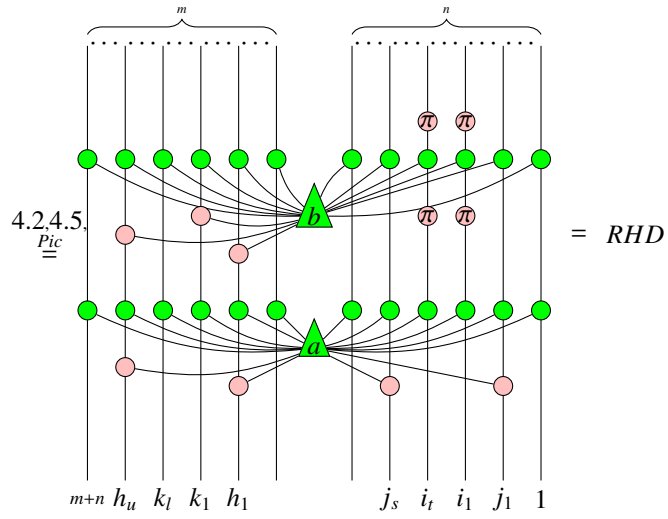
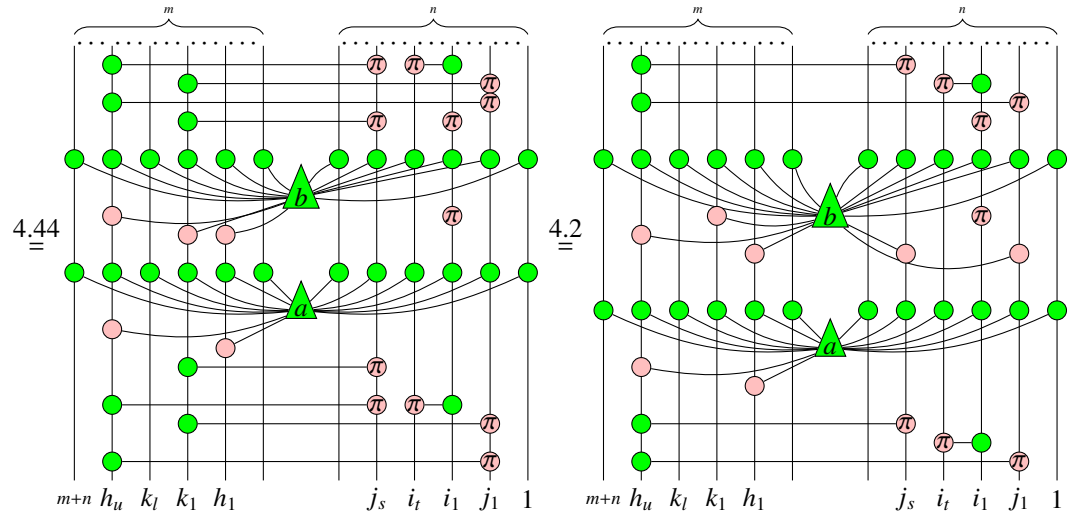
Proof: If $\{h_1, \dots, h_u\} \not\subseteq \{k_1, \dots, k_l\}$, we assume w.l.g that $h_1 \notin \{k_1, \dots, k_l\}$. Then



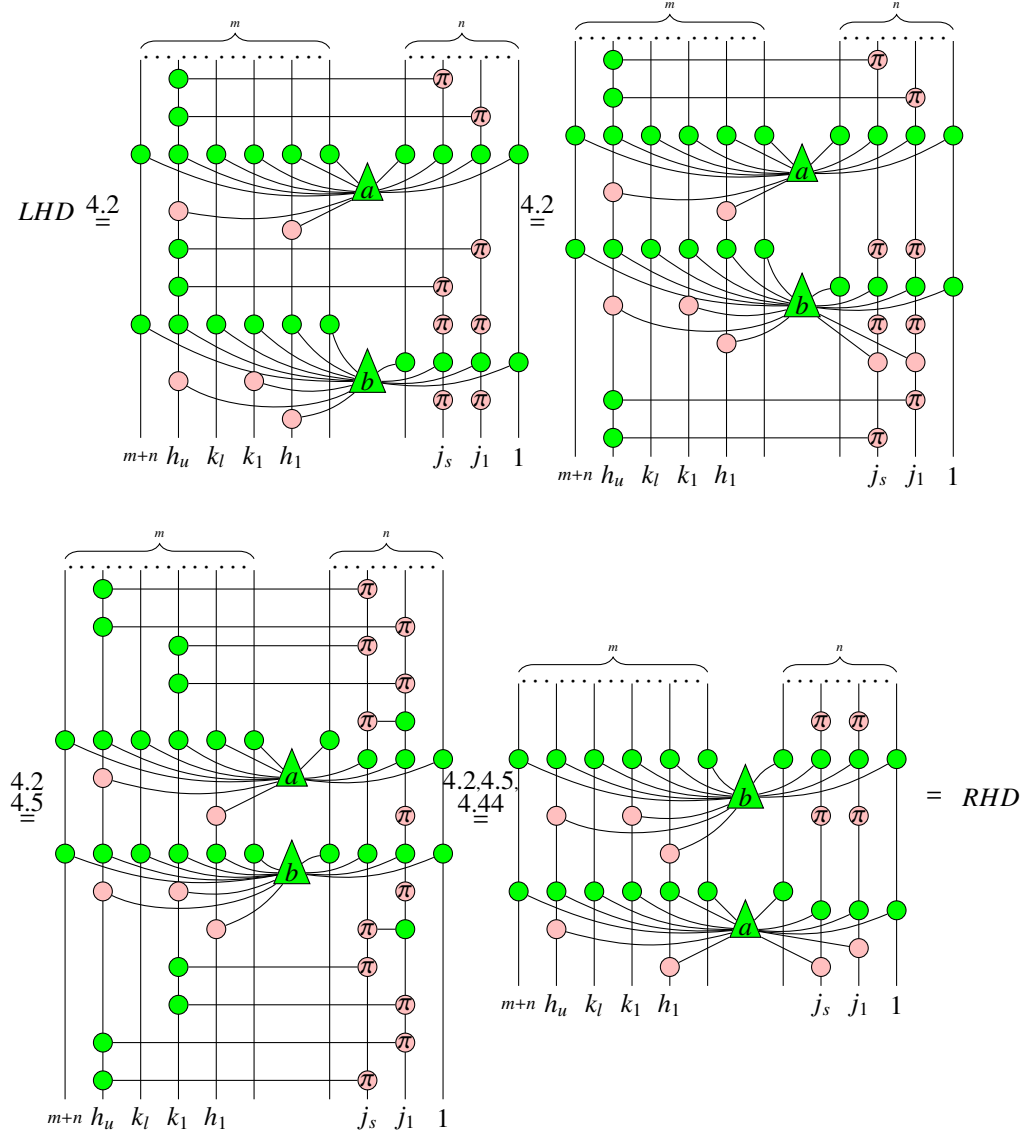
If $\{h_1, \dots, h_u\} \subseteq \{k_1, \dots, k_l\}$, we assume w.l.g that $k_1 \notin \{h_1, \dots, h_u\}$. Here are two

cases. (1) $\{i_1, \dots, i_t\} \not\subseteq \{j_1, \dots, j_s\}$, we assume w.l.g that $i_1 \notin \{j_1, \dots, j_s\}$. Then



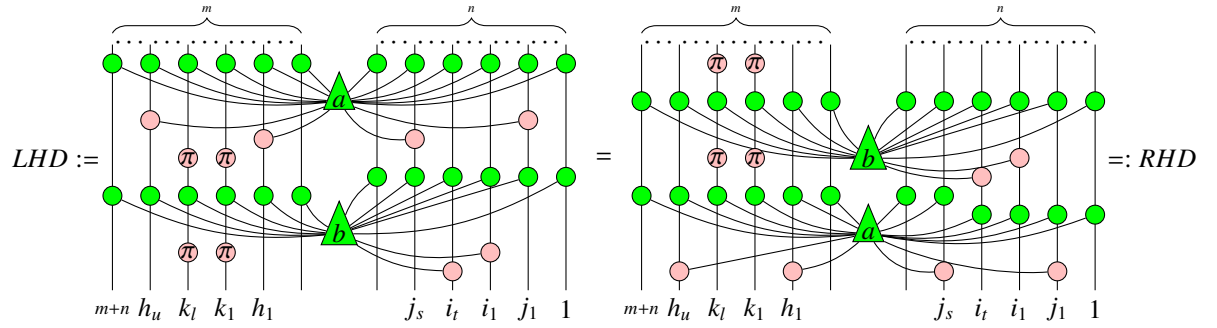


(2) $\{i_1, \dots, i_t\} \subseteq \{j_1, \dots, j_s\}$. Then

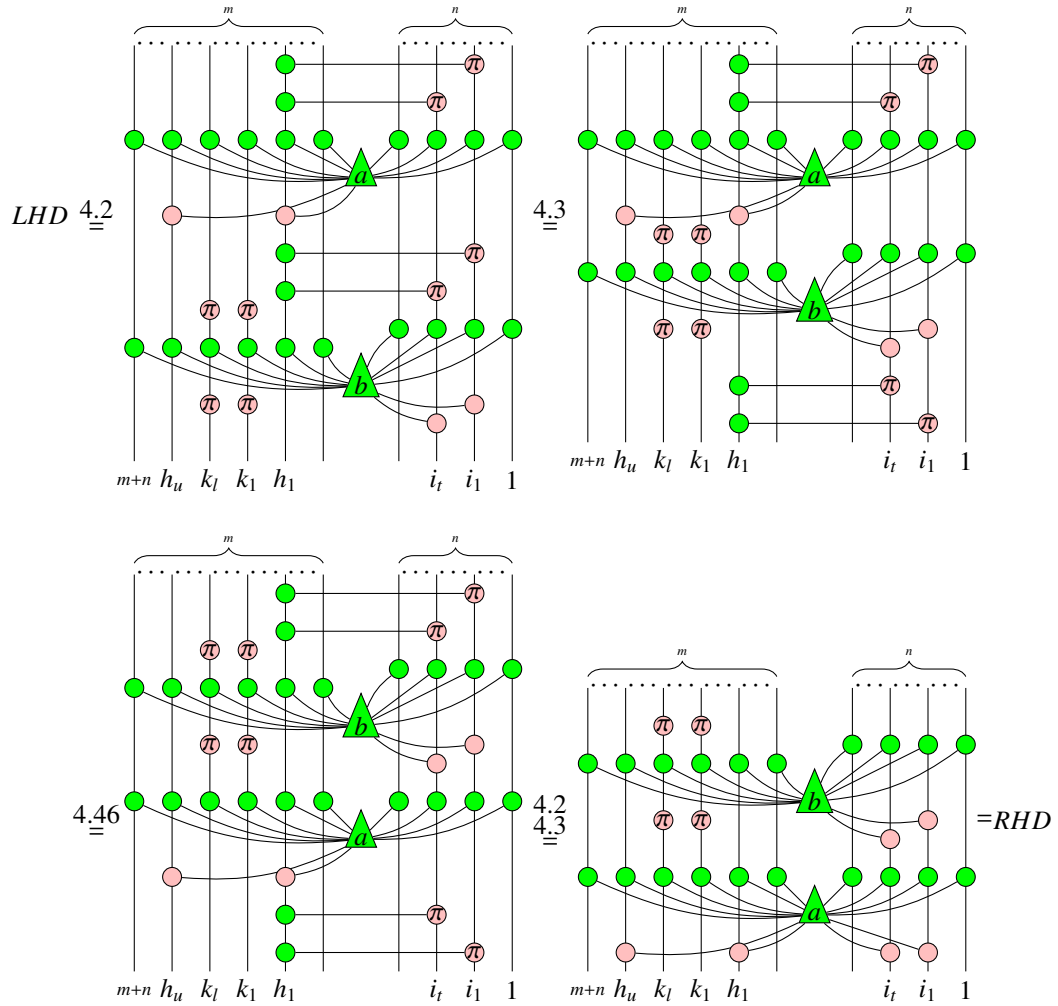


□

Proposition 4.48 Suppose the node a is connected to h_1, \dots, h_u on the left m wires via pink nodes, and is connected to j_1, \dots, j_s on the right n wires via pink nodes; the node b is connected to i_1, \dots, i_t via pink nodes, pairs of red π nodes separated by green nodes connected to b are located on k_1, \dots, k_l . Furthermore, $\emptyset \neq \{i_1, \dots, i_t\} \subseteq \{1, \dots, n\}$, $\emptyset \neq \{j_1, \dots, j_s\} \subseteq \{1, \dots, n\}$, $\emptyset \neq \{h_1, \dots, h_u\} \subseteq \{n+1, \dots, n+m\}$, $\{k_1, \dots, k_l\} \subseteq \{n+1, \dots, n+m\}$, $\{h_1, \dots, h_u\} \neq \{k_1, \dots, k_l\}$. Then

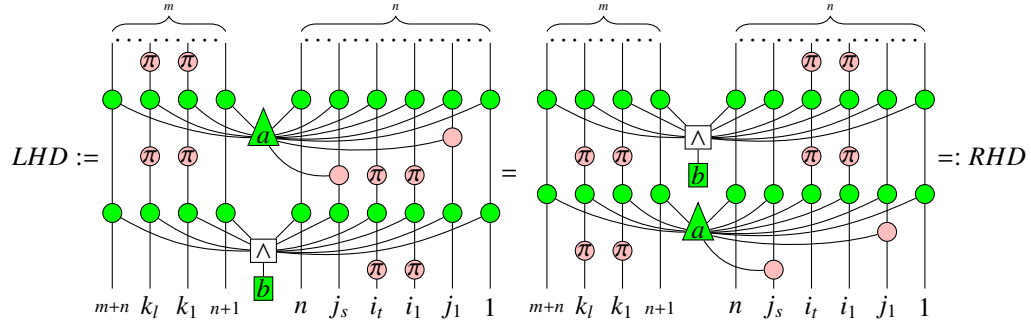


Proof: If $\{k_1, \dots, k_l\} = \emptyset$, then it is just the case of Proposition 4.27. Below we assume that $\{k_1, \dots, k_l\} \neq \emptyset$. Since $\emptyset \neq \{h_1, \dots, h_u\}$, we assume that $\{h_1\} \neq \emptyset$. Then we have



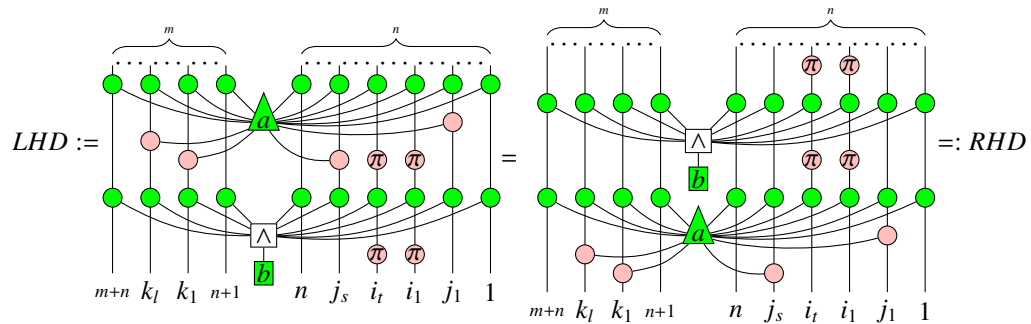
□

Proposition 4.49 Suppose the node a is connected to j_1, \dots, j_s on the right n wires via pink nodes, pairs of red π nodes separated by green nodes connected to a are located on k_1, \dots, k_l , pairs of red π nodes separated by green nodes connected to b are located on i_1, \dots, i_t . Furthermore, $\{i_1, \dots, i_t\} \subseteq \{1, \dots, n\}, \emptyset \neq \{j_1, \dots, j_s\} \subseteq \{1, \dots, n\}, \emptyset \neq \{k_1, \dots, k_l\} \subseteq \{n+1, \dots, n+m\}$. Then



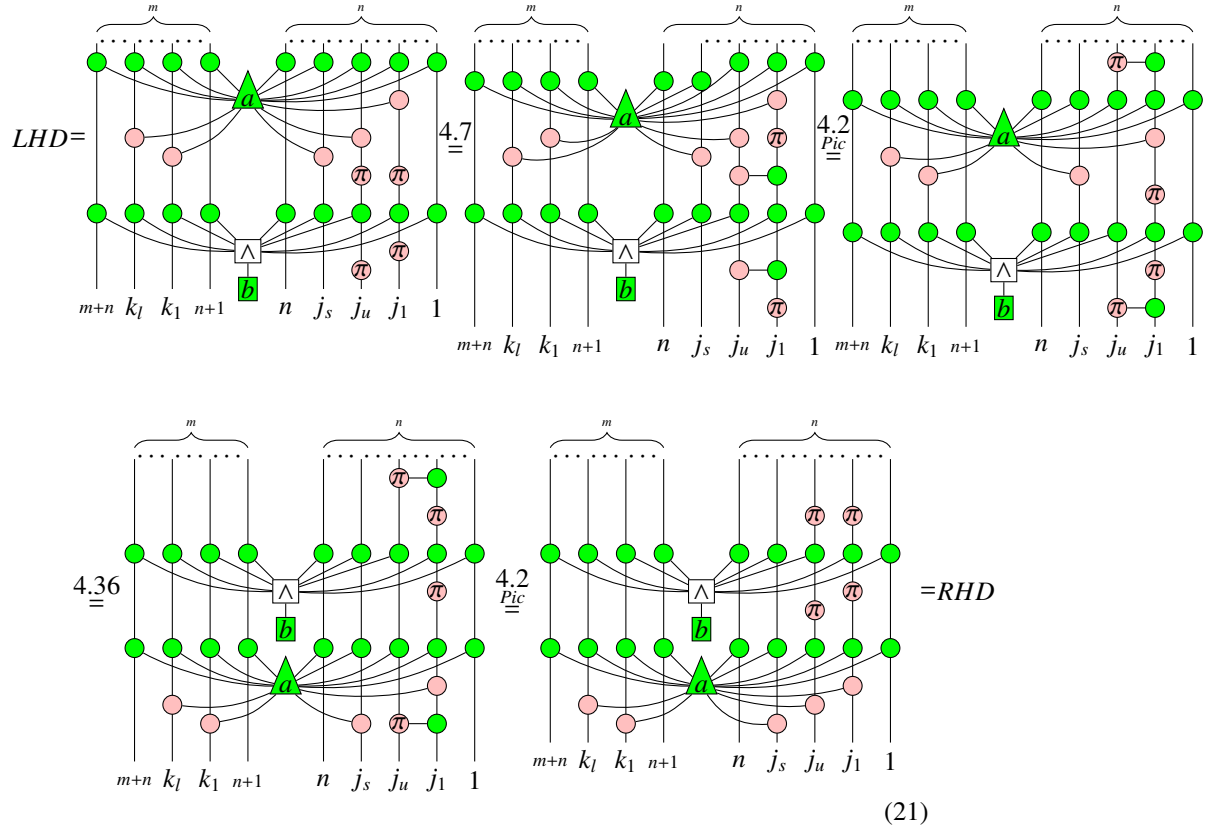
Proof: Since $\{k_1, \dots, k_l\} \cap \{j_1, \dots, j_s\} = \emptyset$, it is just one of the cases of Proposition 4.36, so we are done. □

Proposition 4.50 Suppose the node a is connected to j_1, \dots, j_s on the right n wires via pink nodes, and connected to k_1, \dots, k_l on the left m wires via pink nodes; pairs of red π nodes separated by green nodes connected to b are located on i_1, \dots, i_t . Furthermore, $\emptyset \neq \{i_1, \dots, i_t\} \subseteq \{1, \dots, n\}, \emptyset \neq \{j_1, \dots, j_s\} \subseteq \{1, \dots, n\}, \emptyset \neq \{k_1, \dots, k_l\} \subseteq \{n+1, \dots, n+m\}$. Then



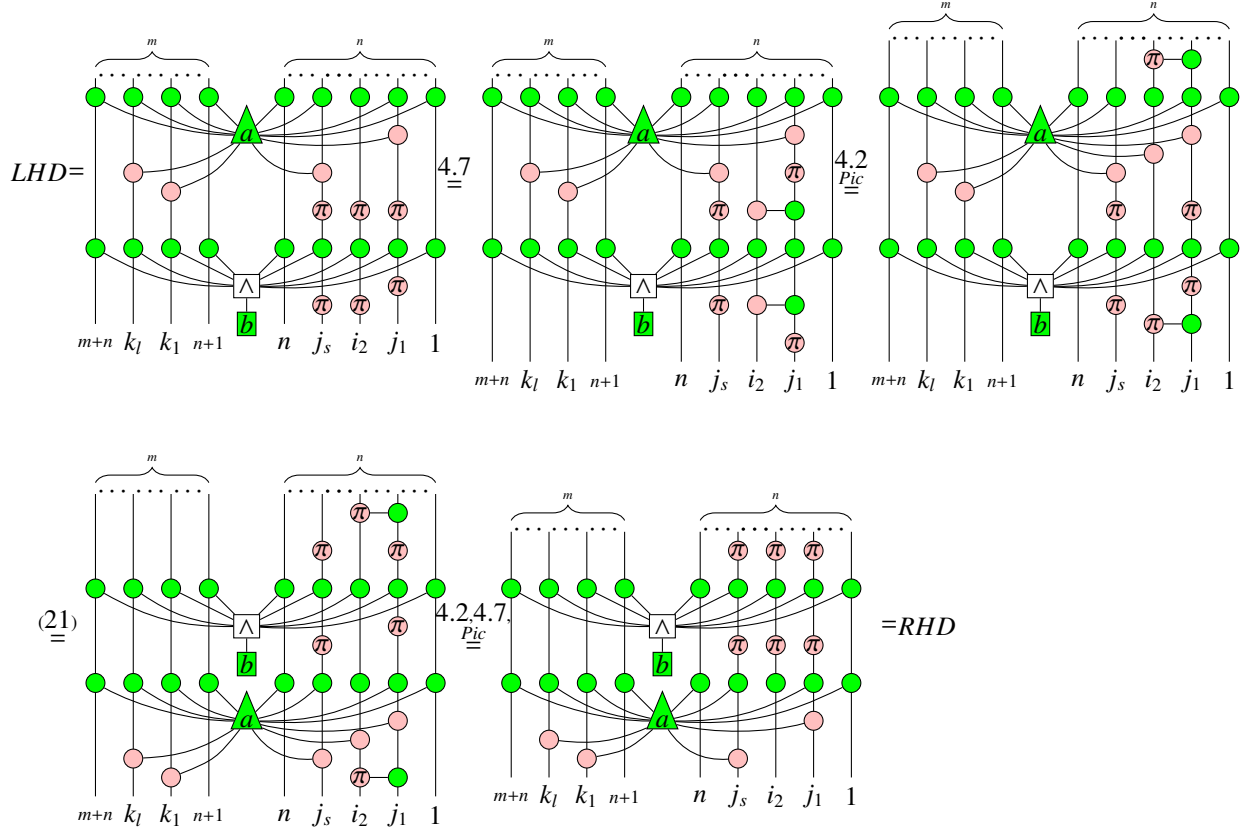
Proof: If $|\{i_1, \dots, i_t\} \cap \{j_1, \dots, j_s\}| \leq 1$, then it is just one of the cases of Proposition 4.36, so we are done. Below we assume that $|\{i_1, \dots, i_t\} \cap \{j_1, \dots, j_s\}| \geq 2$. If

$\{i_1, \dots, i_t\} \subseteq \{j_1, \dots, j_s\}$, we assume w.l.g that $i_1 = j_1, i_t = j_u$. Then we have



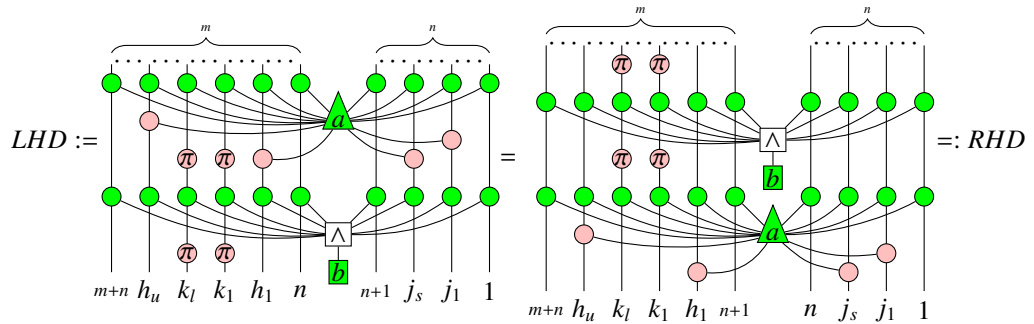
If $\{i_1, \dots, i_t\} \not\subseteq \{j_1, \dots, j_s\}$, we assume w.l.g that $i_1 = j_1, i_t = j_s, i_2 \notin \{j_1, \dots, j_s\}$. Then

by the proof of the last case we have



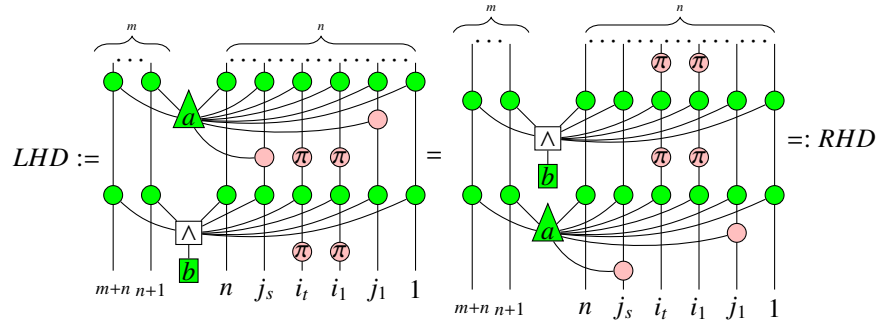
□

Corollary 4.51 Suppose the node a is connected to j_1, \dots, j_s on the right n wires via pink nodes, and connected to h_1, \dots, h_u on the left m wires via pink nodes; pairs of red π nodes separated by green nodes connected to b are located on k_1, \dots, k_l . Furthermore, $\emptyset \neq \{j_1, \dots, j_s\} \subseteq \{1, \dots, n\}, \emptyset \neq \{k_1, \dots, k_l\} \subseteq \{n+1, \dots, n+m\}, \emptyset \neq \{h_1, \dots, h_u\} \subseteq \{n+1, \dots, n+m\}$. Then

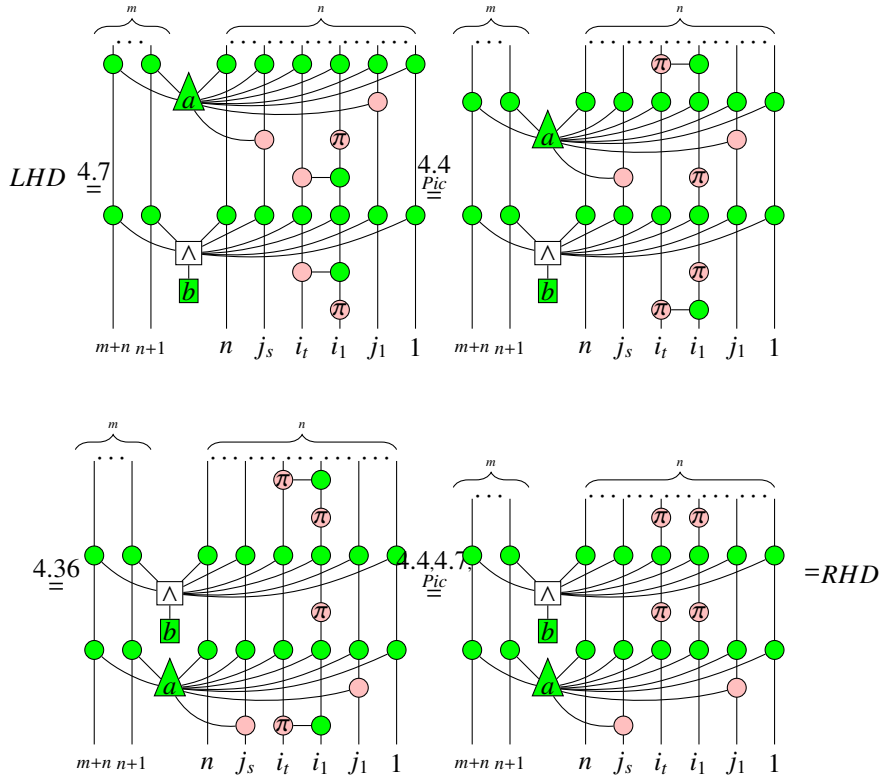


This is just the symmetric case of Proposition 4.50, thus can be obtained by swapping wires.

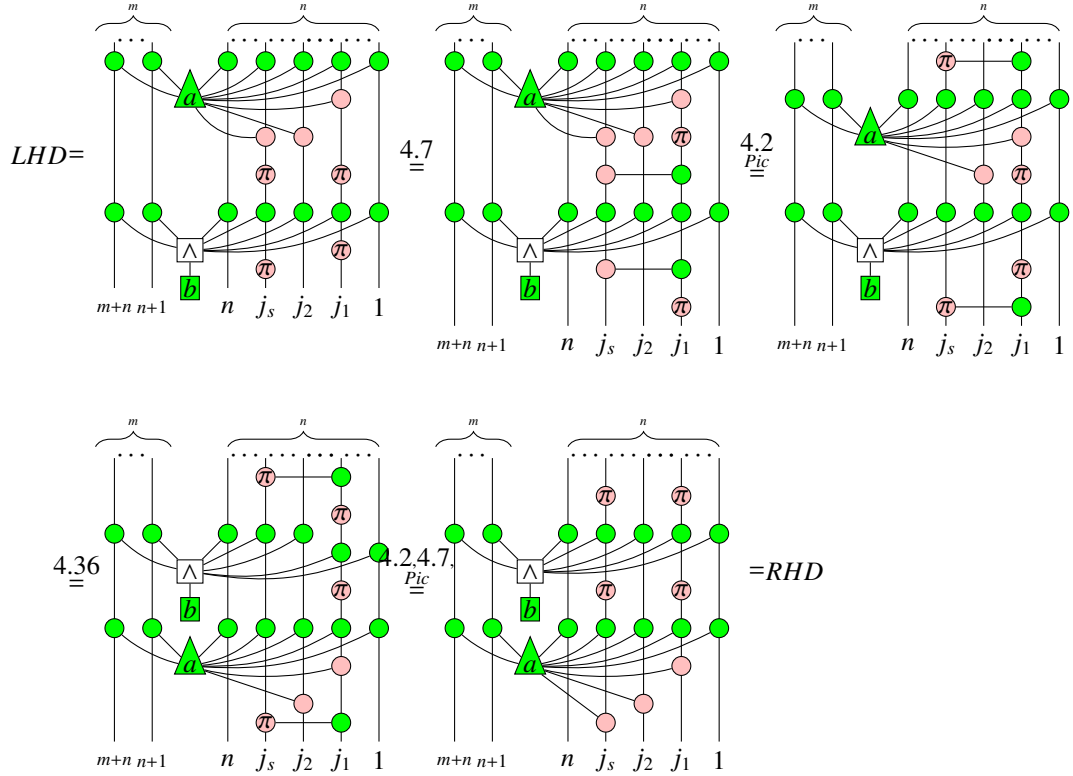
Proposition 4.52 Suppose the node a is connected to j_1, \dots, j_s on the right n wires via pink nodes, pairs of red π nodes separated by green nodes connected to b are located on i_1, \dots, i_t . Furthermore, $\emptyset \neq \{i_1, \dots, i_t\} \subseteq \{1, \dots, n\}, \emptyset \neq \{j_1, \dots, j_s\} \subseteq \{1, \dots, n\}, \{i_1, \dots, i_t\} \neq \{j_1, \dots, j_s\}$. Then



Proof: If $\{i_1, \dots, i_t\} \not\subseteq \{j_1, \dots, j_s\}$, we assume w.l.g that $i_1 \notin \{j_1, \dots, j_s\}$. Then by Proposition 4.36 we have

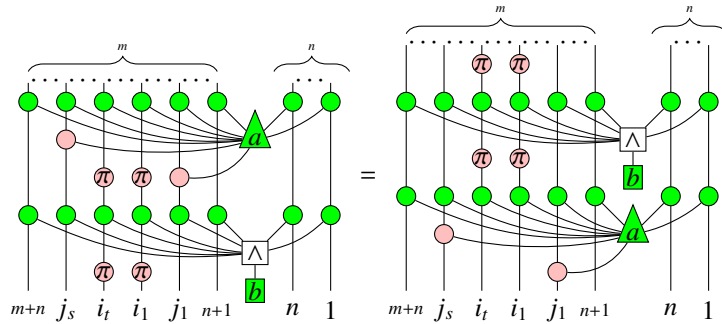


If $\{i_1, \dots, i_t\} \subseteq \{j_1, \dots, j_s\}$, since $\{i_1, \dots, i_t\} \neq \{j_1, \dots, j_s\}$, we assume w.l.g that $i_1 = j_1, i_t = j_s, j_2 \notin \{i_1, \dots, i_t\}$. Then by Proposition 4.36 we have



□

Corollary 4.53 Suppose the node a is connected to j_1, \dots, j_s on the left m wires via pink nodes, pairs of red π nodes separated by green nodes connected to b are located on i_1, \dots, i_t . Furthermore, $\emptyset \neq \{i_1, \dots, i_t\} \subseteq \{1+n, \dots, m+n\}, \emptyset \neq \{j_1, \dots, j_s\} \subseteq \{1+n, \dots, m+n\}, \{i_1, \dots, i_t\} \neq \{j_1, \dots, j_s\}$. Then



This is just the symmetric case of Proposition 4.52, thus can be obtained by swapping wires.

5 Completeness of ZX-calculus via elementary transformations

In this section, we prove the following main theorem based on a normal form of an arbitrary vector which is obtained via elementary transformations.

Theorem 5.1 *The ZX-calculus is complete with respect to the rules in Figure 1.*

5.1 Normal form

Suppose $\{e_k | 0 \leq k \leq 2^m - 1\}$ are the 2^m -dimensional standard unit column vectors (with entries all 0s except for one 1):

$$e_k = \begin{pmatrix} 0 \\ \vdots \\ 1 \\ \vdots \\ 0 \end{pmatrix} \begin{matrix} r_0 \\ \\ r_k \\ \\ r_{2^m-1} \end{matrix}$$

where r_i denote the i -th row, $0 \leq i \leq 2^m - 1$, $m \geq 1$.

Let

$$|0\rangle = \begin{pmatrix} 1 \\ 0 \end{pmatrix}, |1\rangle = \begin{pmatrix} 0 \\ 1 \end{pmatrix}.$$

Then

$$|a_{m-1} \cdots a_i \cdots a_0\rangle = e_{\sum_{i=0}^{m-1} a_i 2^i}, \quad (22)$$

where $a_i \in \{0, 1\}$, $0 \leq i \leq m - 1$ [10].

To have the normal form, we first need to have a graphical representation of elementary row addition. Suppose that $0 \leq j_1 < \cdots < j_s \leq m - 1$, $1 \leq s \leq m$. We claim that the following diagram



where a_j connects to j_1, \dots, j_s via red dots represents the $2^m \times 2^m$ row-addition elementary matrix:

$$A_j = \begin{pmatrix} 1 & \cdots & 0 & \cdots & 0 \\ \vdots & \ddots & & & \vdots \\ 0 & \cdots & 1 & \cdots & a_j \\ \vdots & & & \ddots & \vdots \\ 0 & \cdots & 0 & \cdots & 1 \end{pmatrix} \begin{matrix} r_0 \\ \\ r_j \\ \\ r_{2^m-1} \end{matrix}$$

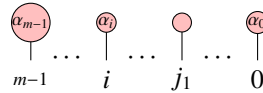
where a_j lies in the r_j row, $j = 2^m - 1 - (2^{j_1} + \cdots + 2^{j_s})$. We demonstrate this in the following. Note that all the columns $\{A_{jk} | 0 \leq k \leq 2^m - 1\}$ of A_j are standard unit vectors except the last (counted from left to right) column. This means

$$A_{jk} = A_j e_k = \begin{cases} e_k, & 0 \leq k \leq 2^m - 2 \\ e_{2^m-1} + a_j e_j, & k = 2^m - 1 \end{cases}$$

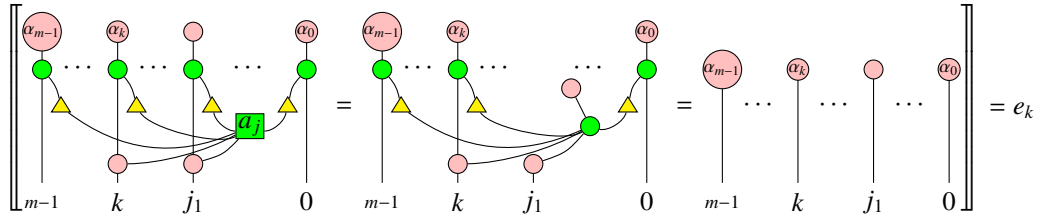
where

$$A_{j2^m-1} = \begin{pmatrix} 0 \\ \vdots \\ a_j \\ \vdots \\ 1 \end{pmatrix} \begin{matrix} r_0 \\ \\ r_j \\ \\ r_{2^m-1} \end{matrix}$$

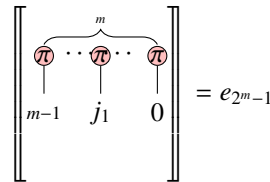
By the equality (22), we let $e_k = |a_{m-1} \cdots a_i \cdots a_0\rangle$. Clearly, if $0 \leq k \leq 2^m - 2$, then some a_i must be 0, $0 \leq i \leq m - 1$. Suppose $a_{j_1} = 0$, then e_k can be represented by the following diagram:



where $\alpha_i \in \{0, \pi\}$, $0 \leq i \leq m - 1$. Then for $0 \leq k \leq 2^m - 2$, we have



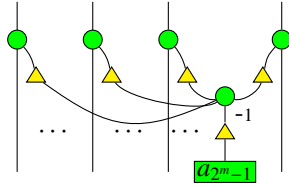
For $k = 2^m - 1$, we have



$$\begin{aligned}
 & \left[\begin{array}{c} \pi \\ \vdots \\ \pi \end{array} \right]_{m-1} \dots \left[\begin{array}{c} \pi \\ \vdots \\ \pi \end{array} \right]_{j_s} \dots \left[\begin{array}{c} \pi \\ \vdots \\ \pi \end{array} \right]_{j_1} \dots \left[\begin{array}{c} \pi \\ \vdots \\ \pi \end{array} \right]_0 = \left[\begin{array}{c} \pi \\ \vdots \\ \pi \end{array} \right]_{m-1} \dots \left[\begin{array}{c} \pi \\ \vdots \\ \pi \end{array} \right]_{j_s} \dots \left[\begin{array}{c} \pi \\ \vdots \\ \pi \end{array} \right]_{j_1} \dots \left[\begin{array}{c} \pi \\ \vdots \\ \pi \end{array} \right]_0 \\
 & = \overbrace{|1 \cdots 1\rangle}^m + a_j | \underset{m-1}{1} \cdots \underset{j_s}{0} \cdots \underset{j_1}{1} \cdots \underset{0}{0} \cdots 1 \rangle \\
 & = e_{2^{m-1}} + a_j e_j
 \end{aligned}$$

where we used (22) for the last equality. Therefore, we have shown that the diagram (23) represents the matrix A_j .

Similarly we can check that the following diagram



represents the row-multiplication matrix:

$$M = \begin{pmatrix} 1 & \cdots & 0 & \cdots & 0 \\ \vdots & \ddots & \vdots & \ddots & \vdots \\ 0 & \cdots & 1 & \cdots & 0 \\ \vdots & & & \ddots & \vdots \\ 0 & \cdots & 0 & \cdots & a_{2^m-1} \end{pmatrix} \begin{matrix} r_0 \\ \vdots \\ r_k \\ \vdots \\ r_{2^m-1} \end{matrix}$$

Given an arbitrary vector $(a_0, a_1, \dots, a_{2^m-1})^T$ with $a_i \in \mathbb{C}, m \geq 1$, we claim that it can be uniquely represented by the following normal form:

$$(24)$$

where for those diagrams which represent row additions, a_i connects to wires with pink nodes depending on i , and all possible connections are included in the normal form. Actually, one can check that there are $\binom{m}{1} + \binom{m}{2} + \cdots + \binom{m}{m} = 2^m - 1$ row additions in

the normal form. By Proposition 4.27, all the row addition diagrams are commutative with each other.

The normal form (24) is actually obtained via the following processes:

$$\begin{pmatrix} 0 \\ 0 \\ \vdots \\ 1 \end{pmatrix} \xrightarrow[\text{addition}]{\text{row}} \begin{pmatrix} a_0 \\ 0 \\ \vdots \\ 1 \end{pmatrix} \xrightarrow[\text{addition}]{\text{row}} \begin{pmatrix} a_0 \\ a_1 \\ \vdots \\ a_{2^m-2} \\ 1 \end{pmatrix} \xrightarrow[\text{multiplication}]{\text{row}} \begin{pmatrix} a_0 \\ a_1 \\ \vdots \\ a_{2^m-2} \\ a_{2^m-1} \end{pmatrix}$$

In the case of $m = 0$, for any complex number a , its normal form is defined as

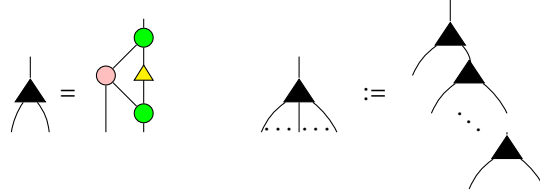


where

$$\begin{bmatrix} \pi \\ a \end{bmatrix} = a$$

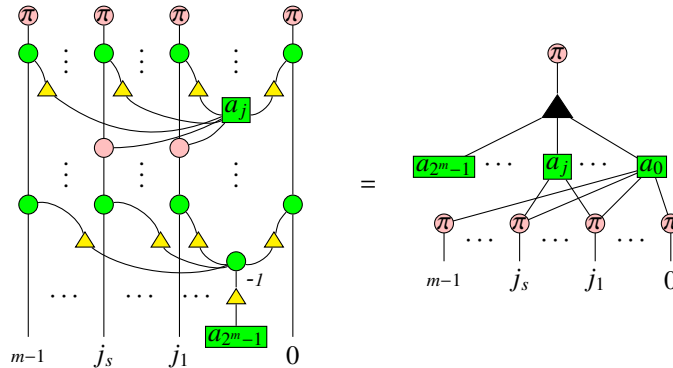
By the map-state duality as given in (25), we obtain the universality of ZX-calculus over \mathbb{C} : any $2^m \times 2^n$ matrix A with $m, n \geq 0$ can be represented by a ZX diagram.

Now we make the following conventions due to the rule (Aso).



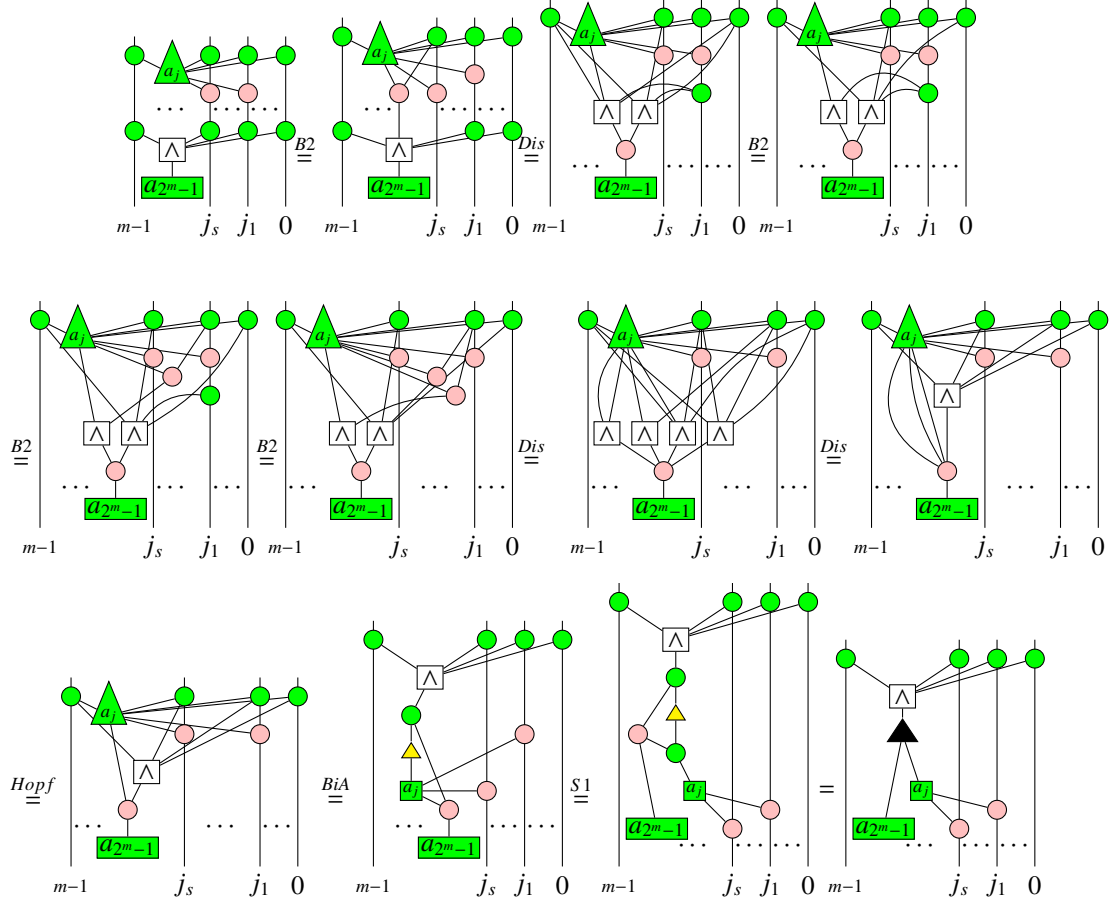
At the end of this subsection, we give another form to the normal form (24) as follows.

Proposition 5.2



where each green box a_j connects to pink π nodes at the locations labelled as j_1, \dots, j_s with $j = 2^m - 1 - (2^{j_1} + \dots + 2^{j_s}), 0 \leq j_1 < \dots < j_s \leq m - 1$. In another words, j_1, \dots, j_s are exactly the locations where the coefficients are 0 in the binary expansion $j = \sum_{i=0}^{m-1} a_i 2^i$.

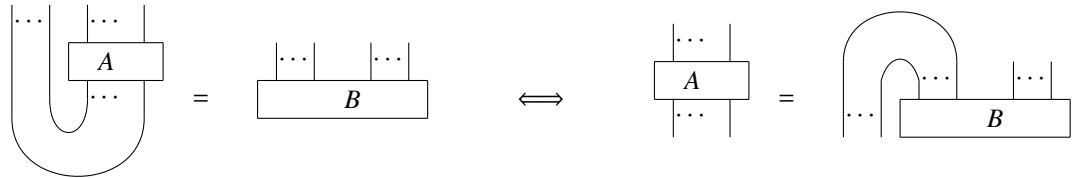
Proof:



Repeat this processes and by the associative rule (Aso) and the π copy rule (B3) we then finish the proof. \square

5.2 Completeness

Completeness means for any two diagrams D_1 and D_2 , if $\llbracket D_1 \rrbracket = \llbracket D_2 \rrbracket$, then $D_1 = D_2$ can be derived from the ZX rules. Because of the following map-state duality, we can assume that each diagram is a state diagram (diagram without any input):



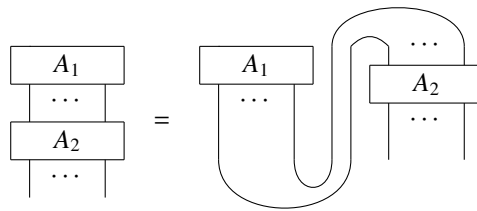
(25)

For proof of completeness, assume that $\llbracket D_1 \rrbracket = \llbracket D_2 \rrbracket$. The proof strategy is to show that each state diagram (including scalars) can be written into a normal form. Then D_1 and D_2 must have the same normal form, since $\llbracket D_1 \rrbracket = \llbracket D_2 \rrbracket$. So we can rewrite D_1 into D_2 by first rewriting D_1 into its normal form then inverting the rewriting (which is a series of equalities) from D_2 to its normal form, which means $D_1 = D_2$ can be derived from the ZX rules.

In general, each state diagram has the following form:



where A_1, A_2, \dots, A_n are diagrams composed of generators in parallel. Since A_1 is a state diagram, it must be composed of cap or \bullet . Also, we have



which means if the tensor of two normal forms can be rewritten into a normal form, a bending of any generator can be rewritten into a normal form, and a self-plugging on a normal form (connecting two outputs of a normal form with a cup) can be rewritten into a normal form, then a normal form sequentially connected with a diagram composed of tensors of generators can be rewritten into a normal form. As a consequence, any state diagram as depicted in (26) can be rewritten into a normal form.

To summarise, we need to prove the following statements:

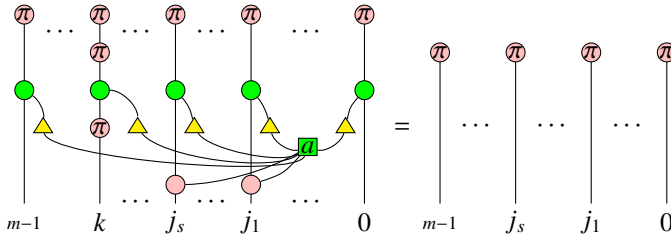
1. the juxtaposition of any two diagrams in normal form can be rewritten into a normal form.
2. a self-plugging on a diagram in normal form can be rewritten into a normal form.
3. all generators bended in state diagrams or already being state diagrams can be rewritten into normal forms.

5.2.1 Rewrite the tensor product of two normal forms into a normal form

First, we note that for $m = 0$, the tensor of two scalar diagrams in normal form is still a normal form:

$$\begin{array}{c} \pi \\ | \\ \square a \end{array} \begin{array}{c} \pi \\ | \\ \square b \end{array} \stackrel{B3}{=} \begin{array}{c} \pi \\ / \quad \backslash \\ \square a \quad \square b \end{array} \stackrel{S1}{=} \begin{array}{c} \pi \\ | \\ \square ab \end{array}$$

Proposition 5.3



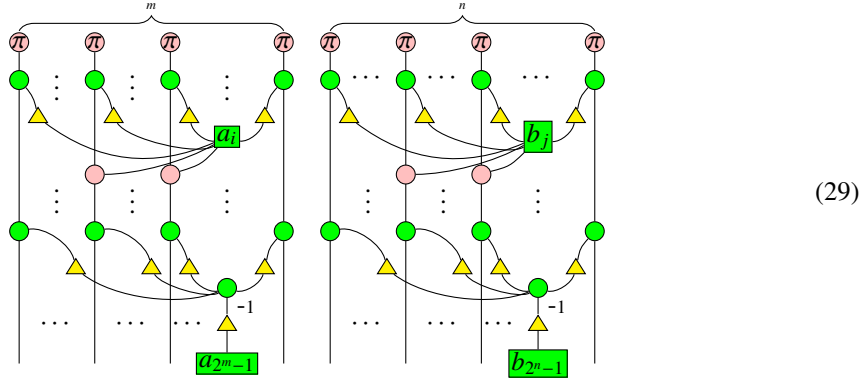
Given two normal forms such that

$$\left[\begin{array}{c} \pi \quad \pi \quad \pi \quad \pi \\ \vdots \quad \vdots \quad \vdots \quad \vdots \\ \square a_1 \\ \vdots \quad \vdots \quad \vdots \quad \vdots \\ \square a_{2^{m-2}} \\ \vdots \quad \vdots \quad \vdots \quad \vdots \\ \square a_{2^{m-1}} \end{array} \right] = \begin{pmatrix} a_0 \\ a_1 \\ \vdots \\ a_{2^{m-2}} \\ a_{2^{m-1}} \end{pmatrix} \tag{27}$$

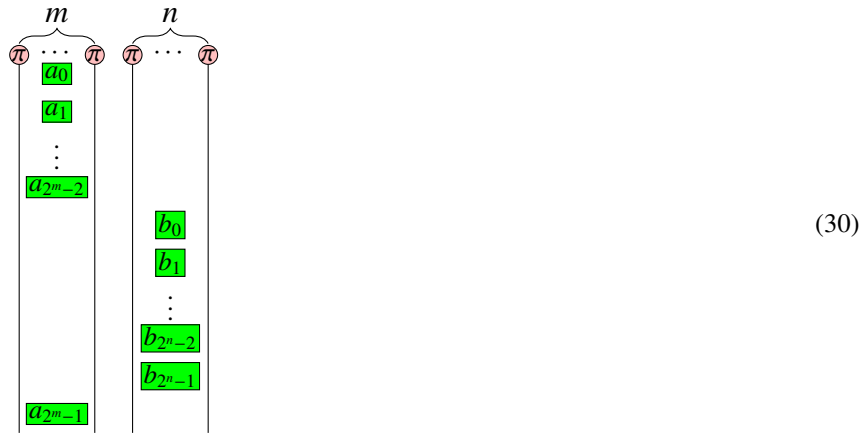
and

$$\left[\begin{array}{c} \pi \quad \pi \quad \pi \quad \pi \\ \vdots \quad \vdots \quad \vdots \quad \vdots \\ \square b_1 \\ \vdots \quad \vdots \quad \vdots \quad \vdots \\ \square b_{2^{n-2}} \\ \vdots \quad \vdots \quad \vdots \quad \vdots \\ \square b_{2^{n-1}} \end{array} \right] = \begin{pmatrix} b_0 \\ b_1 \\ \vdots \\ b_{2^{n-2}} \\ b_{2^{n-1}} \end{pmatrix} \tag{28}$$

where m, n are positive integers, $a_i, b_j \in \mathbb{C}$. We want to rewrite the following tensor product of two normal forms into a single normal form:

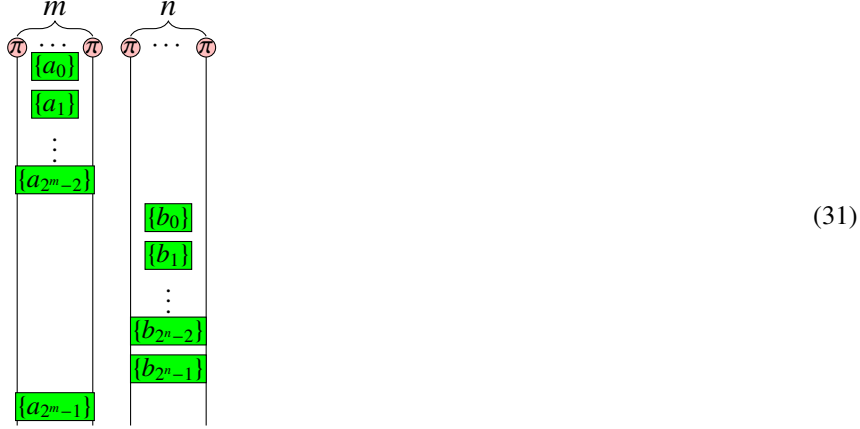


By naturality of the ambient category for ZX-calculus, each diagram can move freely upside and down without going across any other diagrams. Furthermore, the row addition diagrams can commute with each other. Therefore, we can rearrange the order of the diagrams of elementary transformations in the following way:



where for simplicity we use labelled boxes to represent the corresponding diagrams of elementary transformations. Then we apply the equalities (10), (11), (12), (13) which turn the tensor of diagrammatic elementary transformation and parallel wires into a

connected diagram, and we get



where for $0 \leq i \leq 2^m - 1$, $\{a_i\}$ represents the family of 2^n elementary transformations labelled by a_i but with different distribution of red π pairs on the right-most n wires; and for $0 \leq j \leq 2^n - 1$, $\{b_j\}$ represents the family of 2^m elementary transformations labelled by b_j but with different distribution of red π pairs on the left-most m wires. By Proposition 4.32 and Proposition 4.33, diagrams in any $\{a_i\}$ family or $\{b_j\}$ family are commutative to each other. First let the a_{2^m-1} diagram without any red π pair commute with other diagrams in the $\{a_{2^m-1}\}$ family until it is placed at the bottom of the diagram in (31). Then let the b_{2^n-1} diagram without any red π pair first commute with other diagrams in the $\{b_{2^n-1}\}$ family, and furthermore commute with all the a_{2^m-1} diagrams with red π pairs by Proposition 4.36, finally reaches the place right above the a_{2^m-1} diagram without any red π pair. By Corollary 3.42, these two diagrams which have no red π pairs can be combined into a single $a_{2^m-1}b_{2^n-1}$ diagram without any red π pair.

Below we show step by step how to get all the $a_i b_j$ diagrams ($0 \leq i \leq 2^m - 2$, $0 \leq j \leq 2^n - 2$) without any red π pair while cancelling out other diagrams with red π pairs.

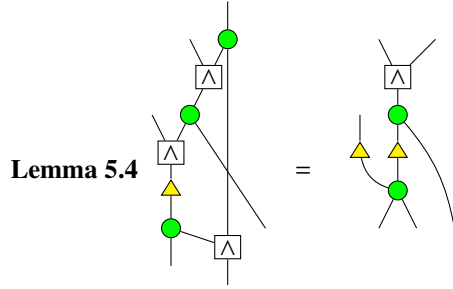
1. In the $\{a_0\}$ family, by Proposition 5.3, each diagram with red π pair will be annihilated by the red π nodes on top, thus only $\{a_0\}$ with no red π pair left, which will be denoted as A_0 .
2. In the $\{b_0\}$ family, there are $2^m - 1$ diagrams with red π pairs, but only one of them has the same location distribution (on the left-most m wires) as that of the pink nodes connected with the output of the a_0 box in A_0 , we denote this diagram by $b_0^{a_0}$. Then $b_0^{a_0}$ commutes with other diagrams of the $\{b_0\}$ family. It also commutes with each diagram of the families $\{a_1\}, \{a_2\}, \dots, \{a_{2^m-2}\}$, following Proposition 4.46. Then $b_0^{a_0}$ can commute to be right below A_0 . Now by Proposition 4.39, we get the diagram $a_0 b_0$ (without any red π pair) and A_0 again, while $b_0^{a_0}$ is consumed. By Proposition 4.27, $a_0 b_0$ commutes with A_0 . Furthermore, $a_0 b_0$ commutes with each diagram in the $\{a_i\}$ family, $0 \leq i \leq 2^m - 2$, by Proposition 4.47; commutes with each diagram in the $\{b_i\}$ family, $0 \leq i \leq 2^n - 2$, by Proposition 4.48; commutes with each diagram in the $\{b_{2^n-1}\}$ family (with red π

pairs), by Corollary 4.51; and commutes with each diagram in the $\{a_{2^m-1}\}$ family (with red π pairs), by Proposition 4.50. Therefore a_0b_0 can be commuted to be right above the diagram $a_{2^m-1}b_{2^n-1}$.

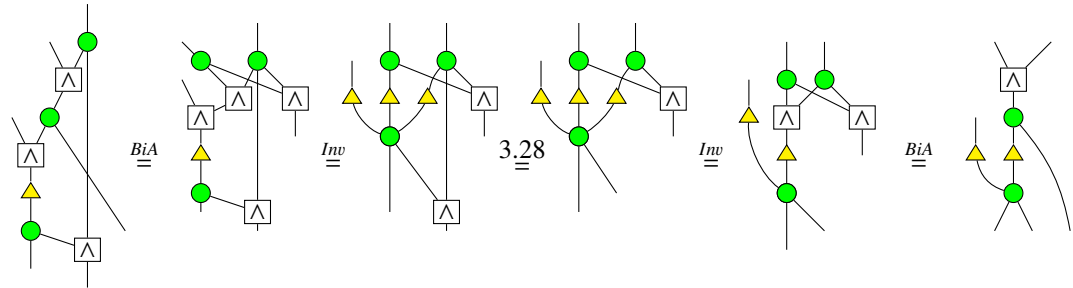
3. Similarly, we can choose $b_i^{a_0}$ from the $\{b_i\}$ family, for $1 \leq i \leq 2^n - 2$, where $b_i^{a_0}$ has the same location distribution (on the left-most m wires) of red π pairs as that of the pink nodes connected with the output of the a_0 box in A_0 . Repeating the method of step 4, we get diagrams a_0b_i located sequentially right above a_0b_0 , for $1 \leq i \leq 2^n - 2$, with all those $b_i^{a_0}$ eliminated.
4. Now choose $b_{2^n-1}^{a_0}$ from the $\{b_{2^n-1}\}$ family, where $b_{2^n-1}^{a_0}$ has the same location distribution (on the left-most m wires) of red π pairs as that of the pink nodes connected with the output of the a_0 box in A_0 . Since all the $b_i^{a_0}$, $0 \leq i \leq 2^n - 2$ have been eliminated, by Proposition 4.36, $b_{2^n-1}^{a_0}$ can commute with all the remaining diagrams of the families b_i , $0 \leq i \leq 2^n - 2$, and commute with all the diagrams with red π pairs in the $\{a_i\}$ families, for $1 \leq i \leq 2^m - 2$. Furthermore, the location distribution (on the left-most m wires) of red π pairs in $b_{2^n-1}^{a_0}$ is different from the location distribution (on the left-most m wires) of pink nodes connected with the output of the a_i for $1 \leq i \leq 2^m - 2$. Then by Corollary 4.53, $b_{2^n-1}^{a_0}$ commutes with each diagram with no red π pairs in the families $\{a_i\}$ for $1 \leq i \leq 2^m - 2$. Therefore, $b_{2^n-1}^{a_0}$ can commute to be right below A_0 . By Proposition 4.38, we get $a_0b_{2^n-1}$ with no red π pairs, while $b_{2^n-1}^{a_0}$ and A_0 are eliminated. Then following the step, $a_0b_{2^n-1}$ can be commuted to the location right above a_0b_i , $0 \leq i \leq 2^n - 2$. So far, we get the products a_0b_i , $0 \leq i \leq 2^n - 1$, and all the diagrams in the $\{a_0\}$ family have been eliminated, the diagrams $b_i^{a_0}$, $1 \leq i \leq 2^n - 1$, are also eliminated, while all the diagrams in the families $\{a_i\}$, $1 \leq i \leq 2^m - 2$, remain unchanged.
5. Repeat the steps 1, 4, 3, 4 for the families $\{a_i\}$, $1 \leq i \leq 2^m - 2$, and $\{b_j\}$, $0 \leq j \leq 2^n - 1$, we get the products a_ib_j , $1 \leq i \leq 2^m - 2$, $0 \leq j \leq 2^n - 1$ at the bottom part. Now what remains is the following diagrams (from top to bottom): families $\{b_j\}$, $0 \leq j \leq 2^n - 2$, without red π pairs; family $\{a_{2^m-1}\}$ with red π pairs; the products a_ib_j , $0 \leq i \leq 2^m - 2$, $0 \leq j \leq 2^n - 1$; and the product $a_{2^m-1}b_{2^n-1}$. We still need to get the products $a_{2^m-1}b_j$, $0 \leq j \leq 2^n - 2$ and eliminate the non-product diagrams.
6. Now each $\{b_i\}$ family without red π pairs just has one diagram b_i , $0 \leq i \leq 2^n - 2$. Denote by $a_{2^m-1}^{b_i}$ the diagram in the family $\{a_{2^m-1}\}$ that has the same location distribution (on the right-most n wires) of red π pairs as that of the pink nodes connected with the output of b_i , $0 \leq i \leq 2^n - 2$. By Proposition 4.52, $a_{2^m-1}^{b_0}$ can commute with each b_i , $1 \leq i \leq 2^n - 2$ to the location just below b_0 . Then by Proposition 4.38, we get $a_{2^m-1}b_0$ with no red π pairs, while $a_{2^m-1}^{b_0}$ and b_0 are eliminated. $a_{2^m-1}b_0$ can commute with each b_i , $1 \leq i \leq 2^n - 2$, and commute with the remaining diagrams in family $\{a_{2^m-1}\}$ with red π pairs, by Proposition 4.52. Therefore, $a_{2^m-1}b_0$ can commute to the location just above the diagrams with products.
7. Repeat the step 6 for b_i , $1 \leq i \leq 2^n - 2$, we can eliminate $a_{2^m-1}^{b_i}$ and b_i , while get $a_{2^m-1}b_i$ for $1 \leq i \leq 2^n - 2$. Now what remains is the red π nodes on top and all

the products $a_i b_j, 0 \leq i \leq 2^m - 1, 0 \leq j \leq 2^n - 1$, which is a normal form.

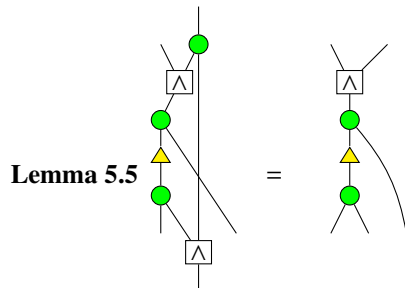
5.2.2 Self-plugging on a normal form



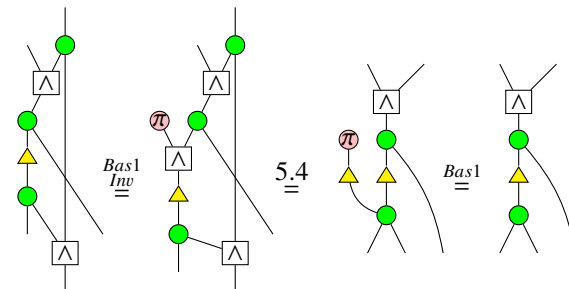
Proof:



□

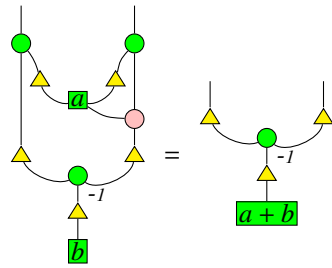


Proof:



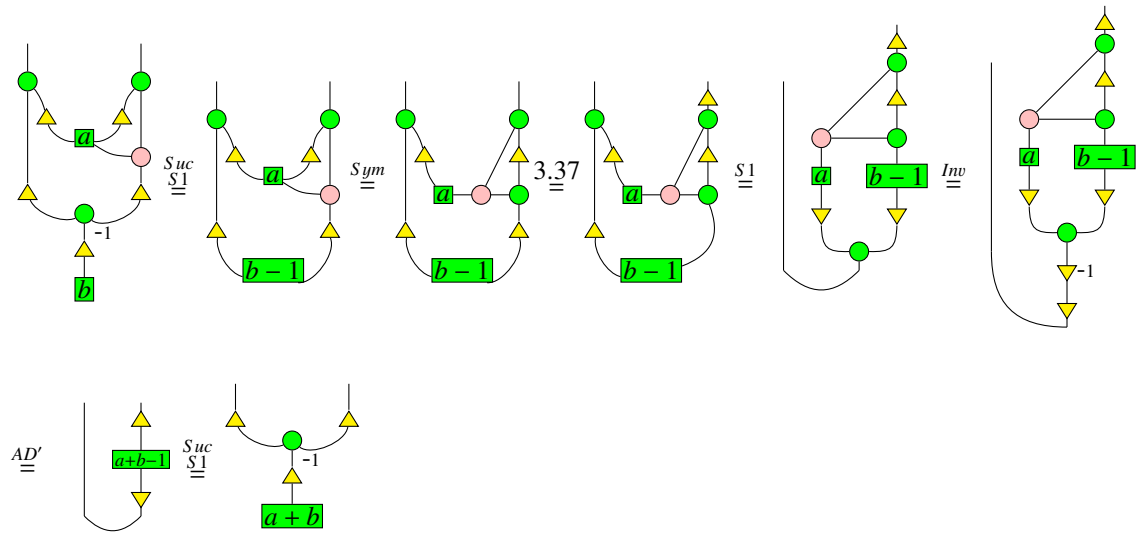
□

Proposition 5.6



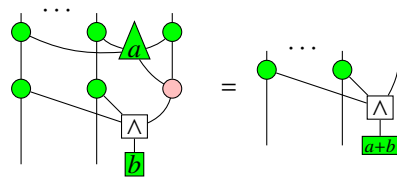
(32)

Proof:

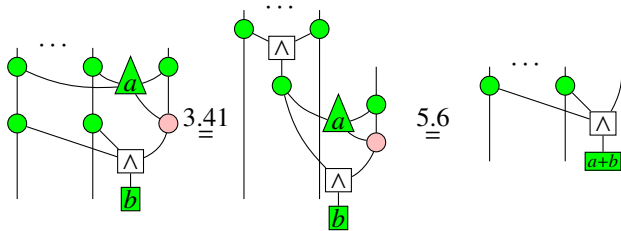


□

Corollary 5.7

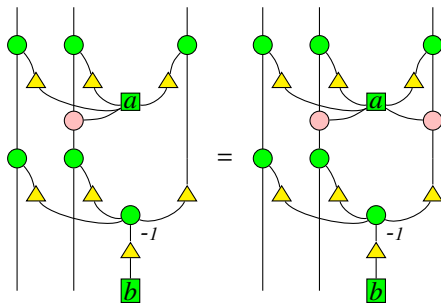


Proof:

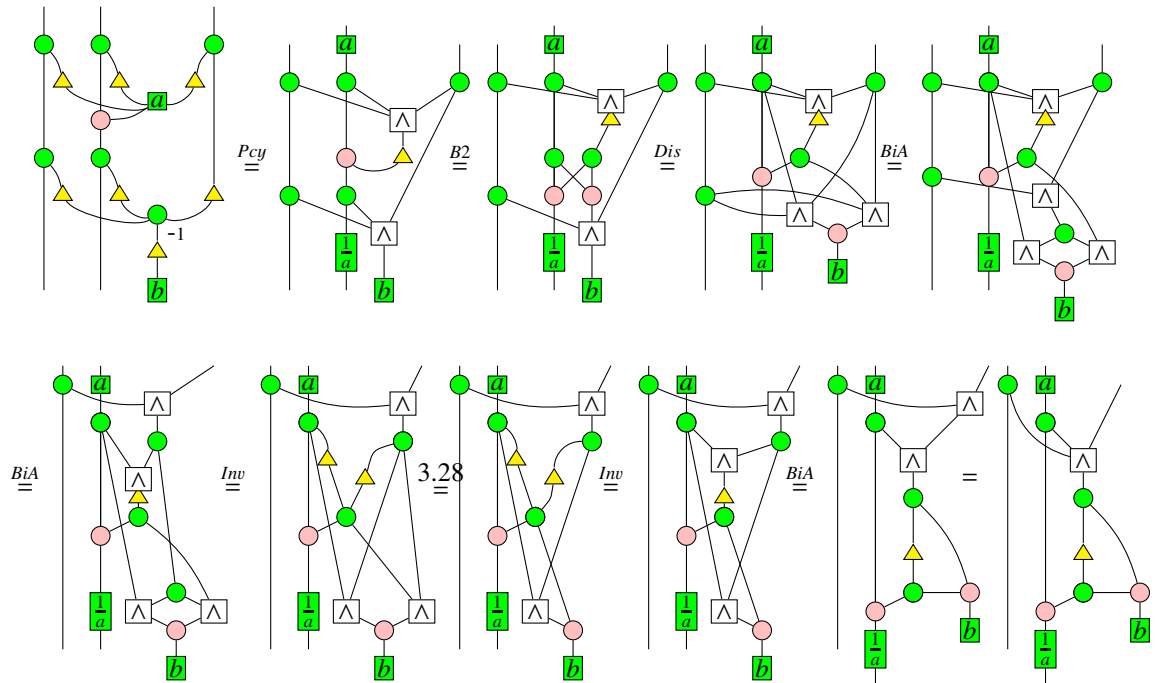


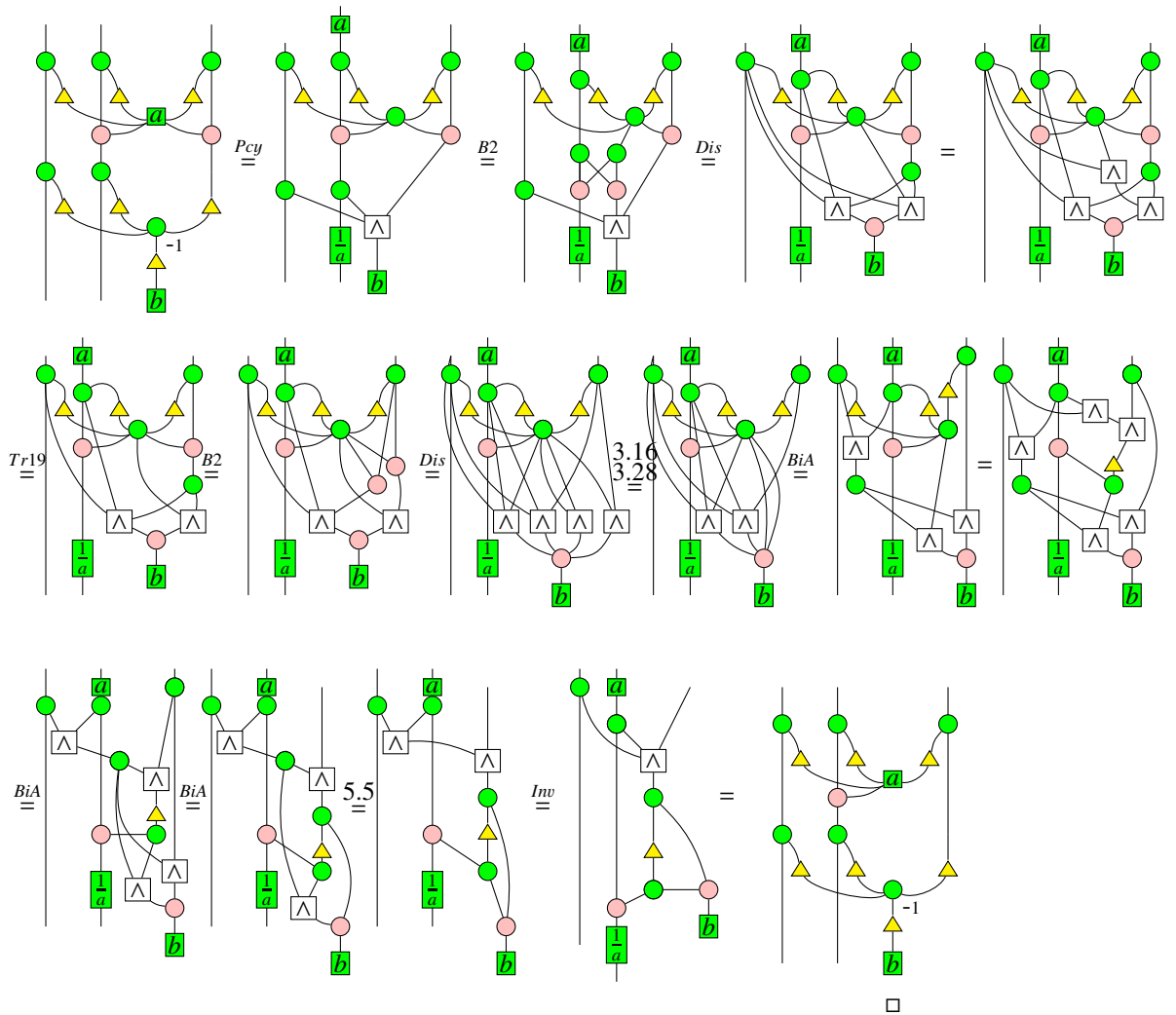
□

Proposition 5.8



Proof: If $a = 0$, then the equality holds trivially. Now we assume $a \neq 0$. Then



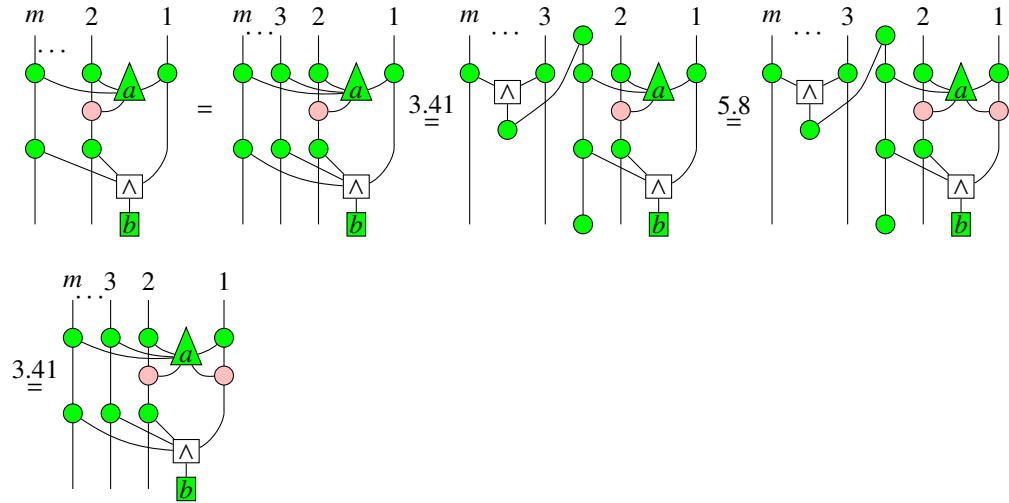


Corollary 5.9 Suppose a is connected to the i -th line via a pink node ($i > 1$). Then

Equation (33) shows two diagrams of a braid-like structure with lines labeled m , i , \dots , 1 . The diagrams are separated by an equals sign. The structure includes green circles, pink circles, yellow triangles, and boxes labeled a , b , and -1 .

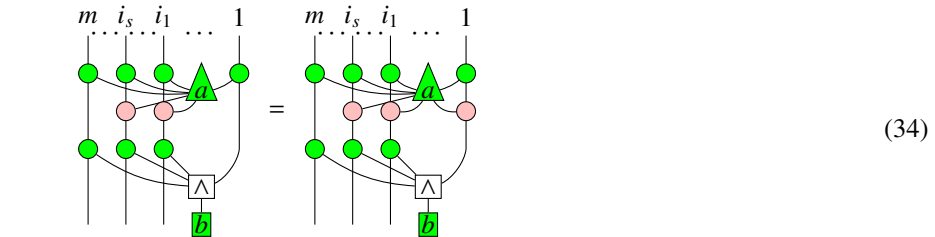
where on the left side of (33) the node a is connected to the i -th line and the 1st line via two pink nodes.

Proof: For simplicity, we prove with the short notation as shown in (2). We assume w.l.g that $i = 2$, otherwise we could swap the i -th line and the 2nd line on both sides of (33). Therefore



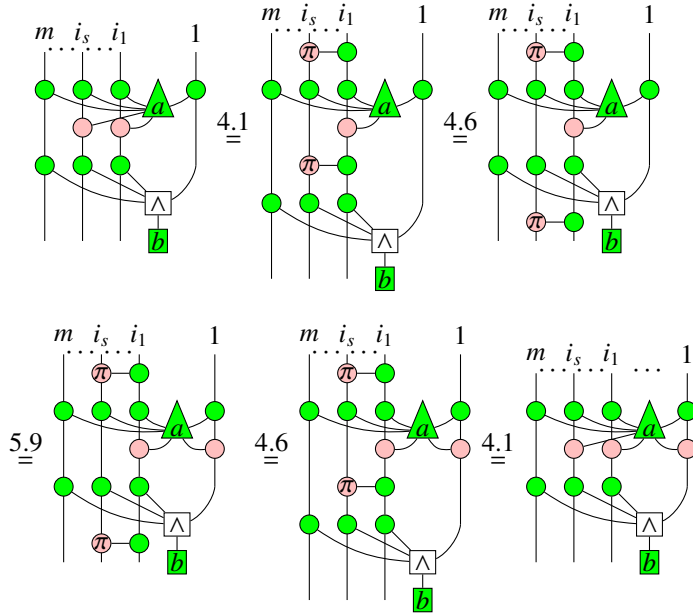
□

Proposition 5.10 Suppose a is connected to the i_1, \dots, i_s via pink nodes ($i_1 > 1$). Then one more connection can be added on the right most line:



Proof: We assume w.l.g that $i_1 = 2$, otherwise we could swap the i_1 -th line and the 2nd

line on both sides of (34). Therefore



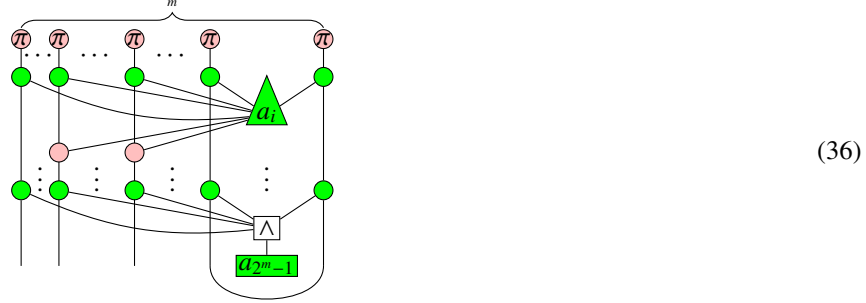
□

Theorem 5.11 *A self-plugged normal form can be rewritten into a normal form.*

Proof: Given a normal form such that

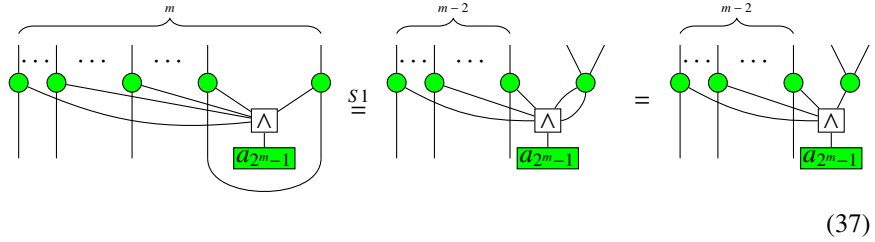
Because of symmetry, we can assume that the normal form is self-plugged on the right-

most two lines and $m \geq 2$:

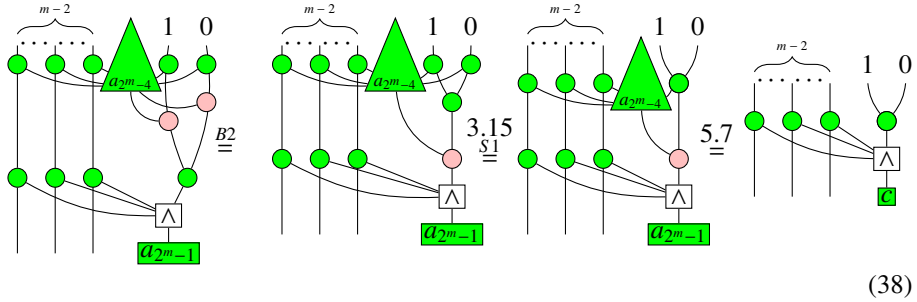


We do the rewriting in an order from bottom to top.

1. Consider the following rewriting:



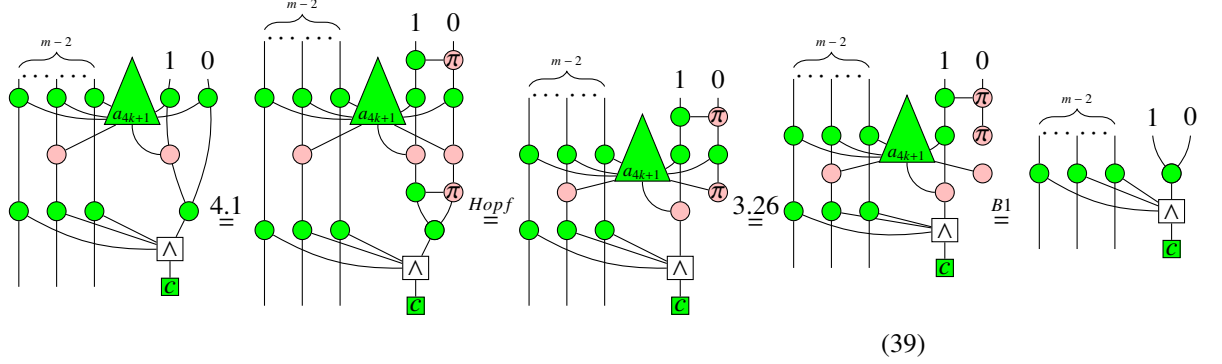
2. Consider the $a_{2^{m-4}}$ term in addition. Since $2^m - 4 = 2^m - 1 - (2^0 + 2^1)$, $a_{2^{m-4}}$ must connect to the 0-th and 1-st lines on the right-most. Then based on (37), we have



where $c = a_{2^{m-4}} + a_{2^{m-1}}$.

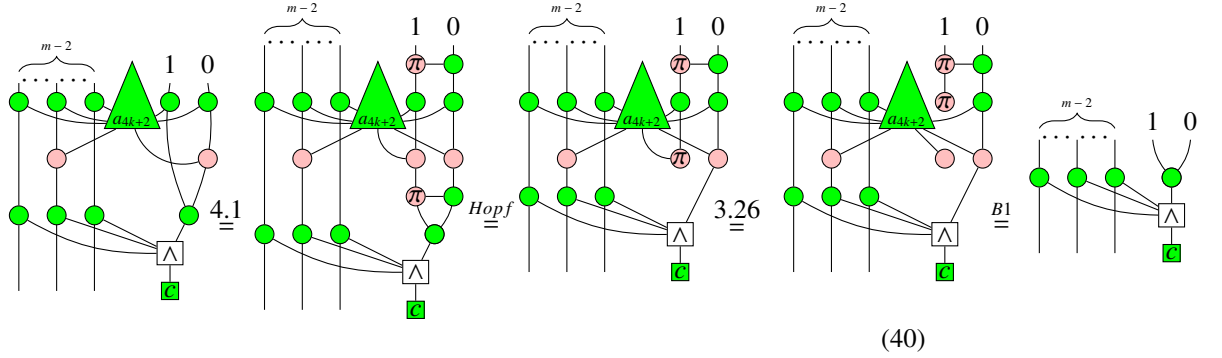
3. Consider a_{4k+1} , $0 \leq k \leq 2^{m-2} - 1$. Since $4k + 1 = 2^m - 1 - (2^{j_1} + \dots + 2^{j_s}) = 4 \cdot 2^{m-2} + 1 - (2 + 2^{j_1} + \dots + 2^{j_s})$, $j_1 < \dots < j_s$, there must exist some j_i such that $j_i = 1$, and $j_k \neq 0$, $k = 1, \dots, s$. This means a_{4k+1} must connect to the 1-st line

via a pink node while not connected to the 0-th line. Then we have



where $c = a_{2^{m-4}} + a_{2^{m-1}}$. So a_{4k+1} are all eliminated.

4. Consider $a_{4k+2}, 0 \leq k \leq 2^{m-2} - 1$. Since $4k + 2 = 2^m - 1 - (2^{j_1} + \dots + 2^{j_s}) = 4 \cdot 2^{m-2} + 2 - (3 + 2^{j_1} + \dots + 2^{j_s}), j_1 < \dots < j_s$, there must exist some j_i such that $j_i = 0$, and $j_k \neq 1, k = 1, \dots, s$. This means a_{4k+2} must connect to the 0-th line via a pink node while not connected to the 1-st line. Then we have



where $c = a_{2^{m-4}} + a_{2^{m-1}}$. So a_{4k+2} are all eliminated.

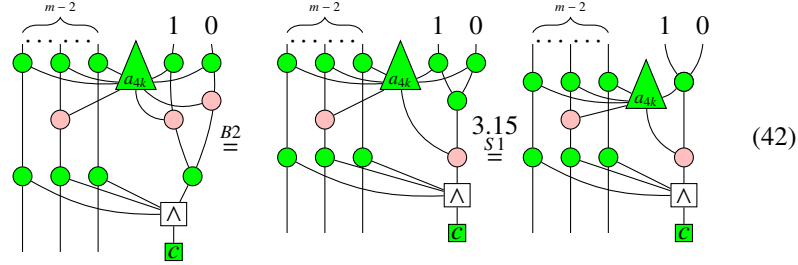
5. Now we consider the case $m = 2$. From the previous cases, a_1 and a_2 are eliminated, a_0 and a_3 are combined as in (38). Therefore we have

$$\begin{array}{c} \pi \\ \pi \\ \bullet \\ \wedge \\ \square \\ c \end{array} = \begin{array}{c} \pi \\ \pi \\ \bullet \\ \square \\ c \end{array} = \begin{array}{c} \pi \\ \bullet \\ \square \\ c \end{array} = \begin{array}{c} \pi \\ \square \\ c \end{array} \quad (41)$$

where $c = a_0 + a_3$. Thus for $m = 2$, we get a normal form.

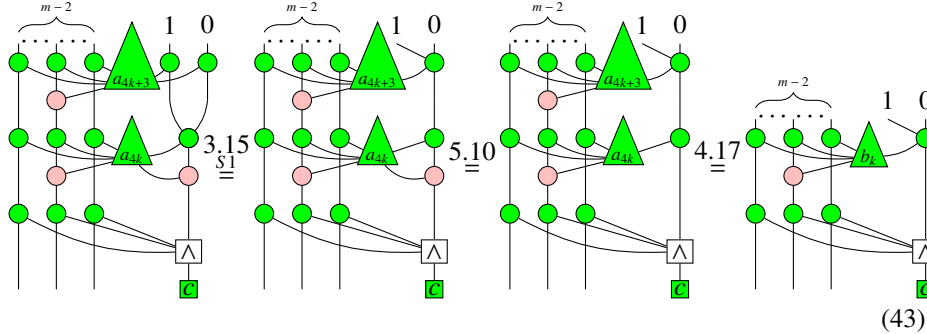
6. Consider $a_{4k}, 0 \leq k \leq 2^{m-2} - 1$. If $m = 2$, it is just the case 2 which we already considered. Now we consider $m \geq 3$ and $4k \neq 2^m - 4$. Since $4k =$

$2^m - 1 - (2^{j_1} + \dots + 2^{j_s}) = 4 \cdot 2^{m-2} - (1 + 2^{j_1} + \dots + 2^{j_s})$, $j_1 < \dots < j_s$, there must be that $j_1 = 0$, $j_2 = 1$, and there is another $j_k \geq 2$, i.e., $4k = 2^m - 4 - (2^{j_{k_1}} + \dots + 2^{j_{k_t}})$, $j_{k_i} \geq 2$. This means a_{4k} is connected with the right-most two wires and at least one wire among the left $m - 2$ wires via pink nodes. Therefore,



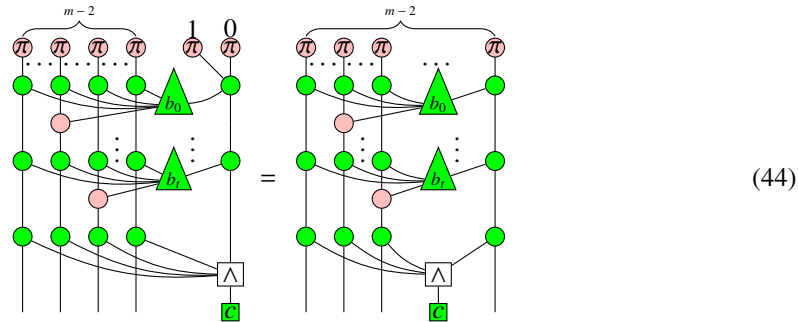
where $c = a_{2^{m-4}} + a_{2^{m-1}}$.

7. Consider a_{4k+3} , $0 \leq k \leq 2^{m-2} - 1$. If $m = 2$, it is just the case 1 which we already considered. Now we consider $m \geq 3$ and $0 \leq k < 2^{m-2} - 1$. By case 6, $4k + 3 = 2^m - 4 - (2^{j_{k_1}} + \dots + 2^{j_{k_t}}) + 3 = 2^m - 1 - (2^{j_{k_1}} + \dots + 2^{j_{k_t}})$, $j_{k_i} \geq 2$. This means a_{4k+3} is not connected with the right-most two wires but with at least one wire among the left $m - 2$ wires via pink nodes in the same way as the case of a_{4k} . Therefore,



where $c = a_{2^{m-4}} + a_{2^{m-1}}$, $b_k = a_{4k+3} + a_{4k}$, $0 \leq k \leq 2^{m-2} - 2$.

8. Finally the self-plugged normal form (36) becomes

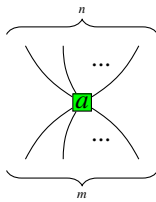


where $c = a_{2^{m-4}} + a_{2^{m-1}}$, $b_k = a_{4k+3} + a_{4k}$, $0 \leq k \leq 2^{m-2} - 2$, $t = 2^{m-2} - 2$. Clearly, the RHS of (44) is a normal form now.

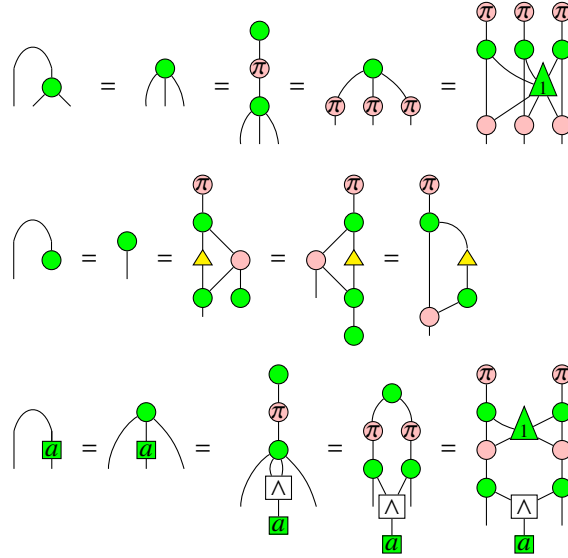
□

5.2.3 Rewriting generators into normal form

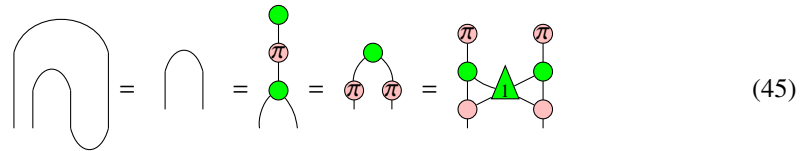
In this section, we prove that all the generators bended in state diagrams or already being state diagrams can be rewritten into normal forms.

1. For the generator , we only need consider the diagrams in (1)

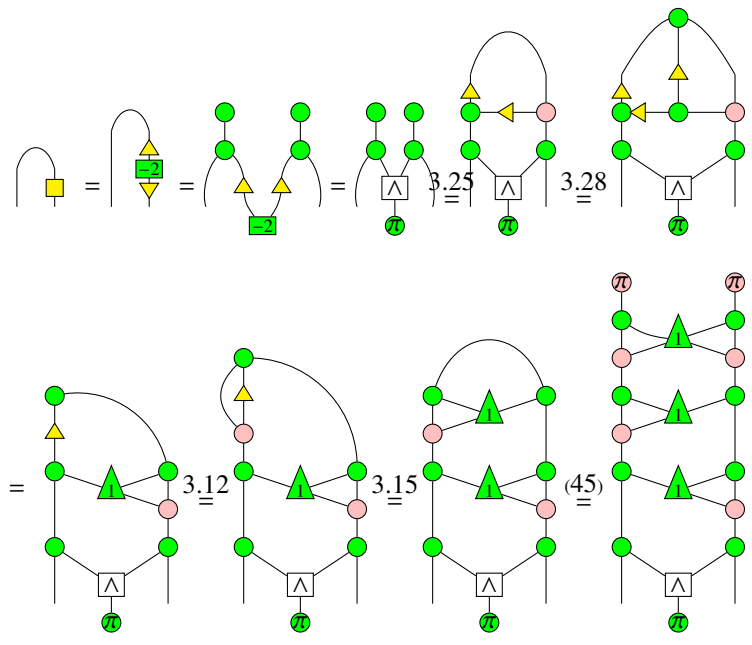
according to Remark 2.2:



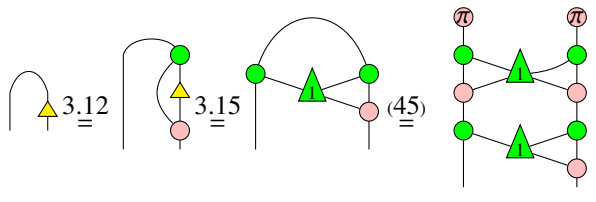
2. For the generators , , and , we have



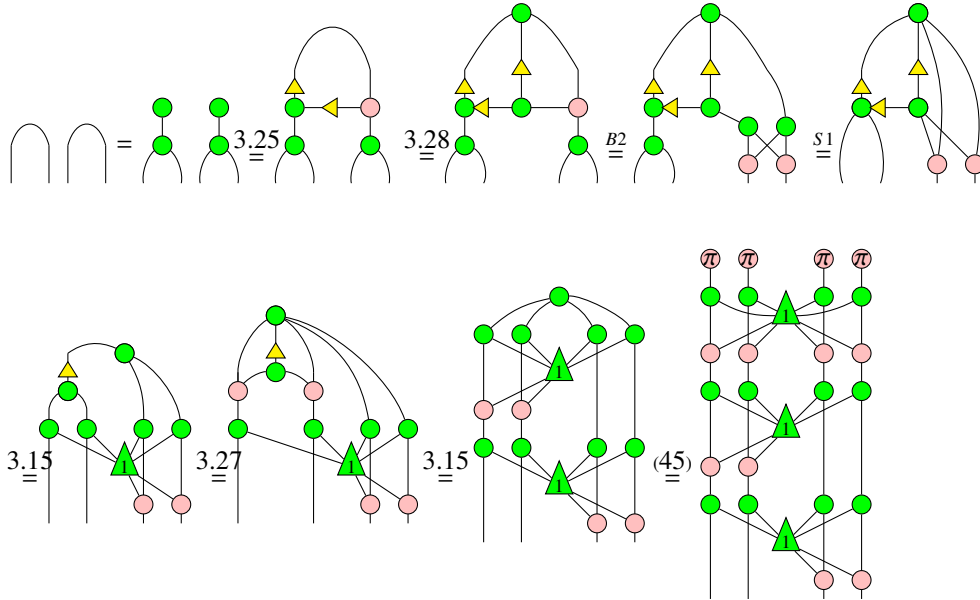
3. For the generator \square , we have



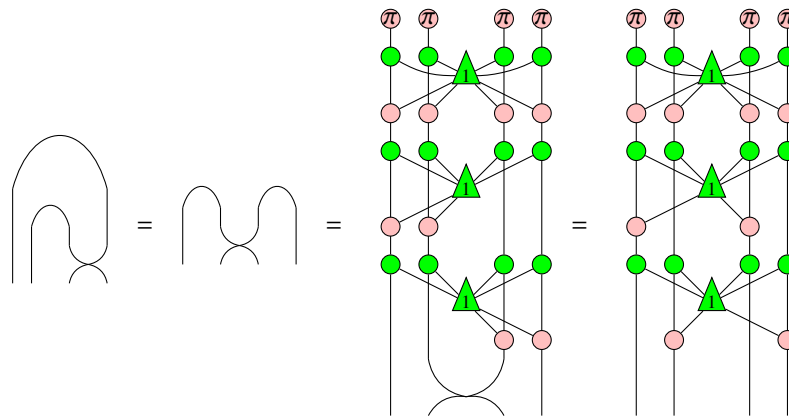
4. Since $\triangleleft^{-1} = \triangleleft$, we only need to consider \triangleleft :



5. For the generator $\begin{array}{c} \text{---} \\ \diagdown \quad \diagup \\ \text{---} \end{array}$, first we have




Then



5.2.4 Rewriting scalars into normal form

Given an arbitrary scalar diagram, it can be seen as a state diagram on top plugged with cups or \bullet from the bottom. Such a state diagram has been shown that it can be rewritten into a normal form, and a normal form plugged with \bullet can be bended up so that we have can still have a normal form with outputs connected by just cups. Since normal form with more than 2 outputs plugged with cups can be reduced to a normal form with outputs as proved in Theorem 5.11, we just need to show that a normal form

with exactly 2 outputs plugged with a cup can be written into a scalar normal form , which has also been obtained in Theorem 5.11.

6 Conclusion and further work

In this paper, we give an algebraic axiomatisation of qubit ZX-calculus and prove its completeness by constructing a normal form of an arbitrary state diagram via elementary transformations in linear algebra. In comparing to previous complete axiomatisation of ZX-calculus, this axiomatisation has no need to resort to either rules with trigonometry functions or other completeness results. Also the techniques used to achieve completeness here are very useful for application of this formalism.

There is lot of work following this direction. First, by the same method of this paper, we will fill all proof details in [17] for ZX-calculus over arbitrary commutative rings and semi-rings. Second, we can generalise the completeness of qubit ZX-calculus to qudit versions which have similar normal form as presented in [19]. Furthermore, since all different dimensional qudit ZX-calculus can be put together in a single framework called qfinite ZX-calculus as described in [19], the completeness could be obtained similarly as proved in this paper. As a consequence, one could reconstruct quantum theory using the qfinite ZX-calculus.

On the application side, we can utilise the techniques invented in this paper to simplify quantum circuits. Also with the diagrammatic representation of elementary matrices, we can solve linear systems in ZX-calculus [16], which would be helpful for tackling problems in quantum machine learning.

Acknowledgements

This work is supported by AFOSR grant FA2386-18-1-4028. The author would like to thank Bob Coecke, KangFeng Ng, and Aleks Kissinger for useful discussions.

References

- [1] Miriam Backens, Simon Perdrix & Quanlong Wang (2017): *A Simplified Stabilizer ZX-calculus*. *Electronic Proceedings in Theoretical Computer Science* 236, pp. 1–20, doi:10.4204/eptcs.236.1. Available at <http://dx.doi.org/10.4204/EPTCS.236.1>.
- [2] Niel de Beaudrap, Xiaoning Bian & Quanlong Wang (2020): *Fast and Effective Techniques for T-Count Reduction via Spider Nest Identities*. In Steven T. Flammia, editor: *15th Conference on the Theory of Quantum Computation, Communication and Cryptography (TQC 2020)*, *Leibniz International Proceedings in Informatics (LIPIcs)* 158, Schloss Dagstuhl–Leibniz-Zentrum für Informatik, Dagstuhl, Germany, pp. 11:1–11:23, doi:10.4230/LIPIcs.TQC.2020.11.

- [3] Titouan Carette, Dominic Horsman & Simon Perdrix (2019): *SZX-Calculus: Scalable Graphical Quantum Reasoning*. In: *44th International Symposium on Mathematical Foundations of Computer Science, MFCS 2019, August 26-30, 2019, Aachen, Germany*, pp. 55:1–55:15, doi:10.4230/LIPIcs.MFCS.2019.55.
- [4] Bob Coecke & Ross Duncan (2011): *Interacting quantum observables: categorical algebra and diagrammatics*. *New Journal of Physics* 13(4), p. 043016. Available at <http://stacks.iop.org/1367-2630/13/i=4/a=043016>. doi:10.1088/1367-2630/13/4/043016.
- [5] Alexander Cowtan, Silas Dilkes, Ross Duncan, Will Simmons & Seyon Sivarajah (2020): *Phase Gadget Synthesis for Shallow Circuits*. *Electronic Proceedings in Theoretical Computer Science* 318, p. 213?228, doi:10.4204/eptcs.318.13.
- [6] Amar Hadzihasanovic, Kang Feng Ng & Quanlong Wang (2018): *Two Complete Axiomatisations of Pure-State Qubit Quantum Computing*. In: *Proceedings of the 33rd Annual ACM/IEEE Symposium on Logic in Computer Science, LICS '18*, p. 502?511, doi:10.1145/3209108.3209128.
- [7] Emmanuel Jeandel, Simon Perdrix & Renaud Vilmart (2018): *Diagrammatic Reasoning Beyond Clifford+T Quantum Mechanics*. In: *Proceedings of the 33rd Annual ACM/IEEE Symposium on Logic in Computer Science, LICS '18*, ACM, New York, NY, USA, pp. 569–578, doi:10.1145/3209108.3209139. Available at <http://doi.acm.org/10.1145/3209108.3209139>.
- [8] Emmanuel Jeandel, Simon Perdrix & Renaud Vilmart (2019): *A Generic Normal Form for ZX-Diagrams and Application to the Rational Angle Completeness*. In: *34th Annual ACM/IEEE Symposium on Logic in Computer Science, LICS 2019, Vancouver, BC, Canada, June 24-27, 2019*, pp. 1–10, doi:10.1109/LICS.2019.8785754. Available at <https://doi.org/10.1109/LICS.2019.8785754>.
- [9] Aleks Kissinger & Arianne Meijer-van de Griend (2020): *CNOT circuit extraction for topologically-constrained quantum memories*. *Quantum Inf. Comput.* 20(7&8), pp. 581–596.
- [10] N. David Mermin (2007): *Quantum Computer Science: An Introduction*. Cambridge University Press.
- [11] Anthony Munson, Bob Coecke & Quanlong Wang (2020): *AND-gates in ZX-calculus: spider nest identities and QBC-completeness*. accepted to QPL 2020. ArXiv:1910.06818.
- [12] Kang Feng Ng & Quanlong Wang (2017): *A universal completion of the ZX-calculus*. ArXiv:1706.09877.
- [13] Kang Feng Ng & Quanlong Wang (2018): *Completeness of the ZX-calculus for Pure Qubit Clifford+T Quantum Mechanics*. arXiv:1801.07993.

- [14] Michael A. Nielsen & Isaac L. Chuang (2010): *Quantum Computation and Quantum Information*. Cambridge University Press, Cambridge, doi:10.1017/CBO9780511976667. doi: 10.1017/CBO9780511976667.
- [15] Renaud Vilmart (2019): *A Near-Minimal Axiomatisation of ZX-Calculus for Pure Qubit Quantum Mechanics*. In: *34th Annual ACM/IEEE Symposium on Logic in Computer Science, LICS 2019, Vancouver, BC, Canada, June 24-27, 2019*, pp. 1–10, doi:10.1109/LICS.2019.8785765. Available at <https://doi.org/10.1109/LICS.2019.8785765>.
- [16] Quanlong Wang: *Solving linear systems in ZX-calculus*. In preparation.
- [17] Quanlong Wang (2019): *ZX-calculus over arbitrary commutative rings and semirings (extended abstract)*. ArXiv:1912.01003.
- [18] Quanlong Wang (2020): *An algebraic axiomatisation of ZX-calculus*. *Proceedings of the 17th International Conference on Quantum Physics and Logic (QPL) 2020*. ArXiv:1911.06752.
- [19] Quanlong Wang (2020): *Enter a visual era: process theory embodied in ZX-calculus*. Presentation at 17th International Conference on Quantum Physics and Logic (QPL), doi:10.13140/RG.2.2.17289.67682.